This is to certify that the

dissertation entitled

SWELLING STRESSES AND DEFORMATIONS

IN WOOD COMPOSITES

presented by

Selim Salim Hiziroglu

has been accepted towards fulfillment
of the requirements for

Ph.D degree in Forestry

Major professor

Date 8.9.1989

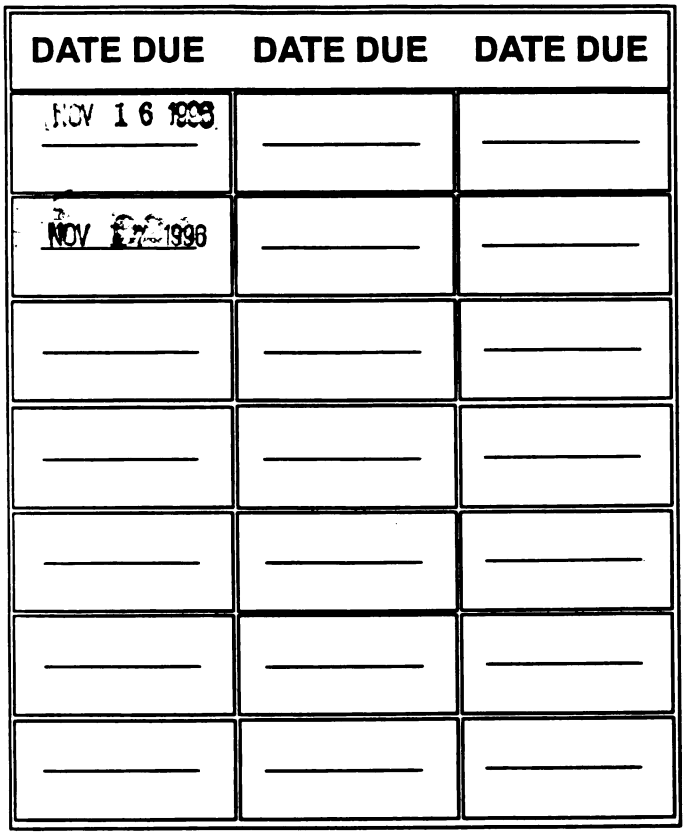

SWELLING STRESSES AND DEFORMATIONS IN WOOD COMPOSITES

By

Selim Salim Hiziroglu

A DISSERTATION

Submitted to
Michigan State University
in partial fulfillment of the requirements
for the degree of

DOCTOR OF PHILOSOPHY

Department of Forestry

1989

ABSTRACT

SWELLING STRESSES AND DEFORMATIONS IN WOOD COMPOSITES

By

Selim Salim Hiziroglu

Wood composites exhibit a dimensional change when they are exposed to different levels of moisture content. These changes occur both in the plane of the board and in thickness. Dimensional changes in the plane of wood composite panels under condition of partial or complete restraint result in swelling or shrinkage stresses which could lead to buckling and development of bending stresses.

It was the objective of this study to determine the development of above stresses and deformations in commercially produced particleboard, waferboard and oriented strandboard under conditions of complete restraint.

Three theoretical approaches were employed within the scope of the study. Firstly, axial swelling and shrinkage stresses were predicted by using experimental expansion and shrinkage coefficients and elastic properties along with theoretically computed buckling deflection values. Secondly, theoretical bending stresses were determined based on actual lateral buckling deformations of restrained specimens exposed to various humidity cycles. The third approach was also based

on experimental lateral buckling deflections of the specimens. However, only the elastic portions of the buckling values were used to predict bending stresses. In all three approaches elastic behaviour of the material was assumed.

The first method resulted in bending stresses in excess of the ultimate strength of each type of composite panel as determined in standard bending tests, while the second method yielded stresses slightly lower than the actual bending strength. The third method indicated that stresses were lower than the ultimate strength of the wood composites tested in this study. It is the visco-elastic characteristics of wood composites that reduce bending stresses to safe values.

Dedicated to my parents

ACKNOWLEDGMENTS

The author wishes to express his deep appreciation and gratitude to his supervisor Dr. Otto Suchsland for the opportunity to study under his guidance, for constant encouragement, assistance and helpful suggestions throughout the progress of this work.

He also wishes to thank for interest and cooperation of the other committee members, Dr. Alan Sliker of the Department of Forestry and Dr. Edward Morash of the Department of Marketing and Transportation Administration.

He is particularly grateful to the Scientific and Technical Research Council of Turkey for awarding him NATO science scholarship. Also, Department of Forestry is acknowledged for the partial financial support of this research.

Numerious suggestions of Dr. Huseyin Hiziroglu in preparing the dissertation are appreciated.

Last, but not least, thanks are due to Mr. Ivan Burton for his help in preparing the experimental set up.

TABLE OF CONTENTS

LIST OF TABLES

LIST OF FIGURES

CHAPTER 1

INTRODUCTION

1.1. Definitions

1.1.1. Particleboard, Waferboard and Oriented Strandboard

The increasing acceptance of wood composites has caused an impressive rise in the consumption of wood based panels as a subtitute for other materials [3,28,70]. Before 1978, the structural panel industry in the United States consisted almost entirely of veneer panels. During that period, timber costs were increasing drastically unfavorable impacting the forest products industry. Wood composite boards such as waferboard and oriented strandboard appeared to offer a good solution to this problem due to their lower cost and their engineering properties being comparable with those of plywood [13,16,86].

As a result, the structural board segment of the wood panel market virtually exploded in capacity in 1986 due to high level of housing demand. Total industry value of structural panels, including plywood, waferboard and oriented strandboard was 25.6 billion ft^2 as can be seen from Figure 1.1. Plywood alone accounted for 22.1 billion ft^2, while the combined production of oriented strandboard and waferboard reached nearly 3.5 billion ft^2. On the other hand particleboard capacity in the United States at the end of 1988 was 4.28

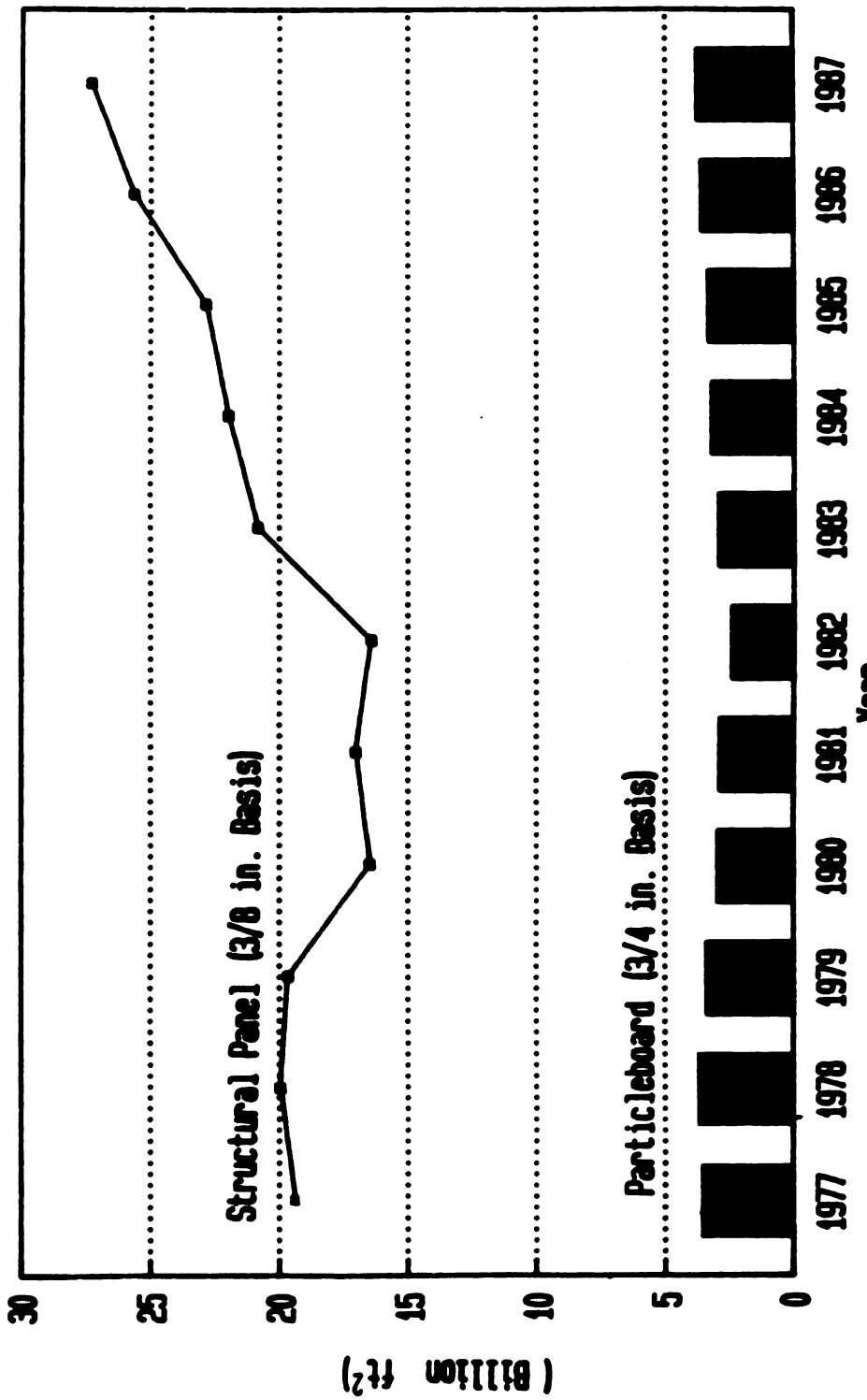

Figure 1.1. Consumption of particleboard and structural wood composites in the United States [16].

billion ft^2 (3/4 inch basis) annually according to National Particleboard Association survey [16]. Particleboard is a generic term for panels manufactured from lignocellulosic material. It is produced from dry wood particles that have been sprayed with a binder and are bonded together under pressure and heat. Particles can be obtained from almost any kind of wood, such as whole logs or wood residue from lumber or plywood manufacturing.

The various kinds of particleboards differ greatly, based on the size and geometry of the particles used, the density to which the panel is pressed and their manufacturing process.

The term "structural particleboard " was used for panels used as roof and wall sheathing as early as 1962. Later, above term was adopted to distinguish structural type of panels made of phenolic bonded flakes from the traditional urea-bonded particleboard. Waferboard and oriented strandboard can be included under the definition of structural flakeboards within the purpose of this discussion. Both types of structural composites because of their relatively large flake size are usually produced from roundwood rather than any kind of mill residue and they are bonded with phenolic resin.

Waferboard, the earliest type of widely used structural wood composites is made from large, almost square particles of predetermined dimensions with uniform thickness. The fiber orientation in such a product is parallel to the board face.

Typical particle thickness and length are about 0.025 inch and 1.0 inch to 2.0 inch, respectively, in waferboard. Because random wafer width may equal or exceed wafer length, manufacture of this composite rules out the use of any alignment process.

On the other hand, oriented strandboard is manufactured from knife cut type particles of uniform thickness with a length at least three times greater than the width, allowing their parallel alignment. Usually three layers of oriented strands are formed with orientation in adjacent layers alternating by a 90° angle. In contrast to waferboad and oriented strandboard, particleboard is made from smaller particles [71]. Figure 1.2 shows the differences in appearence between waferboard, oriented strandboard and particleboard.

Wood composites are being utilized in more applications today than ever before. Furniture and cabinet parts, floor underlayment and decking, wall sheathing can be given as some of the applications of wood composites.

During the last decade, plywood had a relatively constant 14 % share of the total wall sheathing market from the early 1960's through 1978 [3]. However, oriented strandboard and waferboard have been largely utilized to replace plywood in sheathing and roofing in residential construction as illustrated in Figures 1.3, 1.4, 1.5, and 1.6. They have 24%

Figure 1.2. Structural wood composites.


WAFERBOARD
ORIENTED STRANDBOARD
PARTICLEBOARD

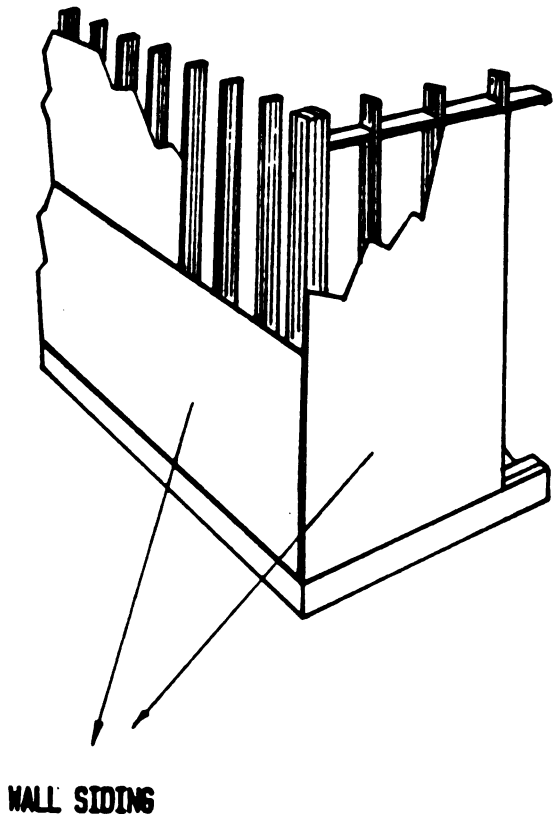

Figure 1.3. Conventional wall sheathing.

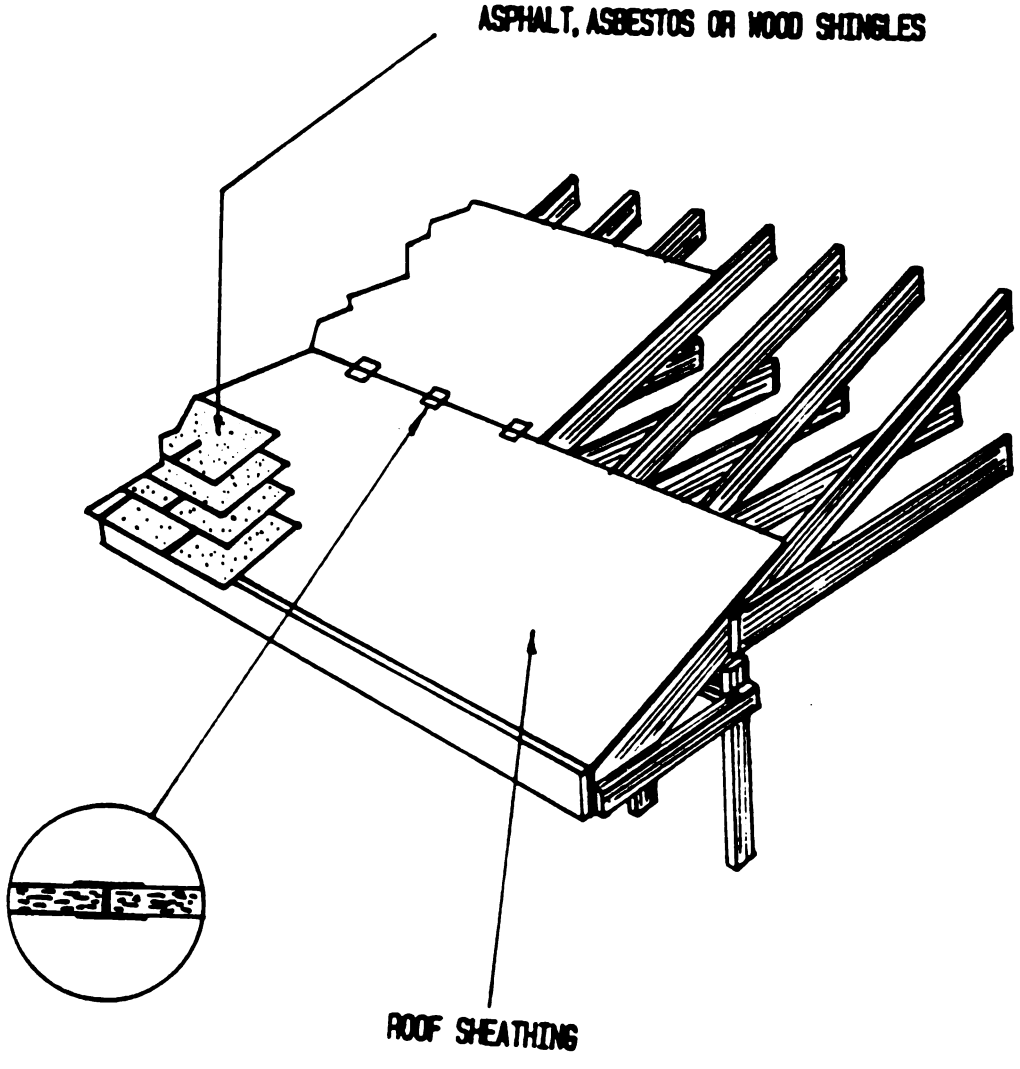

Figure 1.4. Application of roof decking.

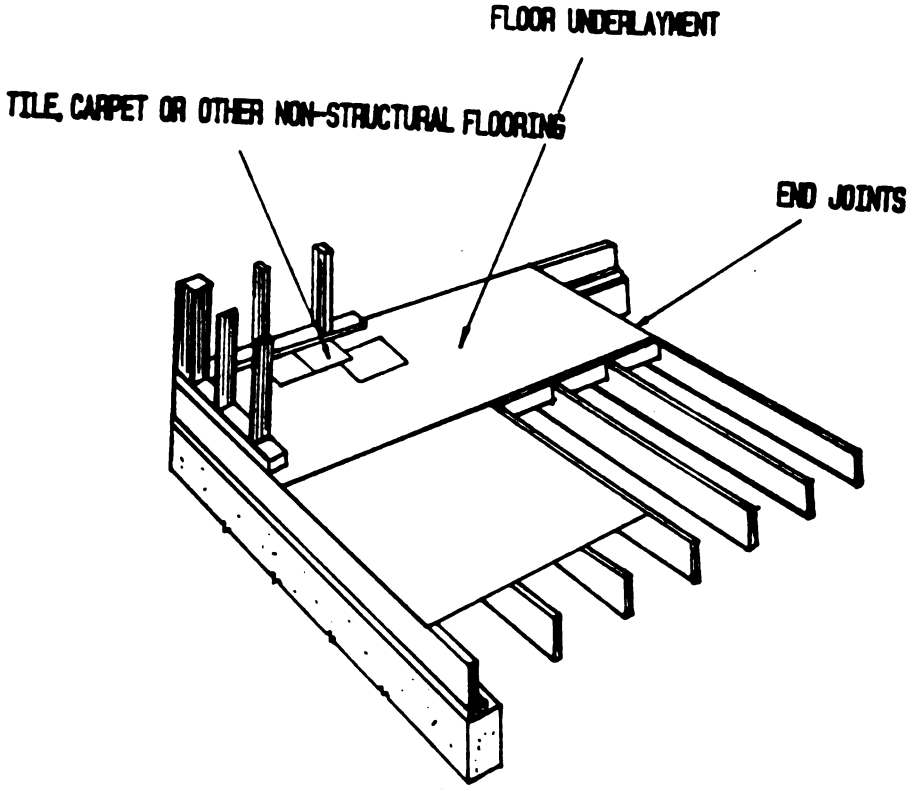

Figure 1.5. Floor underlayment.

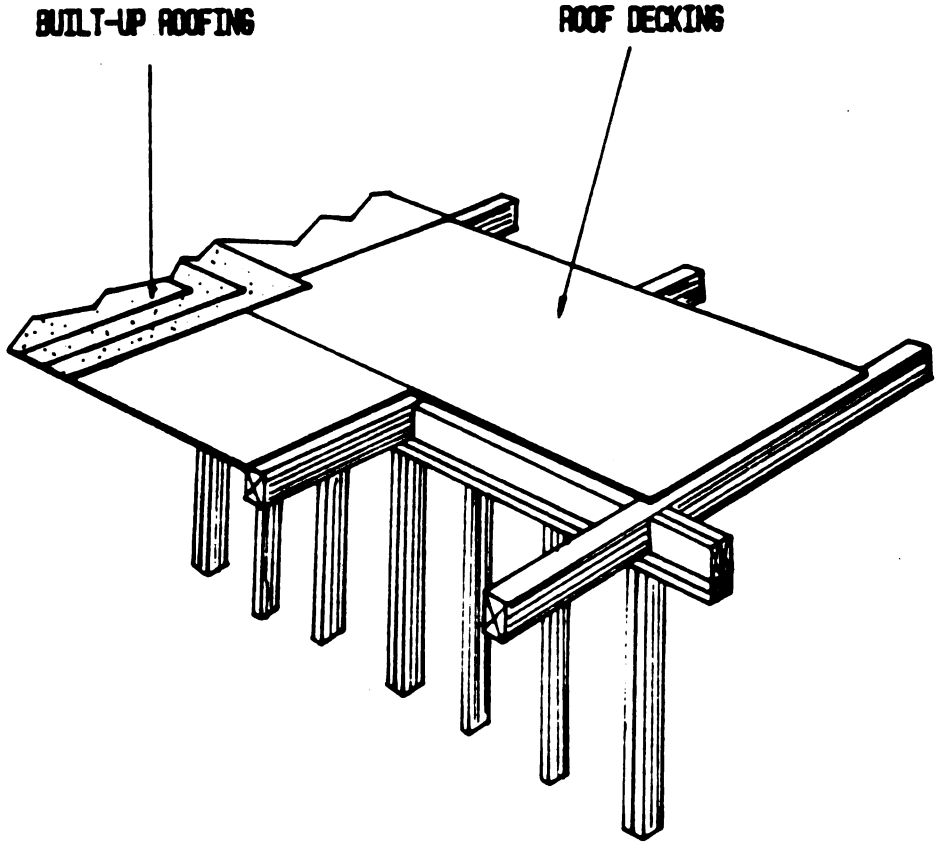

Figure 1.6. Roof decking with built-up roofing

market share in the wood panel industry [70]. Among the structural uses of particleboard, one of the most important in terms of volume consumed is underlayment floor covering, particularly in mobile homes.

1.2. Production Processes of Particleboard, Waferboard and Oriented Strandboard

1.2.1. Particleboard

Most of the particleboards are produced by the method known as platen method. In this method, the board is manufactured by pressing a mat of particles coated with a bonding agent between parallel platens in a hot press with the pressure applied perpendicularly to the faces.

After particles are dried to 2-4 % moisture content (MC) in a dryer, they are classified by size. The furnish then proceeds to a blender where resin and wax are applied to the material. Forming is the next step in which particles are deposited onto a moving conveyor to form a mat. Final thickness of the board is determined by densification either in single or multi-opening hot presses. After the cured boards are unloaded from the press, they are trimmed to various sizes and sanded to uniform thickness and may undergo various fabricating process such as filling or overlaying. Figure 1.7 depicts the basic steps of this method.

Three different types of board configurations can be used

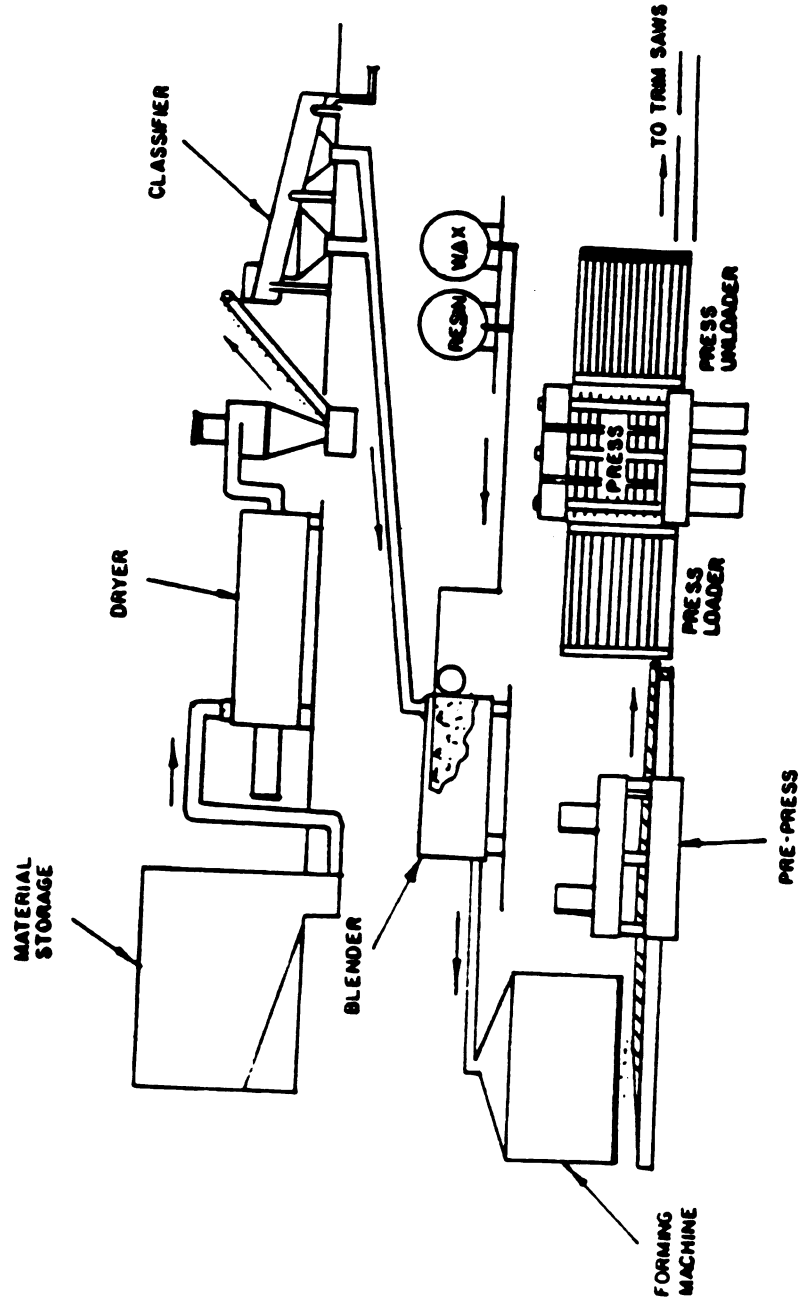

Figure 1.7. Particleboard manufacturing process [50].

for conventional particleboard as far as the number of layers is concerned. The first kind is a homogeneous board in which the total furnish is uniformly distributed throughout the mat. In three-layer boards the furnish is divided into core and face fractions. Thin flakes of finer material, for instance could be located in each face whereas coarser particles would be used for the core of the board. A third configuration is the multi-layer board. In this kind of board, the finest material is on the faces and particle size gradually inreases toward the core of the board.

1.2.2. Waferboard

Disk flakers are commonly used for the reduction of debarked logs into the desired wafer configuration [22,36]. Wafers are dried and then screened for removal of fines. In the next step a spray-dried phenolic resin is applied in blenders at a rate of between 2-5 % by weight. Approximately 1 % wax is also applied to the wafers. Wafers are deposited into a mat before final thickness of the panel is determined by densification in the hot pres at a temperature of 325° to 350° F. Edge trimming and cutting to size completes waferboard manufacture (See Figure 1.8).

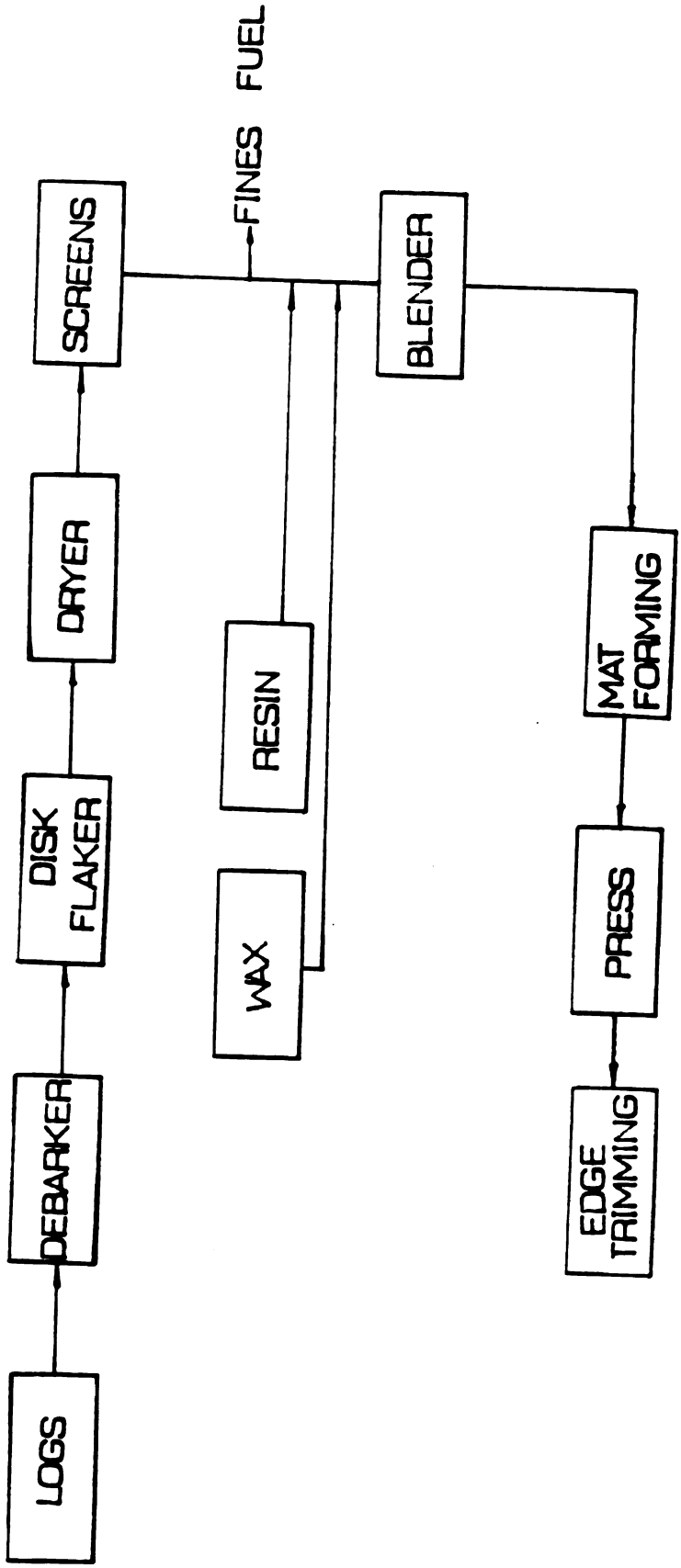

Figure 1.8. Typical process flow chart of waferboard manufacture.

1.2.3. Oriented Strandboard

Ring and drum flakers are used for the reduction of raw material (round wood) to both face and core strands. Similarly to waferboard production, strands are dried and screened before resin application. Oriented strandboard is usually manufactured by using liquid phenolic resol resins which are applied with the wax additive in a spray type blender.

Face strands which could be longer and /or thinner than core strands are aligned parallel to the machine direction during the orientation process. Core strands are laid down at a 90° angle to the face layers [17]. Figure 1.9 depicts a typical forming process for oriented strandboard. Finally, either multi-opening or single-opening presses densify the board to the final panel thickness. A flow diagram of oriented strandboard manufacture can be seen in Figure 1.10.

1.3. Properties of Structural Wood Composites

Particle geometry, particle size, particle alignment as well as resin content are four factors which affect both physical and mechanical performances of structural wood composites. Static bending strength, tension strength parallel and perpendicular to the surface are examples of important mechanical properties while density, thickness swelling and linear expansion are the most important physical

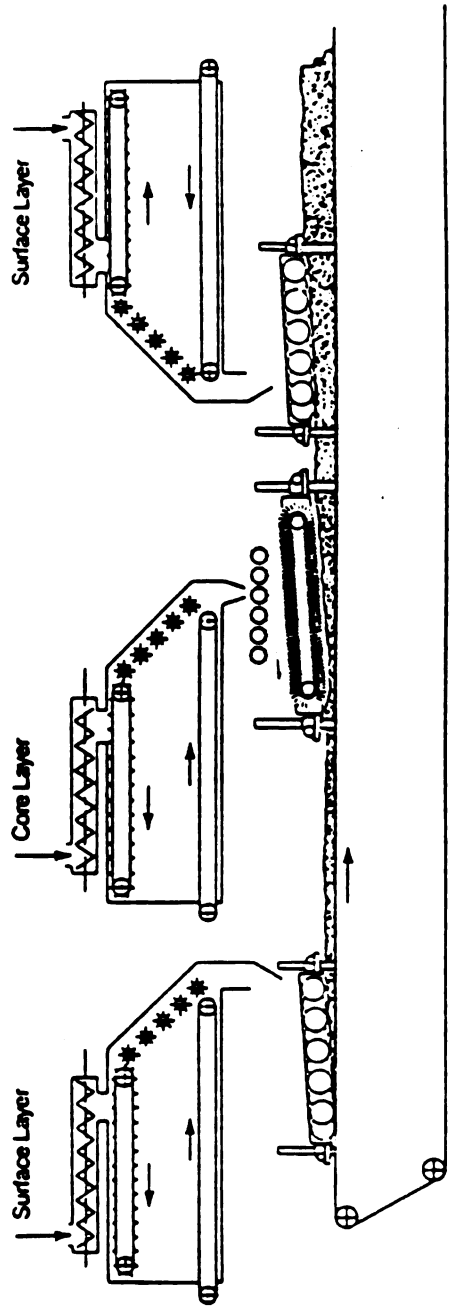

Figure 1.9. Mat forming of oriented strandboard [71].

Figure 1.10. Typical process flow chart of oriented strandboard manufacture.

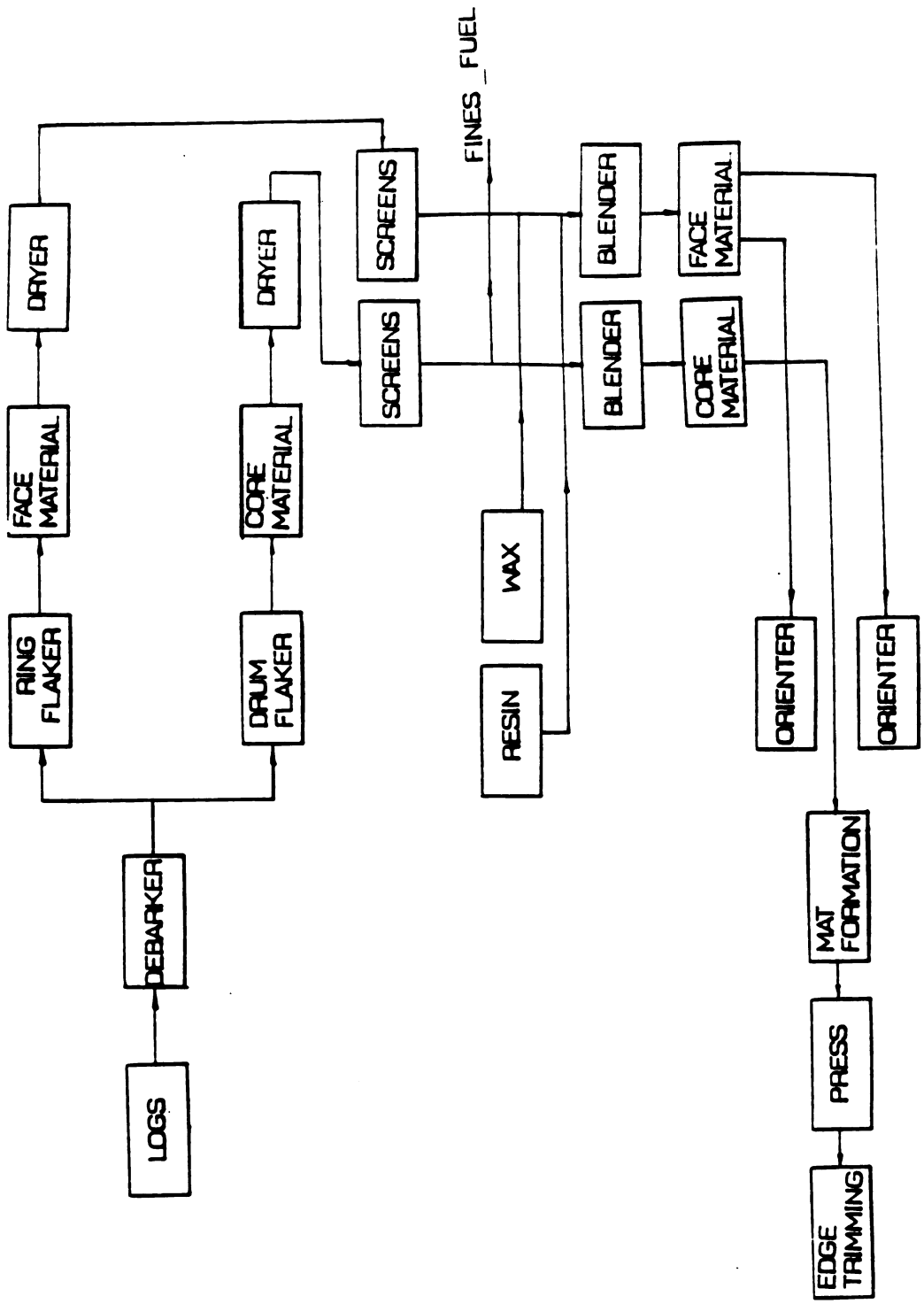
LOGS
DEBARKER
RING FLAKER
DRUM FLAKER
FACE MATERIAL
CORE MATERIAL
DRYER
DRYER
SCREENS
SCREENS
FINES_FUEL
WAX
RESIN
BLENDER
BLENDER
FACE MATERIAL
CORE MATERIAL
ORIENTER
ORIENTER
MAT FORMATION
PRESS
EDGE TRIMMING

characteristics. Therefore, optimization of board performance requires knowledge of relationships between these raw material and process variables and basic properties of structural panels.

Previuos research has found that bending properties increase directly with particle length and decrease with flake thickness [19,22,36,46,61,64,67,84].

Gatchel et al. [19] reported that reduction in flake thickness resulted in an incresed modulus of elasticity (MOE) and modulus of rupture (MOR) (These two mechanical properties are explained in section 2.5.1). This could be related to the more uniform distribution of thinner particles which diminishes the discontinuities in the board. In the same study it was observed that variation of the flake length did not significantly affect the MOE values of boards. Another study conducted by Lehmann [46] presented findings similar to the work done by Gatchel et al. [19].

Slenderness ratio can be considered as an important measure to determine effect of flake geometry on mechanical properties of wood composites. It is defined as the ratio of flake length to flake thickness. The higher slenderness ratios of the large flakes used as raw material for waferboard and oriented strandboard results in bending properties superior to those of conventional particleboard [9,58]. Figure 1.11 depicts the direct effect of the slenderness ratio on MOR values of

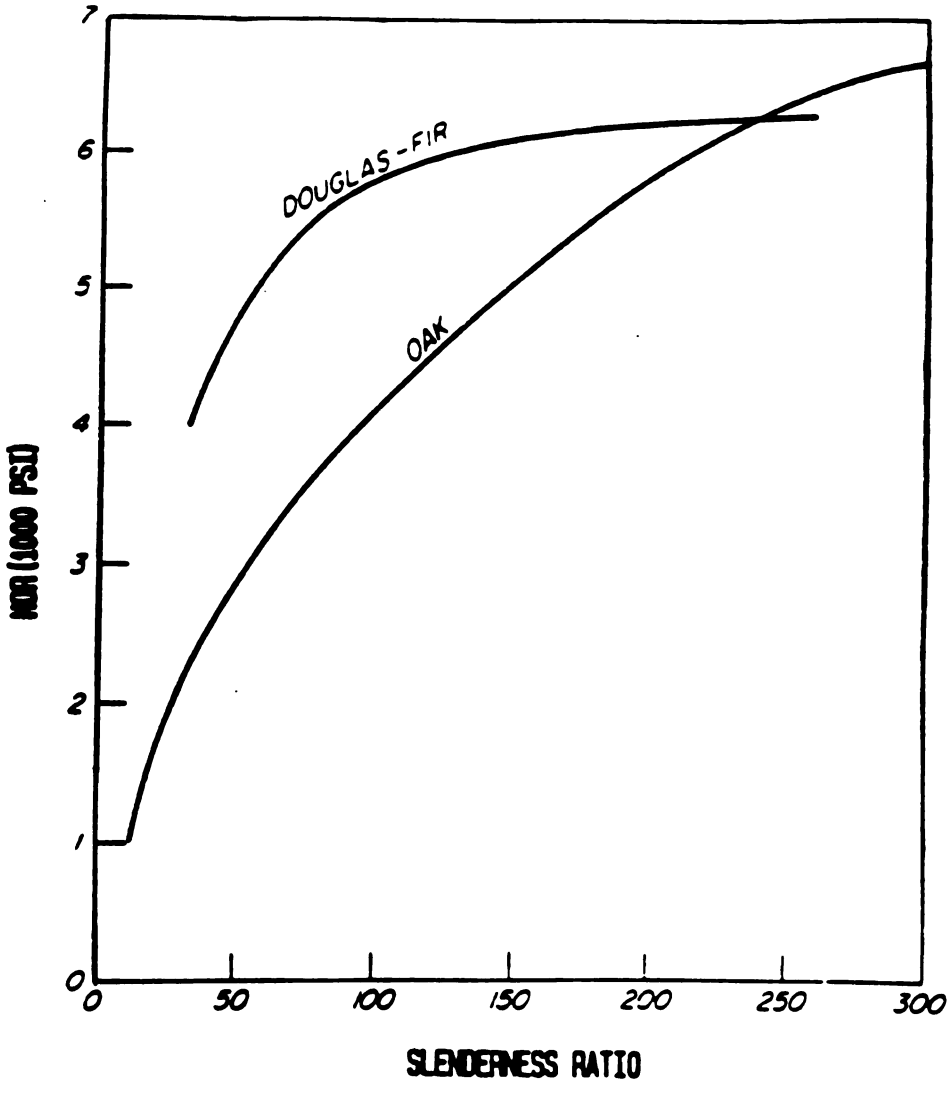

Figure 1.11. Slenderness ratio versus modulus of rupture [9,58].

structural board made from oak and Douglas fir flakes.

Post [58] also determined that the MOR of particleboard manufactured from oak flakes increased as particle length was increased from 0.5 inch to 4.0 inch. On the other hand, the same study indicated that particle thickness did not have as significant an effect on MOR as did particle length. Flake geometry also has a very important influence on durability of structural panels because of its association with the sringback phenomenon. Springback can be defined as irreversible thickness swelling resulting from release of compressive stresses in the board. Fluctuating humidity is the most important factor which triggers the release of these stresses. As flake thickness decreases, thickness swelling improves.

McNatt [51] reported greater thickness changes for waferboard compared to those of particleboard as a result of cyclic relative humidity exposure from 30 % to 90% . Flake thickness was found to be a more important variable than flake length with regard to springback in the equilibrium moisture content range between 10 % and 21 % [51]. On the other hand, it was also indicated that the stablest flakeboard could be produced by combining thinner flakes with higher resin content.

Another important characteristic which has a very significant role in the structural performance of wood

composites is flake alignment. Particles or flakes can be lined up in one direction according to their length. Most oriented strandboard, however, is manufactured by forming alternately oriented layers which provides balanced mechanical characteristics as found in plywood. Alternating layer orientation provides expansion resistance as is the case in plywood. As Figure 1.12 illustrates, flake alignment of three layer oriented strand board improves both linear expansion and modulus of elasticity of the board in the direction of face orientation.

1.4. Objectives of the Study

Wood based panels experience a dimensional change when they are exposed to varying moisture content. Particularly, flake type structural board such as waferboard and oriented strandboard may be exposed to very high levels of moisture content in their practical application as roof decking and sheathing material. Consequently, panel expansion and attendent buckling deformation of the material with respect to the framing can be considered as a significant constructional problem.

Particleboard may also present similar problems in its application as underlayment and floor decking in mobile homes.

Therefore, it is the main objective of this study to

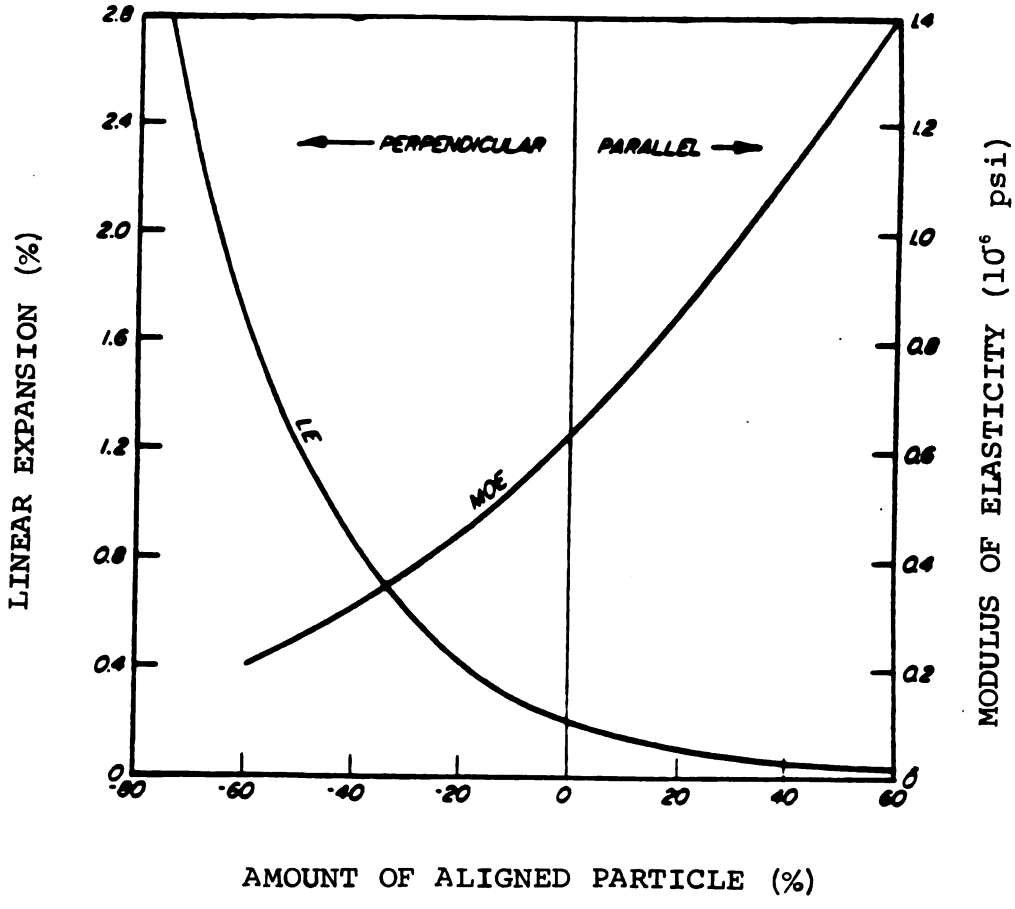

Figure 1.12. Effect of particle alignment on linear expansion and modulus of elasticity of three-layer oriented strandboard [21].

(Shown on the horizontal axis is the relative quantity of face material oriented in the parallel direction (+%) and in the perpendicular direction (-%) , rest of the flakes and the core are random.)

investigate the development of stresses and deformations under changing relative humidity levels under controlled laboratory conditions to determine whether such stresses reach levels where they may impair the performance of particleboard, waferboard and oriented strandboard.

Three theoretical approaches were used to determine the bending stresses of restrained structural wood composite columns due to change in relative humidity within the scope of the study. First, bending stresses were determined for various dimensional and exposure conditions based on measured expansion and shrinkage coefficients and measured elastic properties. Later, actual lateral buckling deflections were obtained from restrained specimens exposed to various humidity cycles and were used as input to computation of bending stresses. Finally, elastic portions of the lateral buckling deflection from the experiments were employed to calculate bending stresses.

These approaches necessitated the determination of swelling and shrinkage coefficients, the determination of bending strength (MOR) and modulus of elasticity (MOE) of the material under consideration.

1.5. Organization of the Thesis

In Chapter 1, a brief introduction of wood composites, their basic production processes and the objectives of the

study were given and explained.

The mechanism of buckling of wood composites due to hygroscopic expansion is presented in Chapter 2 in the light of previous investigations.

The experimental details, including material and sample design, relative humidity cycles, mechanical and physical tests are described in Chapter 3.

Chapter 4 is devoted to the results and discussions of experimental and theoretical investigations.

Finally, conclusive remarks are presented in Chapter 5.

CHAPTER 2

THE MECHANISMS OF BUCKLING OF WOOD COMPOSITES CAUSED BY HYGROSCOPIC EXPANSION

2.1. General

In this chapter, firstly, buckling of wood composites due to hygroscopic expansion will be described. Secondly, swelling stresses and deformations of wood composites will be explained in the light of previous works. Thirdly, theoretical swelling, shrinkage, and bending stresses and deformations of wood composites in analogy to the analysis of thermal stresses under the assumption of elasticity will be described.

Later, hygrocopic swelling and shrinkage of wood and wood composites under both free and restraint conditions will be illustrated.

Finally, major factors such as MOE and linear expansion which have significant effect on development of stressess and deformations in wood composites caused by hygroscopicity will be presented.

2.2. Mechanisms of Buckling

Buckling is the sudden lateral deformation of a slender column or a thin sheet under compressive load [78,65]. If a

slender column is exposed to a relatively small load, it will be axially shortened. As the load on such a slender member is increased gradually, it will reach a level at which lateral deflection will occur suddenly without further load increase. This load and stress at this point are called critical load (Euler load) and critical stress, respectively. The compressive axial deformation at this point is called the critical strain. Critical load is a significant factor in buckling of a column, and is the maximum load which a slender column can support.

In most structural applications of materials, buckling is synonymous with structural failure. There are, however, situations where buckling is caused not by structural loads but by internal forces. This would be the case when a sheet or column would be subjected to hygroscopic or thermal expansion while they are restrained in the axial direction. Buckling, in this case would be a manifestation of the hygroscopic or thermal expansion but would not necessarily indicate failure. The forces acting in such cases are hygroscopic swelling or thermal forces. Hygroscopic properties of wood and wood based composites are presented in section 2.3.

The swelling and shrinkage of wood composite panels is not hazardous in itself unless above mentioned deformations

occur. However, buckling and warping present significant problems which are of great practical importance in the application of these panel products [80].

The equivalence of the effect of external forces and forces generated by restrained expansion on the buckling of a column is illustrated in Figure 2.1. The column on the left is being compressed by the external force P. When the compression strain reaches the critical level

$$\epsilon_{cr} = \frac{\pi^2 \, h^2}{3 \quad L^2}$$

where, ϵ_{cr} = Critical strain (inch/inch)

h = Column thickness (inch)

L = Column length (inch)

the column deflects laterally. The column on the right is held in a rigid clamp. As its moisture content (MC) increases, it wants to expand but is prevented from doing so. As a result a swelling force develops.

If the restrained expansion is equal to ϵ_{cr} , the column buckles. This restrained expansion is the product of the expansion coefficient, α, (expansion per 1 % ΔMC) and the moisture content change (ΔMC). At this point the loads P on both columns are the same and critical strain can be expressed

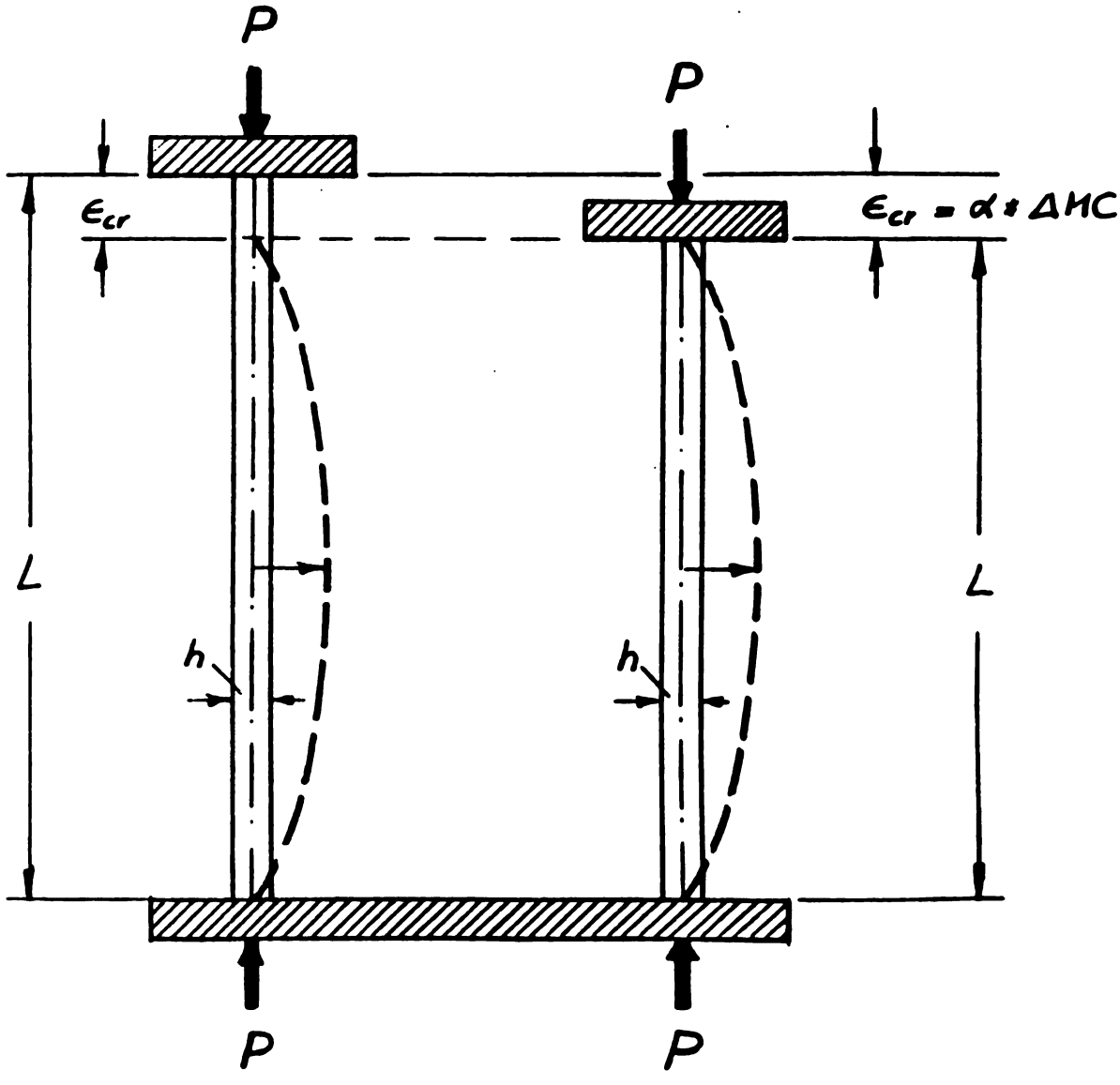

Figure 2.1. Buckling of a column due to external load (left) and hygroscopic expansion (right)[80].

as follows :

$$\epsilon_{cr} = \alpha \Delta MC = \frac{\pi^2}{3} \frac{h^2}{L^2}$$

where α = Coefficient of hygroscopic expansion (1/%)

ΔMC = Change in moisture content (%)

The same result would be obtained by letting the column on the right expand without restraint, and then compressing it back to its original length by applying an external force P.

In the following, the phenomenon of buckling under external loads will be described. This will be followed by an explanation of stresses occuring during hygroscopic expansion of wood material restrained in one direction (swelling stresses) including the consequence of axial compression, namely buckling deformation and bending stresses associated with buckling deformations.

2.2.1. Elastic Buckling

Elasticity assumption was used to determine theoretical development of swelling and bending stresses and deformation throughout the study. Therefore, elastic buckling of columns will be described in the following.

In order to accurately explain the behaviour of a column by employing Hook's law, stresses in the member must remain below the proportional limit of the material. This is the case for a slender column (Figure 2.2) in which the critical stress (Euler stress) is reached before the axial stress exceeds the proportional limit [81,65]. Moreover, it is assumed that the load is concentric throughtout the cross section of the material. However, these conditions exist neither in any actual engineering structures nor in wood composites. Consequently, it is desirable to investigate the behavior of an imperfect column and compare the results with those predicted by Euler's theory [12].

A column may have different boundary conditions based on its end positions as illustrated in Figure 2.3. This figure represents various conditions and effective length which is the distance between adjacent points of inflection locations for a column.

The internal resisting moment at any section of a particular column with hinged ends will be :

$$M_x = -EI \frac{d^2y}{dx^2} \qquad (2.1)$$

As can be seen from Figure 2.4 equating this expression to the externally applied bending moment which is Py gives

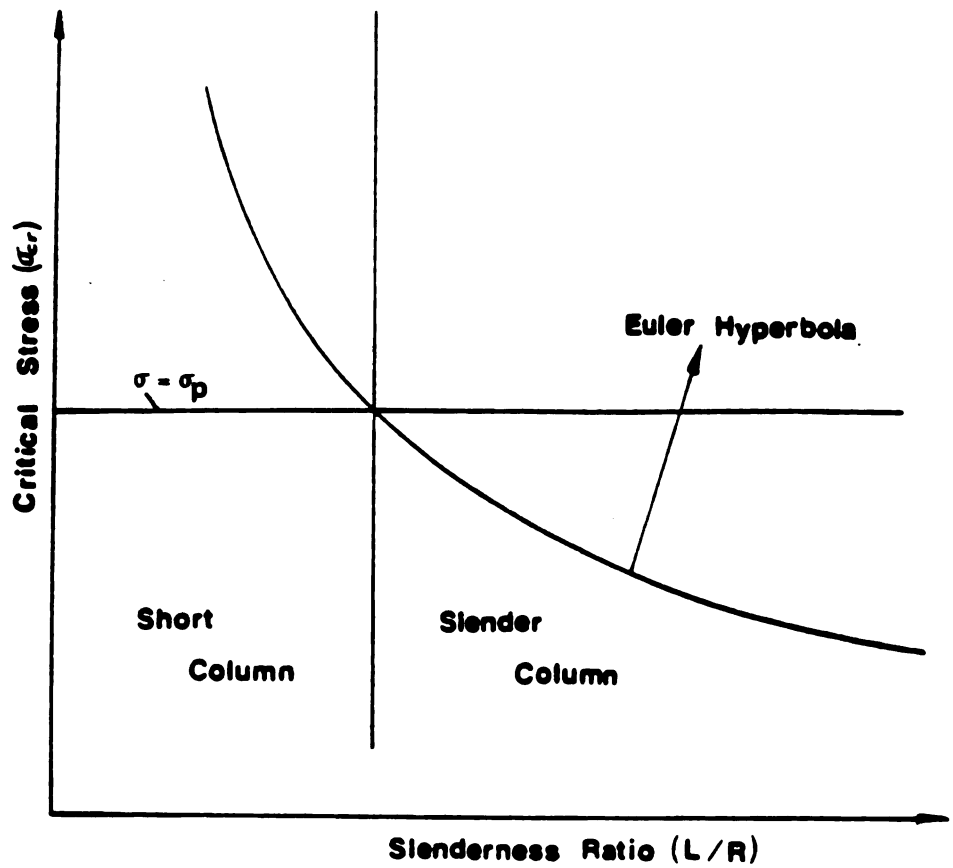

σ_p = Proportional limit stress (psi)
L = Length of column (inch)
R = Column thickness (inch)

Figure 2.2. Illustration of column curve [12].

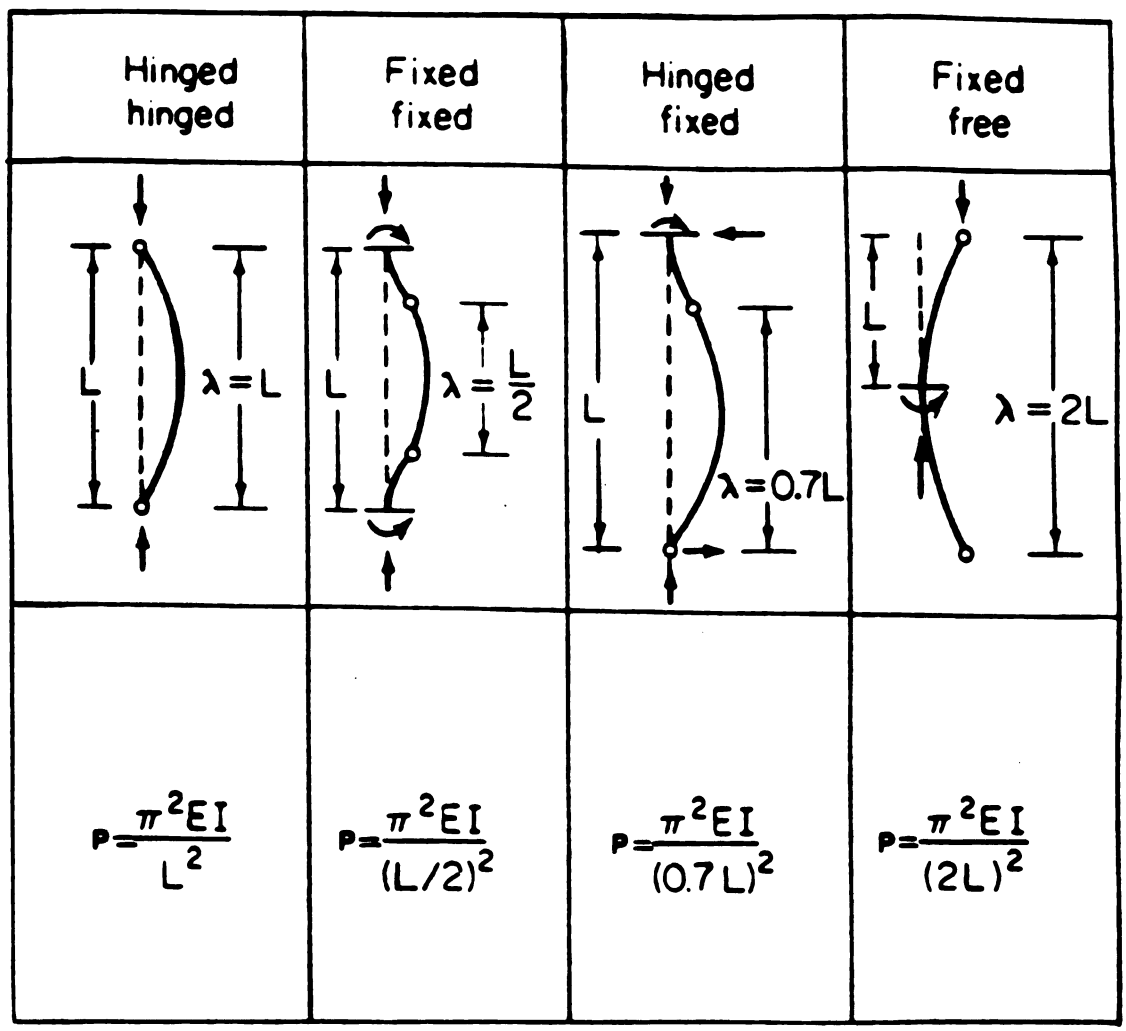

Figure 2.3. Effective length and critical load of variuos boundary conditions of columns [65,85].

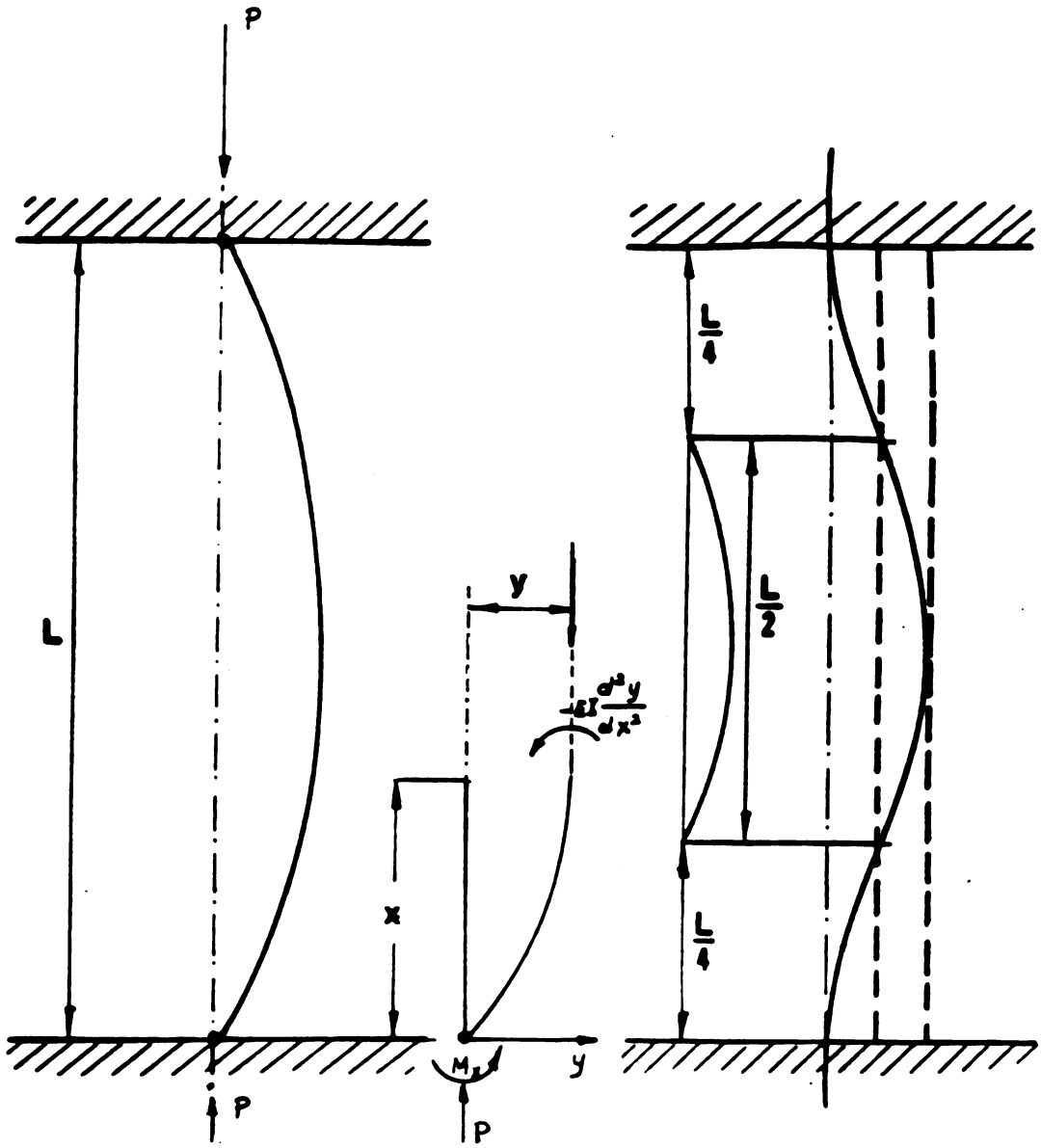

Figure 2.4. Illustration of internal resisting moment of a hinged-ends column (center), buckling deflections of hinged-ends (left) and fixed-ends (right) column [12].

$$M_x = Py$$

$$Py + E\ I\ \frac{d^2y}{dx^2} = 0 \qquad (2.2)$$

or

$$\frac{d^2y}{dx^2} + k^2y = 0 \qquad (2.3)$$

where $k^2 = \frac{P}{E\ I}$

In the above equation,

E : Modulus of elasticity (psi) P : Load (lb)

I : Moment of inertia ($inch^4$) y : Deflection(inch)

$\frac{d^2y}{dx^2}$: Deflection at distance x (inch)

Py : Externally applied bending moment (lb-inch)

Solution of homogeneous linear differential equations with constant coefficients is always of the form

$$y = e^{ax} \tag{2.4}$$

Substitution of this expression into Eq. (2.2) leads to,

$$y(x) = A_1 \; e^{ikx} + A_2 \; e^{-ikx} \tag{2.5}$$

By using Euler's formulas, exponential functions can be written as,

$$\begin{aligned} e^{ia} &= \cos a + i \sin a \\ e^{-ia} &= \cos a - i \sin a \end{aligned} \tag{2.6}$$

The general solution for Eq. (2.3) can be expressed as,

$$y(x) = A \sin kx + B \cos kx \tag{2.7}$$

where A and B are arbitrary constants depending on the boundary conditions. The arbitrary constants A and B can be determined by using the following boundary conditions :

$$x = 0 \qquad \text{at} \quad y = 0$$

$$x = L \qquad \text{at} \quad y = 0$$

$$y(0) = 0 \longrightarrow A = 0$$

$$y(L) = B \sin kL = 0$$

for the second condition, where $y = 0$ and $x = L$,

$$A \sin kL = 0 \qquad (2.8)$$

This relation can be satisfied in one of two ways,

$$\text{either } A = 0 \quad \text{or} \quad \sin kL = 0$$

If $A = 0$, P can have any value .

$$\text{If } \sin kL = 0 \quad \text{then,}$$

$$kL = n\pi \quad , \quad \text{where, } n = 1,2,3,4,...$$

Substition of this expression into equation (2.3) and (2.8) leads to

$$P = \frac{n^2 \pi^2 E I}{L^2} \qquad (2.9)$$

At the load given by equation (2.9), the column can be in equilibrium in a slightly bend form [12]. For n = 1 (column

with hinged ends),

$$P_{cr} = \frac{\pi^2 \, E \, I}{L^2} \qquad (2.10A)$$

$$\sigma_{cr} = \frac{\pi^2 \, E \, h^2}{12 \, L^2} \qquad (2.10B)$$

Equations 2.10A and 2.10B yield the critical load (Euler load) and critical stress, respectively. Critical load is the smallest load at which a state of neutral equilibrium is possible.

If a column is fixed at both ends,

$$EIy'' + Py = M_o$$

$$y'' + k^2 y = M_o / I E \qquad (2.11)$$

where, $k^2 = P / E I$

Equation (2.11) consists of two parts namely, the complementary part and the particular part. The complementary part is the solution of the homogeneous equation which is given in Eq. (2.7). The particular part is any solution to the entire equation such as,

$$y = \frac{M_o}{E\ I\ k^2} \qquad (2.12)$$

Therefore, the entire solution is :

$$y(x) = A \sin kx + B \cos kx + M_o / P \qquad (2.13)$$

A and B are arbitrary constants which can be evaluated by using the boundary conditions.

$$y' = 0, \qquad y = 0 \qquad \text{at} \quad x = 0$$

$$y = 0 \qquad \text{at} \quad x = L$$

$$A = 0 \quad \text{and} \quad B = - \frac{M_o}{P}$$

Therefore, $$y(x) = \frac{M_o\ (1 - \cos kx)}{P} \qquad (2.14)$$

the last condition leads to the trancendental equation

$$\cos kL = 1.0$$

The smallest non-zero root to this equation is :

$$kL = 2\pi$$

$$P_{cr} = \frac{4\ \pi^2\ E\ I}{L^2} \qquad (2.15A)$$

Equation 2.15A represents the critical load of a column with fixed ends. It is four times as large as the critical load of a hinged-end-column [12]. Equation 2.15B can also be used to determine the critical stress for a column with fixed ends.

$$\sigma_{cr} = \frac{\pi^2\ E\ h^2}{3\ L^2} \qquad (2.15B)$$

2.2.2. Hygroscopic Swelling Stresses.

Swelling stresses could be either hygroscopic or thermal stresses. Thermal stresses in metals are much more critical than either thermal or hygroscopic swelling stresses in wood and wood composites. As a result, considerable theoretical work has been done in the field of thermal stresses in metals which can be applied directly to hygroscopic swelling stresses in

wood and wood composites.

As the dimensions of a piece of metal increase with an increase in temperature, so do the dimensions of a piece of wood or wood composite increase as its moisture content increases. Hygroscopic swelling stresses may be defined as stresses that must be applied to the panel during the changing moisture content in order to prevent expansion and shrinkage from its original length [57].

Another way of looking at this stress development is as follows :

One allows a piece of wood to expand freely with increasing moisture content and then applies a stress just sufficient to compress the wood back to its original dimensions.

$$\sigma = \epsilon E = \alpha \Delta MC E$$

where,

σ = stress (psi)

ϵ = elastic strain (inch/inch)

E = Modulus of elasticity (psi)

α = coefficient of hygroscopic expansion (1/%)

ΔMC = change in moisture content (%)

The above equation describes two equivalent cases. The left hand term explains stress as the product of the elastic strain and the modulus of elasticity, and the right hand term

subsitutes the free expansion (α ΔMC) for the elastic strain. The hygroscopic expansion is the product of the expansion coefficient, α ,(expansion per 1/% moisture content change) and the moisture content change, ΔMC. All of the following derivation are based on this important equivalence.

Equation 2.15B given in section 2.2 represents the critical stress of a column with fixed ends. Using the above subsititution the critical stress for this column can be written as follows:

$$\sigma_{cr} = \epsilon_{cr} E = \frac{\pi^2 h^2 E}{3L^2} = (\alpha \Delta MC)_{cr} E$$

where, E is modulus of elasticity at the end condition (high moisture condition). It must be pointed out again that elasticity is assumed.

There is considerable literature on the subject of swelling and shrinkage stresses in wood products and their measurement.

In one of the studies, buckling due to the linear expansion of hardboard siding was investigated by McNatt[52]. In this study, 16-inch long and 3-inch wide hardboard siding samples were conditioned at a relative humidity of 30 % before they were exposed to 90 % relative humidity, restrained in a rigid frame. Over a 4 week period of time, readings of center

deflection were taken to the nearest 0.001 inch by using a dial gage on the samples. It was found that buckling deflection reached a maximum by the end of the 4 week exposure period. Residual buckling was also determined as specimens were removed from the frame. Furthermore, free hardboard samples were included in the conditioning chamber to determine free linear expansion between 30 % and 90 % relative humidity levels. Another important result of the study was that buckling of restrained samples correlated well with linear expansion characteristic of boards as they were exposed from 30 % to 90 % relative humidity.

Suchsland [76] investigated swelling stresses and deformations in hardboard. In this study, 0.25-inch thick, 1.0 inch by 20 inch hardboard strips were conditioned at 20 % and 80 % relative humidity at 100° F before they were placed into a metal frame which had a load cell connected to a strain indicator at its end. Samples were exposed to relative humidity cycles changing between 20 % and 80 % to determine axial shrinkage and swelling stresses as well as deformations due to hygroscopic expansion and contraction. Figure 2.5 shows the axial stresses and midpoint deflections of the hardboard strips as a function of moisture content. Specimens were mounted dry (4% moisture content) and exposed to two cycles of high relative humidity as indicated by numbers on the graph. Compressive stresses developed very rapidly and then

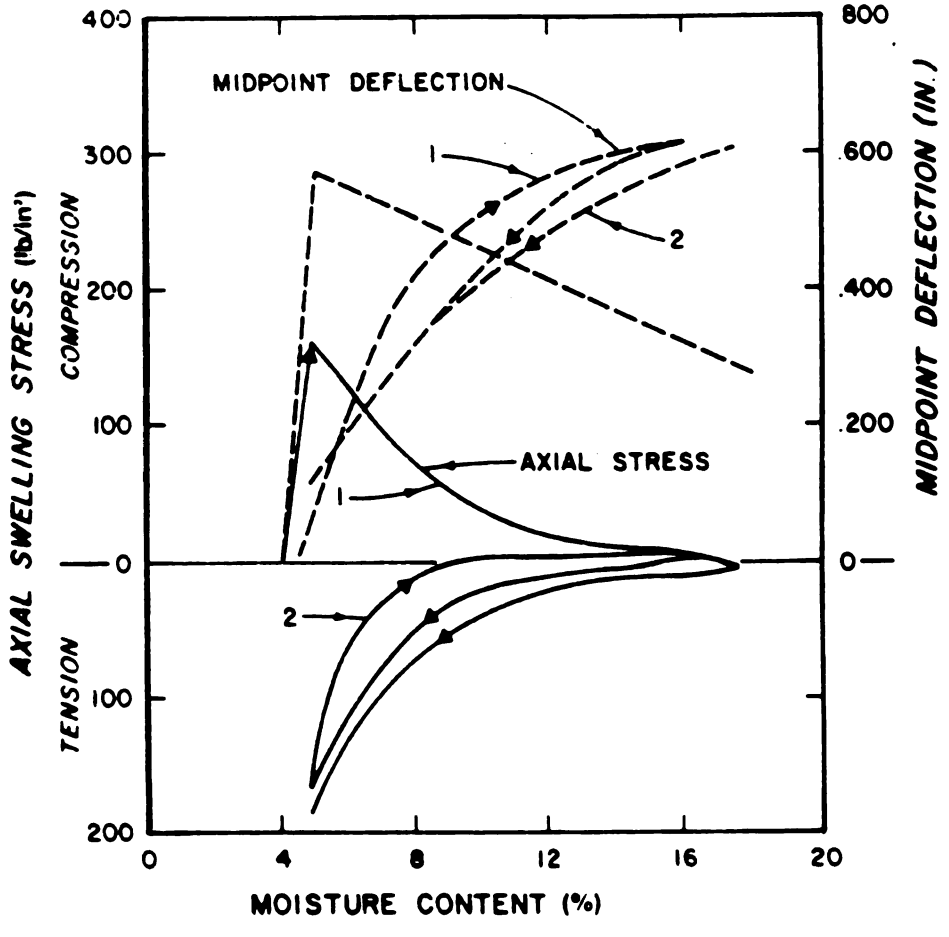

Figure 2.5. Axial stresses and midpoint deflections of restrained hardboard strips as function of moisture content. Numbers refer to cycle sequence [76].

completely relaxed. The tensile stresses developed approximately the same magnitude as the initial compressive stresses. The maximum lateral deflection value for the 20 inch span sample was 0.060 inch [76].

Figure 2.6 also depicts the axial stress and midpoint deflections of an identical sample. However, this sample was mounted at 14.5 % moisture content in this cycle. Later it was exposed to 20 % relative humidity. Maximum axial tension stress was found to be about 350 psi.

Furthermore, theoretical bending stresses were also calculated under the assumption of elasticity. Figure 2.7 depicts theoretical bending stresses of 0.25 inch thick hardboard strips. It was found that the elastic approach cannot be used to correctly predict development of swelling and shrinkage stresses of hardboard. It was also concluded that actual swelling stresses were distributed over the cross section of the sample and maximum bending stresses were affected by the moisture content gradient [76]. In the same study, it was stated that wood composite panels could be subjected to two different types of stresses if they were used as construction materials. One of these stresses is due to the structural loading, while the other one is the consequence of relative humidity changes.

Spalt and Sutton [69] determined buckling of thin surfacing materials due to restrained hygroexpansion within the

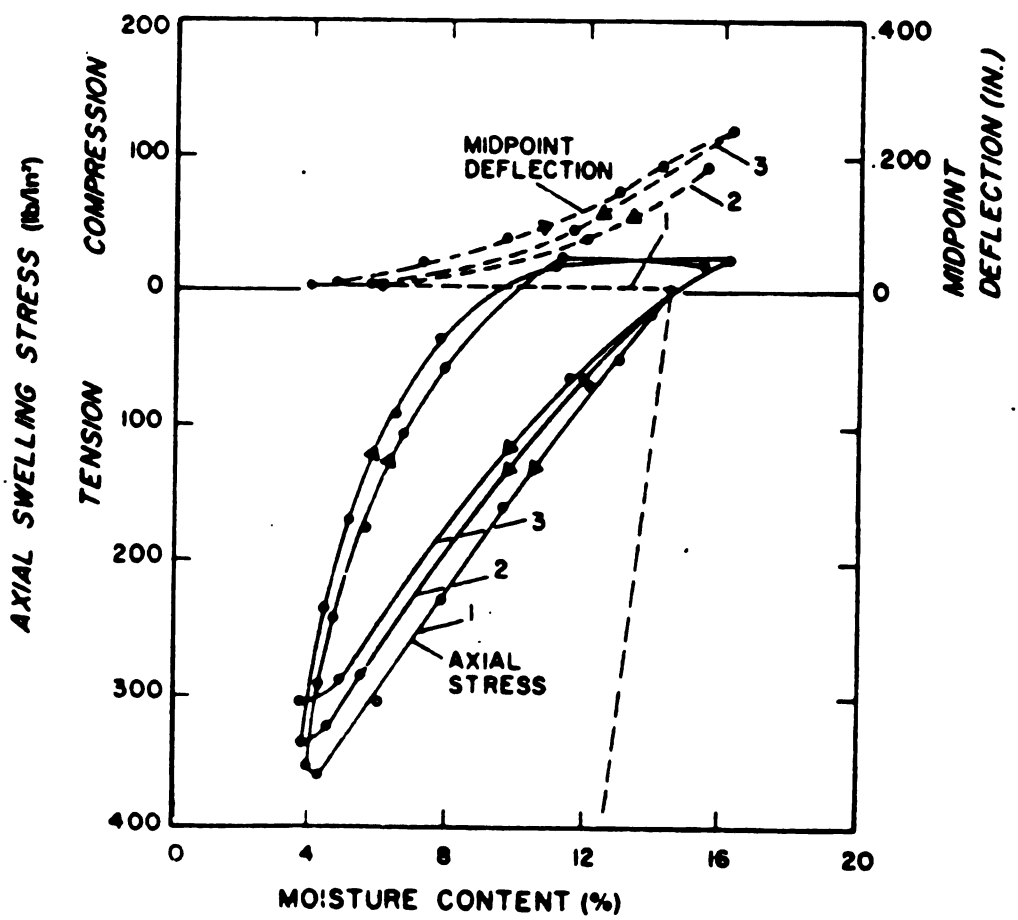

Figure 2.6. Axial stresses and midpoint deflections of restrained hardboard strips as function of moisture content. Number refer) to cycle sequence. (Tension) [76].

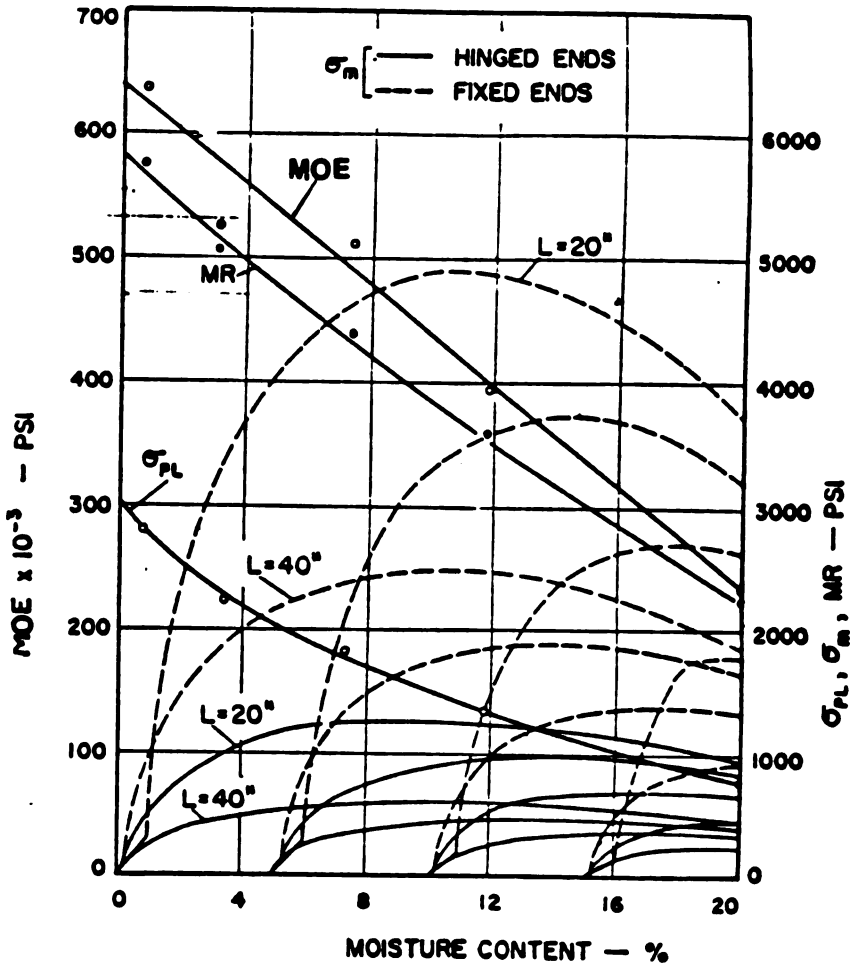

Figure 2.7. Theoretical bending stresses of hardboard strips due to buckling caused by restrained swelling [76].

perspective of column mechanics. The test specimen were subjected to increasing relative humidity while they were rigidly restrained in a metal frame.

The method of theoretical buckling calculation due to changing relative humidity which was described in section 2.2.1 was also employed by Spalt and Sutton. The findings obtained by restrained hygroexpansion are shown in Figure 2.8. In this figure, the curves are theoretical results of buckling as a function of restrained expansion while the plotted points are experimental observations. As can be seen from Figure 2.8 a good agreement was observed between calculated and experimental buckling values. It was found that the magnitude of buckling could be correlated to the moisture content changes and hygroexpansion properties of the material [69].

Swelling stresses of wood under complete uniaxial restraint are described by Perkinty [57]. As indicated in Figure 2.9 after maximum swelling stress has been reached, a certain amount of reduction in stress will occur.

Buckling of plywood, waferboard and particleboard under laboratory conditions was investigated by O'Halloran [55]. In this study, 6-inch by 48-inch strips of differant wood composites and full scale samples under restrained conditions were continuously wetted and dried by using intermittent sprinklers for two weeks. Results from laboratory and full

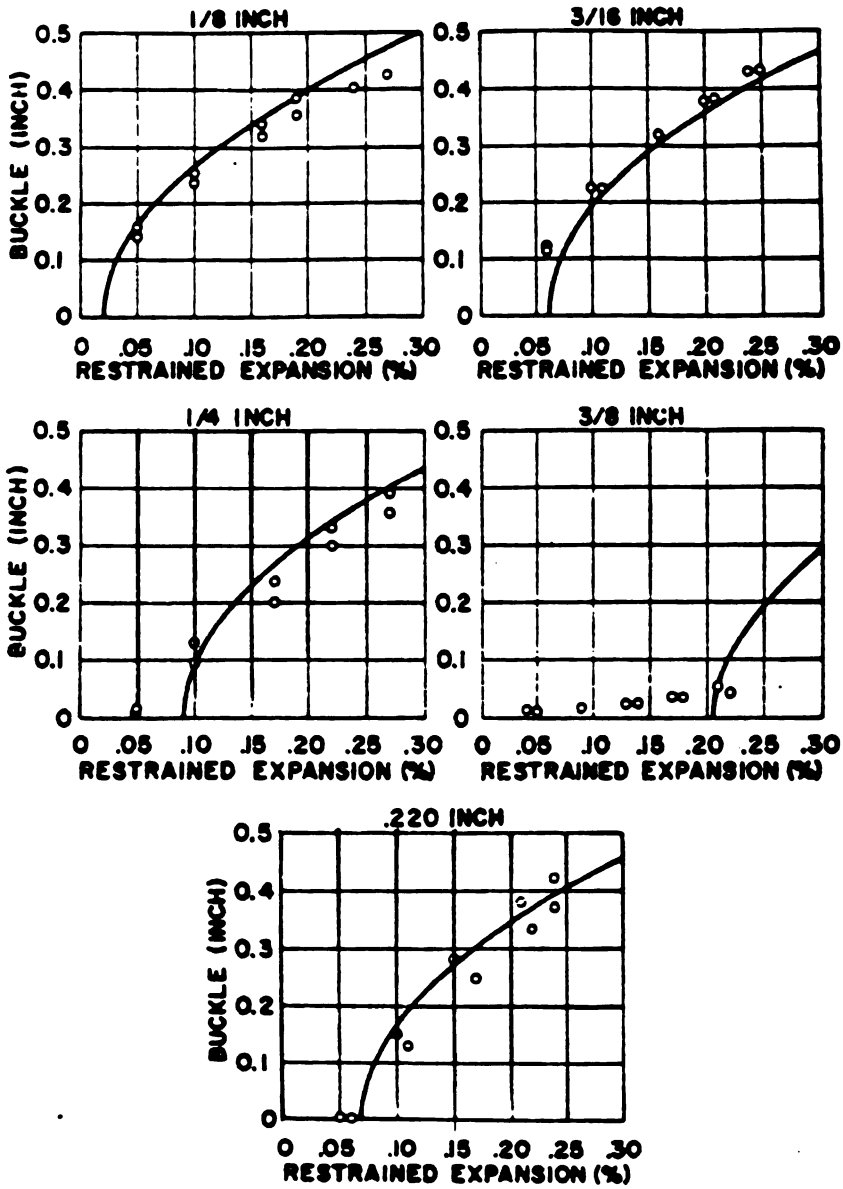

Figure 2.8. Relationship between buckling deflections and restrained expansion of hardboard [69].

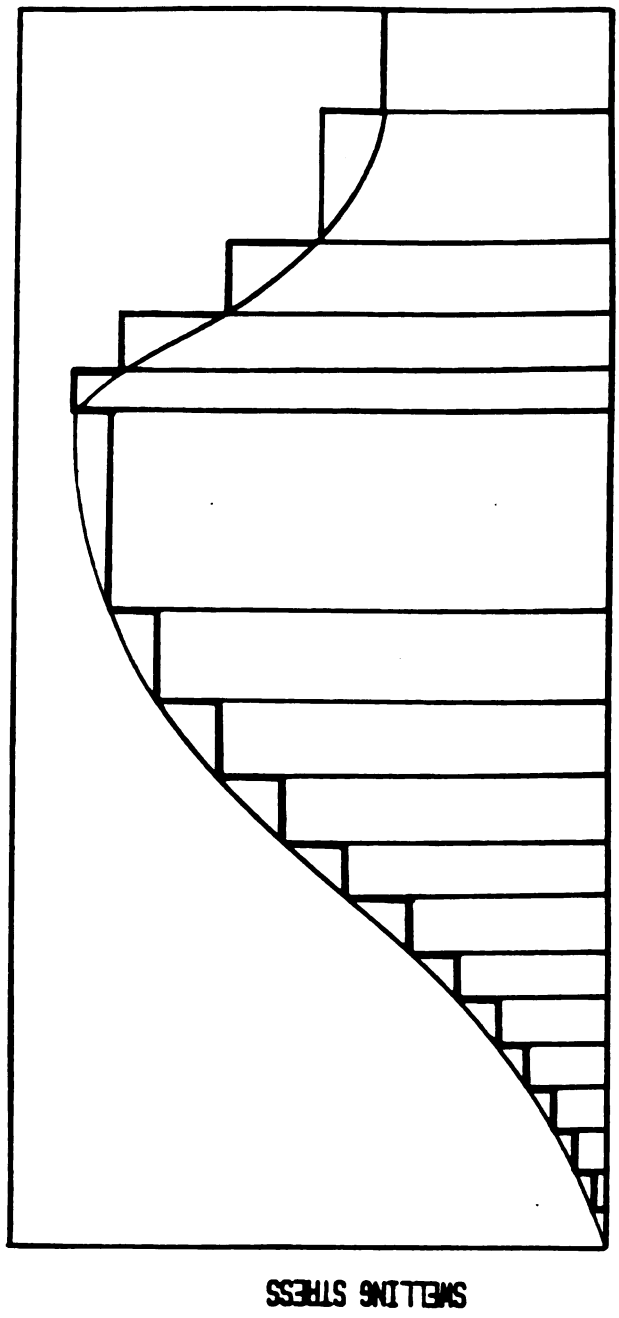

Figure 2.9. Swelling stresses under restrained conditions [39].

scale tests were used for the determination of a stability index. Since the 6-inch by 48-inch strip method correlated adequately with full scale testing, this method was recommended to determine buckling behaviour of wood composites in laboratory conditions [55]. In the following, the stability index approach used in O'Halloran study is described.

If a strip of wood composite with a length of L is considered, Δ L will be the expansion as its moisture content is increased. The equivalent mechanical effort to move the strip the distance Δ L may be calculated by using Hook's law. The resulting equation is [55] :

$$\Delta L = \frac{P L}{E A} \qquad (2.16)$$

where, Δ L : Differential expansion of the material (inch)

P : Load required to cause a movement equal to L (inch)

E : Modulus of elasticty (psi)

L : Column length (inch)

A : Column cross section ($inch^2$)

Equation (2.16) results from simple elastic assumptions. Linear expansion of panel materials over a range of moisture content can be measured. Assuming the critical expansion which is

sufficient to cause buckling can be approximated and Eq.(2.16) can be written as :

$$\Delta L = \alpha \, (\Delta MC) \, L \qquad (2.17)$$

Substitution of Eq.(2.17) into Eq. (2.16) and solving for the absolute value of the load P, the following results :

$$P = \alpha \, (\Delta MC) \, E \, A \qquad (2.18)$$

where $\alpha \, \Delta MC$ is the linear expansion (inch /inch), and P is the load that may cause buckling in the column. Therefore, this load can be considered to be equal to the critical load in Eq. (2.10A), (hinged ends)

$$P_{cr} = \frac{\pi^2 E I}{L^2} \qquad (2.19A)$$

By rearranging terms, the following expression can be obtained,

$$E A = \frac{\pi^2 E I}{(\alpha \Delta MC) L^2} \qquad (2.19B)$$

E A is called the stability index [55]. The larger E A the

more resistant is the material to buckling. As mentioned previously buckling due to hygroscopic expansion is related to material properties and geometry of the application as described by Euler for slender columns [55]. The right side of Eq. (2.19B) contains both material properties and the geometrical dimensions of a slender column. Therefore, it can be employed as a stability index which predicts the possibility of composite panel buckling. The stability index is based on the elasticity assumption, and it provides means to estimate the buckling behaviour of a wood composite product by using experimentally determined physical and mechanical properties [55]. Figure 2.10 illustrates the data from laboratory scale test results of O'Halloran's study[55].

Several different methods have been developed for measuring stresses in wood due to the change of relative humidity [24,38,54,70,73,76]. The procedures employ an external force sensing device which measures the developed stress in the sample. Particularly, two methods have been used extensively to determine uniaxial stresses in wood [38]. In one of these methods, the sample is connected directly to the plate of a dynomometer to acquire the force exerted on the specimen which is exposed to different humidities. Although this method is simple and practical, total stress and strain include the deformations occuring in the dynomometer as well. Therefore, this method cannot be considered as a precision measurement

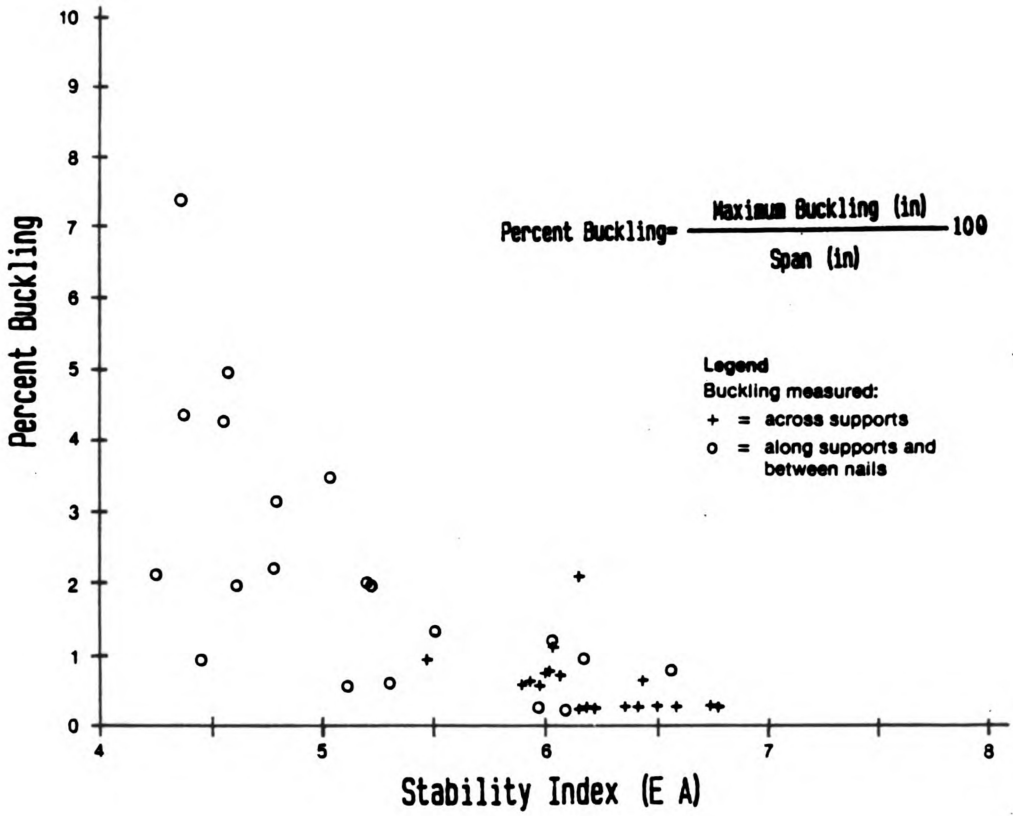

Figure 2.10. Stability index of plywood from full-scale tests [55].

technique. The other method, however, employs the specimen to be placed between two rigid plates which are connected to the dynomometer. This system is also equipped with a gage which determine the distance between two plates with an accuracy of 0.005 mm [38].

Based on the results of the previous works, sorption stresses in wood are found to be a function of the degree of restraint, magnitude of the change in relative humidity, temperature and the time required for a complete sorption process [35]. In addition to above mentioned environmental factors, the mechanical properties such as the modulus of elasticty (MOE), the potential shrinkage, the geometry of cross section, and the type of wood composite influence the stress development extensively [35].

Therefore, the accurate knowledge of the material properties is essential to better understanding the swelling stress development in the wood composites. However, the dynamic change in MOE with fluctuating relative humidity causes considerable complications in precise prediction of the stress development in wood composites [38]. Moreover, raw material characteristics such as particle size and its geometry, wood species as well as manufacturing variables play important roles on the development of restrained stresses in wood composites.

2.3. Development of Theoretical Swelling ,Shrinkage and Bending Stresses and Deformations due to Hygroscopicity.

2.3.1. Theoretical Swelling and Shrinkage Stresses without Buckling.

Elastic swelling and shrinkage stresses without buckling are derived as follows :

$$\epsilon = \frac{L_1 - L_2}{L_1} = \frac{\Delta L}{L_2} = \alpha \quad \Delta MC \qquad (2.20)$$

where, ϵ is elastic strain, L_1 and L_2 are initial and final lengths of the material in inches, respectively. α is the expansion coefficient (inch/inch/%) and Δ MC is the moisture content change in percent.

Since,

$$\sigma = E \epsilon \qquad (2.21)$$

$$\sigma = \alpha \ (\Delta MC) \ E \qquad (2.22)$$

where, σ is the axial swelling stress in psi, α is the linear expansion coefficient in inch/inch/% and finally, Δ MC is the percentage moisture content change.

2.3.2 Theoretical Bending Deformations.

In the following, theoretical bending deflection of wood

composites will be derived under the assumption of elasticity. For that purpose deflection values will be calculated as a function of moisture content in analogy to the analysis of thermal stresses described by Gatewood [18].

Deflection configuration of a buckled column can be approximated by one half of a sine wave. Consequently, the change in column length can be given as follows :

$$\Delta L = \int_0^L \left\{ \left[1 + \left(\frac{dw}{dx} \right)^2 \right]^{1/2} - 1 \right\} dx \qquad (2.23)$$

where L is the original length of the column in inch and

$$w = w_m \sin \left(\frac{\pi x}{L} \right) \qquad (2.24)$$

w_m being the maximum deflection in inch. Eq. (2.23) can be rewritten approximately as,

$$\Delta L = \frac{1}{2} \int_0^L \left(\frac{dw}{dx} \right)^2 dx = \frac{\pi^2 w_m^2}{4 L^2} \qquad (2.25)$$

If the initial deflection of the column (w_i) is approximated by

$$w_i = w_{mi} \sin \frac{\pi x}{L} \tag{2.26}$$

then the maximum deflection of the material w_m can be expressed as,

$$w_m = \frac{w_{mi}}{1 - \frac{P}{P_{cr}}} \tag{2.27}$$

where Pcr and P are critical load and applied load in lb, respectively.

Since the column is exposed to moisture content change, the load in Eq. (2.27) is determined by strain. Therefore, Eq. (2.27) leads to

$$w_m = \frac{w_{mi}}{1 - \frac{\epsilon_o}{\epsilon_{cr}}} \tag{2.28}$$

where ϵ_o is the strain in the middle plane of the wood composite while ϵ_{cr} is the critical strain. In anology to the theory of thermal stresses [18] , the following two equations can be written,

$$\epsilon_o = (\alpha \ \Delta M)_o$$
$$\epsilon_{cr} = (\alpha \ \Delta M)_{cr} \qquad (2.29)$$

As Figure 2.3 illustrates a column might have different end conditions, such as hinged, fixed or one end fixed. If a strip with hinged ends is exposed to moisture content change, by using Eq.(2.25), the following expression can be written :

$$\alpha \ \Delta M = (\alpha \ \Delta M)_o + \frac{\Delta L}{L} = \epsilon_o + \left(\frac{\pi w_m}{2L}\right)^2 - \left(\frac{\pi w_i}{2L}\right)^2 \qquad (2.30)$$

where ΔL is the change in column length in inch. If both sides of Eq. (2.30) are divided by the critical strain,

$$\epsilon_{cr} = \frac{\sigma_{cr}}{E} = \frac{\pi^2 I}{A L^2} = \frac{\pi^2 \rho^2}{L^2} \qquad (2.31)$$

where σ_{cr} is the critical stress in psi, A is the cross section of the column in inch^2 and finally, ρ is the radius of gyration in inch^4. One obtains,

$$K_{\Delta m} = \frac{\alpha \ \Delta M}{(\alpha \ \Delta M)_{cr}} = \frac{\epsilon_o}{\epsilon_{cr}} + \frac{w_m^2}{4\rho^2} - \frac{w_{mi}^2}{4\rho^2} \qquad (2.32)$$

There is no initial deflection then the deflection is zero up to $\epsilon_o = \epsilon_{cr}$. For $\alpha \Delta MC \geq (\alpha \Delta MC)_{cr}$, $K_{\Delta m}$ can be rewritten as follows,

$$K_{\Delta m} = 1 + \frac{w_m^2}{4\rho^2} \tag{2.33}$$

From the above equation, the maximum deflection, $(w_m)_h$ for a column with hinged ends will be :

$$(w_m)_h = 2\rho \sqrt{\frac{\alpha \Delta MC L^2 A}{\pi^2 I} - 1} \tag{2.34A}$$

$$(w_m)_h = 2\rho \sqrt{K_{\Delta m} - 1} \tag{2.34B}$$

where $(w_m)_h$ is the center deflection of column with hinged ends. Furthermore, as Figure 2.4 depicts, deflection of a column with fixed ends is as twice the deflection of a hinged end column of half length [11,76,81].

$$(w_m)_f = 4\rho \sqrt{\frac{\alpha \Delta MC L^2}{4 \pi^2 I} - 1} \tag{2.24C}$$

where $(w_m)_f$ is center deflection of column with fixed ends.

2.3.3. Theoretical Bending Stresses with Buckling

Under the assumption of elasticity, the theoretical deflection calculated in section 2.3.2 causes bending stresses in combination with the axial stresses. The following two equations can be written [65,76],

$$\epsilon_m = \epsilon_o + \frac{A\ \epsilon_o\ w_m\ c}{I} \qquad (2.35)$$

$$\sigma_m = \epsilon_o\ E + \frac{\epsilon_o\ E\ A\ w_m\ c}{I} \qquad (2.36)$$

where, σ_m is the maximum stress in the composite panel, ϵ_o is the axial strain and finally c is the distance of the centroid axis from the center of the sample which can be expressed as $c = h/2$ in inch , where h is the thickness.

For $\epsilon_o = \epsilon_{cr}$

$$\sigma_m = \epsilon_{cr}\ E + \frac{\epsilon_{cr}\ E\ A\ w_m\ c}{I} \qquad (2.37)$$

If we substitute ϵ_{cr} and w_m from equations (2.31) and

(2.34B) in Eq. (2.37) [76,18].

$$\sigma_m = \epsilon_{cr} E \left(1 + \frac{6 w_m}{h} \right) \qquad (2.38)$$

Equation (2.38) can be employed to calculate maximum theoretical bending stresses in compression of restrained wood composites due to the change in moisture content.

Development of tension stresses of restrained wood composites are associated with shrinkage when relative humidity is decreased and can be calculated as simple axial stresses.

2.4. Hygroscopic Swelling and Shrinkage of Wood and Wood Composites

Dimensional changes (swelling and shrinkage) of solid wood are caused by the gain or loss of water molecules by/ from the wood cell wall. The wood cell is the microscopic element of solid wood. It is a hollow cyclider, the approximate dimensions and structure of which are schematicaly illustrated in Figures 2.11 and 2.12. Figure 2.12 shows the layered structure of the cell wall with different arrangements and orientations of the so-called macrofibrils which are the reinforcing elements embedded in an amorphous matrix. Macrofibrils are composed of even smaller elements, the microfibrils, which are either very

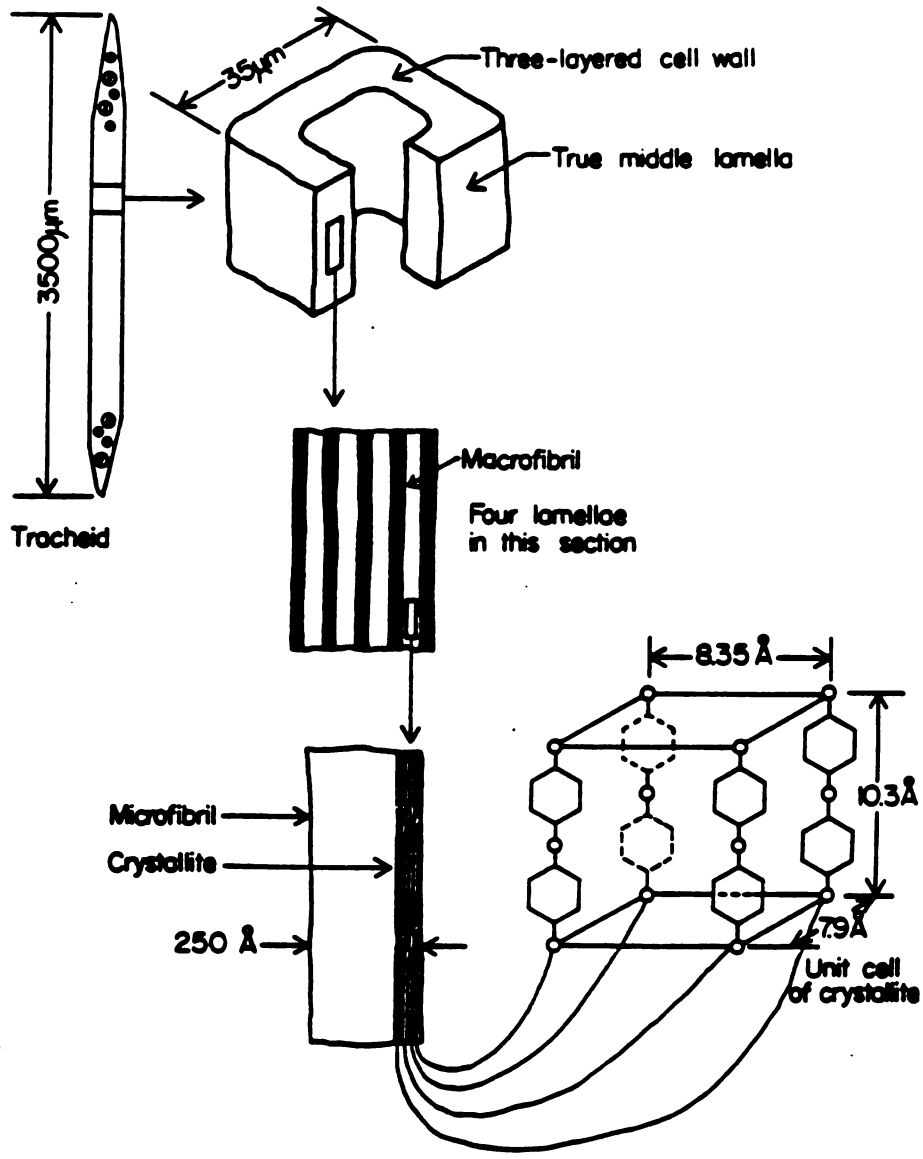

Figure 2.11. Relationships between the elements of cell wall [68].

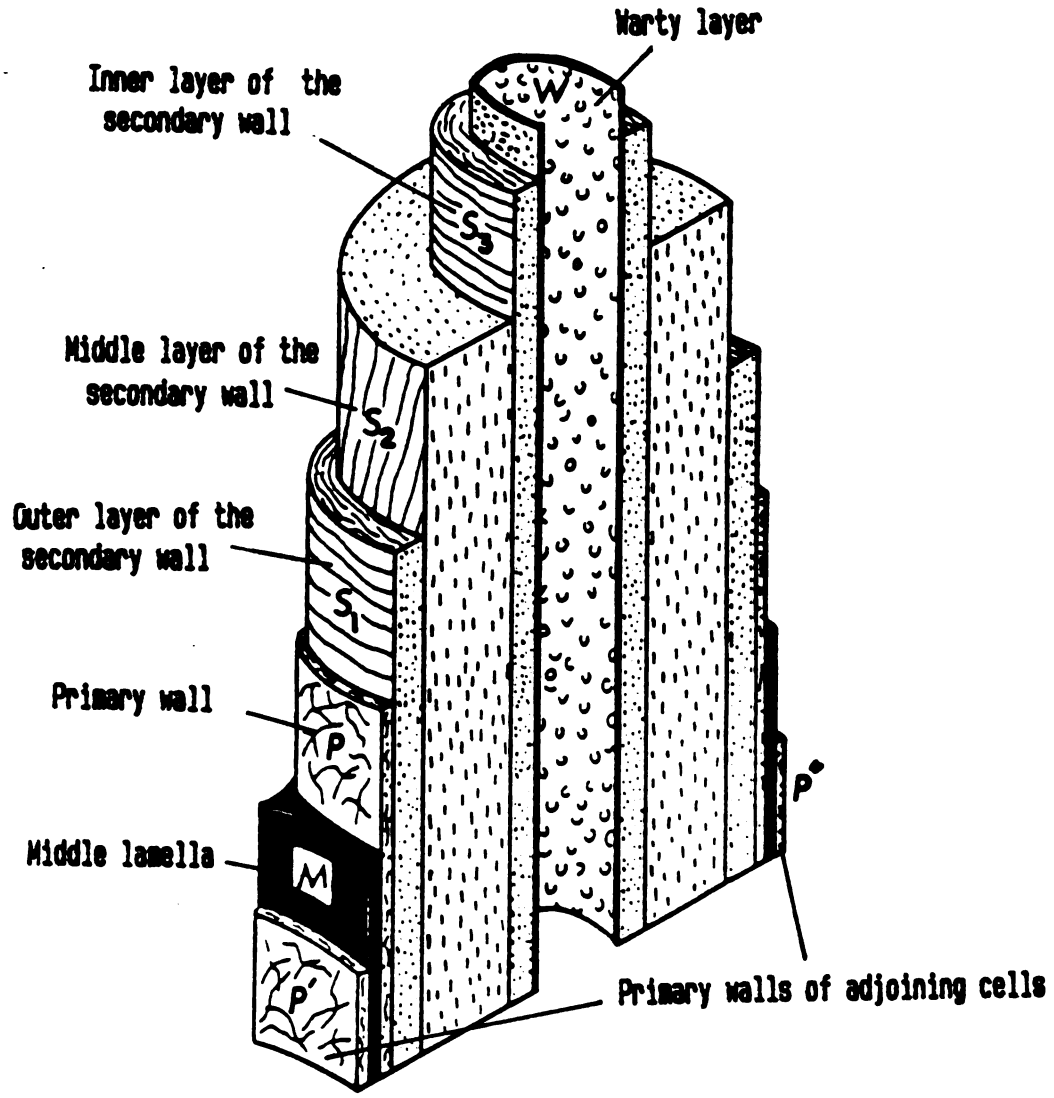

Figure 2.12. Structure of cell wall [68].

closely associated in crystalline regions or less close in amorphous regions. They consist of cellulose chains (Figure 2.11). When water is absorbed, water molecules will enter the amorphous region of the fibrils, forcing the cellulose chains apart. This causes the thickness of the cell wall to increase and the wood to swell, or shrink when the reverse takes place.

Due to the layered structure of the cell wall, the shape of the cells and their arrangement in the tree (substantially parallel to one another), the dimensional changes of solid wood upon moisture gain or loss are different in the three principles directions (longitudinal, radial and tangential) relative to the axis of the tree. Changes are largest in the tangential direction (about 5 to 12 % maximal), somewhat smaller in the radial direction (about 3 to 7 %) and very small in the longitudinal direction (0.2 %). These changes would correspond to a relative humidity interval from 0 % (absolute dry) to 100 % which is a condition at which water begins to condense in the hollow interior of the cell. This so-called free water, however, does not contribute to dimensional changes nor to changes in any other property which is affected by varying moisture content. The point at which condensation begins is called the fiber saturation point, because the cell walls are saturated. It corresponds to a moisture content (MC) of about 30 % for most species [41,85].

The moisture content is defined as

$$MC = \frac{\text{weight of absorbed water}}{\text{weight of dry wood}} \quad 100 \ (\%)$$

When solid wood is broken down to particles of various sizes and shapes as in the manufacture of wood composite boards, and then recombined into sheet form, the arrangement of the cells is, of course, very different from what it was in the tree. In addition, the material is laminated, heated in layers and press, the particles are laminated in varying configurations etc. All these factors result in a modification of the behaviour of the composite as compared with the solid wood. This transformation has been the subject of considerable interest and scientific activity.

The amount of water absorbed during a particular relative humidity interval is governed by the so-called sorption isotherm, which illustrates the relationships between relative humidity of the air and moisture content of wood. Figure 2.13 shows such isotherms for both solid wood and two types of wood composites, particleboard and hardboard. The wood isotherm is valid for most species. Relative to it the isotherms for particleboard and hardboard are lower indicating a smaller moisture content change for any given relative humidity change. This is one of the consequences of transformation of solid wood

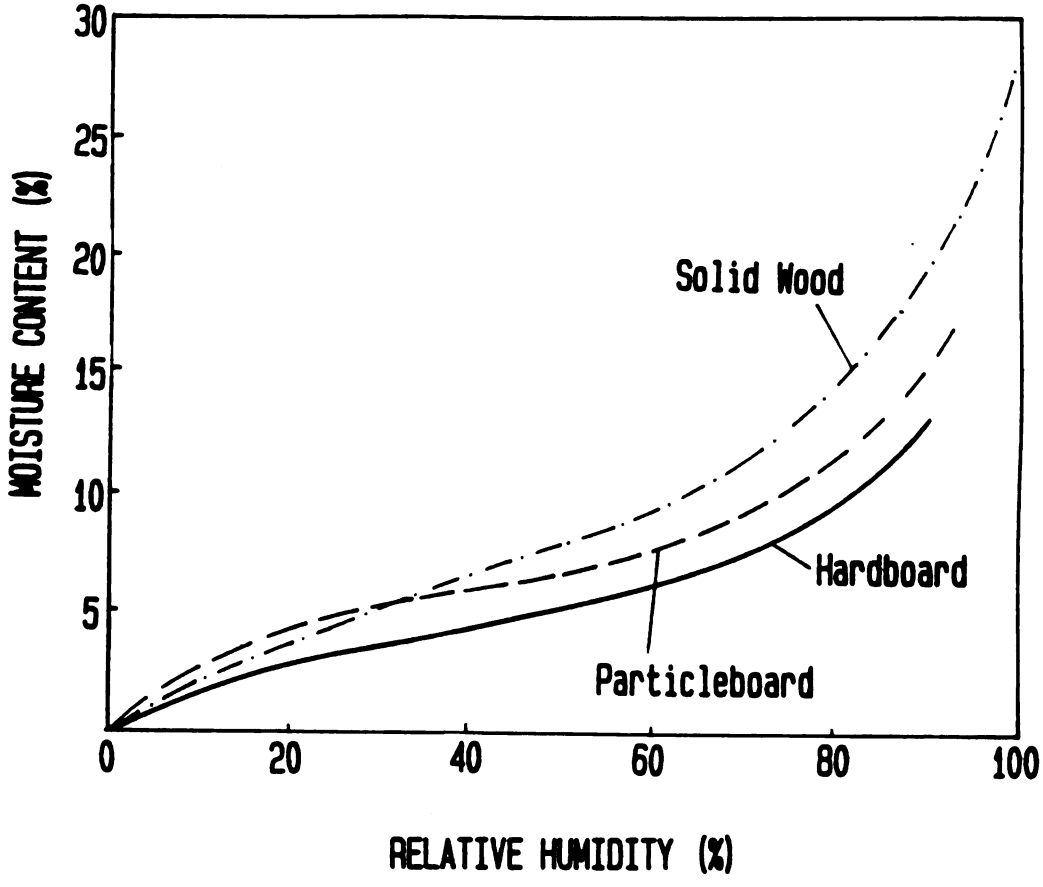

Figure 2.13. Adsorption curves of solid wood, hardboard and particleboard [40].

properties occuring in the board process.

The actual swelling and shrinkage of such composites in response to moisture content changes is affected by quite a number of factors such as particle geometry, orientation of particles, resin content and many others.

In studying the dimensional stability of such materials one distinguishes between changes in thickness (thickness swelling) and changes in the plane of the board (linear expansion). Some factors affect both of them, others either one or the other.

In our study we are mainly concerned with the latter, the linear expansion. It is much smaller than thickness swelling but it is of practical importance because of the large dimensions of the boards. The total linear expansion can be viewed as the product of the expansion coefficient, α, and the moisture content change, Δ MC.

$$\text{Linear Expansion} = \alpha \quad \Delta \text{ MC}$$

There are considerable numbers of investigations on the subject of linear expansion characteristics of wood composites [8,61,75,78,79,82,83,84]. Results of some of these studies were presented in the previous part of section 2.5. In addition to that, Figure 2.14 and Tables 2.1, 2.2 and 2.3 represent a comparison of linear expansion properties of various types of

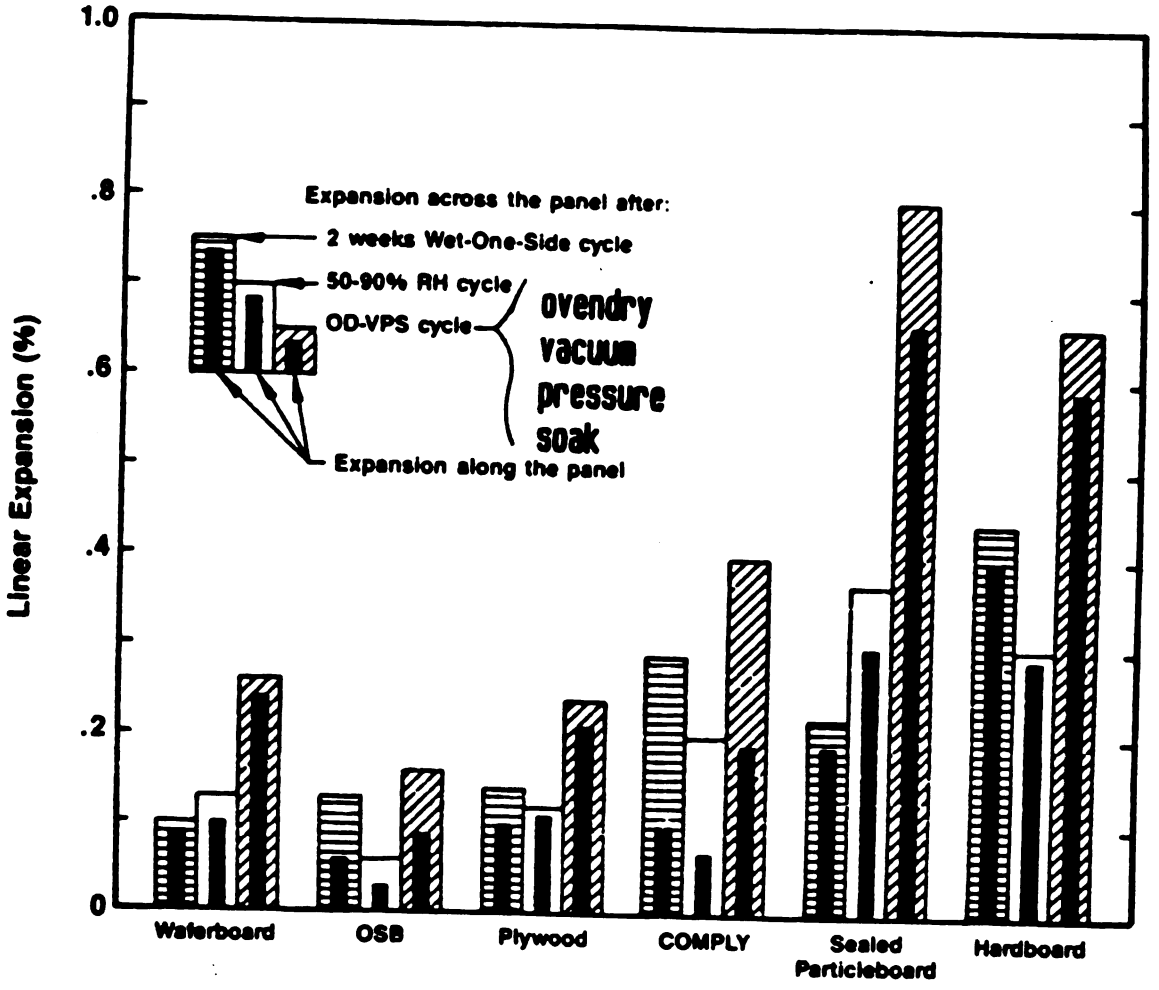

Figure 2.14. Linear expansion values of various wood composites under different conditions [87].

Type of flakeboard	Property					
	Density[2]	Water absorption	Thickness swell	Linear expansion	Modulus of rupture	Modulus of elasticity
	Pcf	---------- *Percent* ----------			*Psi*	*1,000 psi*
Waferboard	38–45	10–30	10–16	0.08–0.15	2,000–3,500	450–650
Oriented strand board						
Parallel to alignment	38–50	10–30	10–20	.05–.10	4,000–7,000	750–1,300
Perpendicular to alignment	—	—	—	.12–.30	1,500–3,500	300–500

Table 2.1. Physical and mechanical properties of flake-type wood composites [87].

Type of particleboard	Property										
					Tensile strength		Shear strength				
	Density	Specific gravity	Modulus of elasticity (bending)	Modulus of rupture	Parallel	Perpendicular	In board plane	Across board plane	24-hour water adsorption	Thickness swelling, 24-hour soaking	Linear expansion[2]
	Pcf		*1,000 psi*	*Psi*	*- - - - Psi - - - -*		*- - - Psi - - -*		*Pct by wt*	*Pct*	*Pct*
Low density	[4]25 – 37	[4]0.40 – 0.59	[5]150 – 250	[5]800 – 1,400	—	[5]20 – 30	—	—	—	—	[6]0.30
Medium density	37 – 50	.59 – .80	250 – 700	1,600 – 3,000	500 – 2,000	30 – 200	100 – 450	200 – 1,000	10 – 50	5 – 50	.2 – .6
High density	50 – 70	.80 – 1.12	350 – 1,000	2,400 – 7,500	1,000 – 5,000	125 – 450	200 – 800	—	15 – 40	15 – 40	.2 – .85

Table 2.2. Physical and mechanical properties of various types of particleboard [85].

Properties	Values
Linear hygroscopic expansion (30–90 pct RH)	<.020 pct
Linear thermal expansion	0.0000034 in/in/°F
Flexure (psi):	
Modulus of rupture	7,000–10,000
Modulus of elasticity	1,200,000–1,500,000
Tensile strength (psi)	4,000–5,000
Compressive strength (psi)	4,500–6,000
Shear through the thickness (edgewise shear) (psi):	
Shear strength	800–1,000

Table 2.3. Physical and mechanical properties of three-ply plywood [85].

wood composites. As can be seen from the above tables particleboard exhibits considerably higher linear expansion values than those of two flake types of structural wood composites due to the smaller particle size.

Sorption and linear expansion characteristics of commercially produced particleboard were investigated by Suchsland [75]. Specimens 0.75 inch by 0.75 inch by board thickness and 12 inch by 1.5 inch were used for the sorption hysteresis and linear expansion tests, respectively. Samples were conditioned in six different environments provided by six different salt solutios. It was found that commercially manufactured particleboards showed a relatively wide range of linear expansion coefficients [75]. Particle geometry was also considered to be one of the most important factors which controls dimensional stability.

Post [59] indicated that linear stability is substantially affected by both flake thickness and flake length. In the same study, it was pointed out that any decrease in flake length reduces the linear stability of the particleboard.

Linear expansion properties of structural flakeboard was studied by Lehmann [45]. He noted that boards made from 2 inch long flakes were the most stable in terms of linear expansion. He also determined that decreased flake thickness and increased flake length along with increased resin content resulted in

lower linear expansion as determined by a soaking test.

Gatchel et al. [19] found increased linear expansion of Douglas fir particleboard at different relative humidities when flake thickness was increased to above 0.015 inch.

McNatt [51] reported that particleboard had higher expansion values than waferboard for relative humidity intervals between of 30 % and 90 % . Random distribution of overlapping flakes in waferboard provides mutual restraint of wafers and results in lower linear expansion. As is evident from the above discussion ,particle size and geometry have a very significant effect on swelling and shrinkage of wood composites.

2.5. Important Factors Affecting Development of Hygroscopic Stress and Deformations of Wood Composites

The previous discussion clearly established that two material characteristics determine the buckling behaviour of wood and wood composites. These are the linear expansion and the modulus of elasticity. Both of these properties are directional in solid wood and depend on the species or its specific gravity. In the case of wood composites these are also influenced by particle size, structure of composite, resin content, alignement of particles and others. Both, of course, are directly affected by the moisture content of the wood. In the following, the moisture content change of wood in response

to changing air condition and the effect of change in mechanical properties wood composites will be described.

2.5.1. Mechanical Properties of Wood Composites as Fuction of Moisture Content Change

The relationship between stress and strain of elastic materials is expressed by Hook's law [12,62,81]

$$\sigma = E\,\epsilon \qquad \text{or} \qquad E = \frac{\sigma}{\epsilon}$$

where σ and E are the stress in psi and modulus of elasticity in psi, respectively, and ϵ is the strain inch/inch. The modulus of elasticity is a measure of the stifness of a solid body. Because of the assumption of linear elastic behaviour the flexture formula cannot be used to calculate ultimate stress in a member. However, nominal failure stress for a material is called modulus of rupture (MOR) [10,62].

Liiri [49] determined that bending and internal bond (tensile strength perpendicular board plane) strength of three-layer particleboard were reduced approximately 50% by increase in moisture content from 10 % to 20% .Reduction in MOR values of particleboard samples which were subjected to 10 cycles of 30 % and 95 % relative humidities was 25 % . Morover, it was also determined that the rate of strength loss increased as the

number of exposure cycles increased.

Hann et al. [32] reported that urea formaldehyde bonded flake type Douglas fir particleboard showed significant decrease in strength and increase in thickness swelling as a result of exposure to 80°F and 90 % relative humidity for 1 year. In the same investigation, three factors namely, springback, deterioration of adhesion and failure in wood due to the shrinkage and swelling stresses were considered as major causes of reduction in mechanical properties of particleboard.

Lehmann [45] pointed out that reduction in strength of particleboard due to the change in moisture content can be reduced by increasing the resin content during the manufacturing process of the product. Optimum resin content can be determined by the performance requirement of the composite material.

McNatt [51] investigated the influence of cyclic relative humidity conditions on static bending properties of particleboard and waferboard. Samples were kept at 30 % and 90 % relative humiditiy levels for an equal period of one week. Later the same relative humidity levels were used for two weeks for each exposure condition.

Lee and Biblis [44] pointed out when the relative humidity decreased from the initial 65 % to 30 %, MOE of particleboard produced from Southern yellow pine increased by 4 % . Board specimens 0.625-inch thick were subjected to one cycle of

65 % ,30 % ,65 %, 95 % relative humidity levels. As a result, it was determined that MOE decreased 70 % due to the increase in relative humidity from 30 % to 95 % .On the other hand, MOE and MOR values were reduced 20 % and 16 % for a single cycle, respectively.

Bryan and Schniewind [7] investigated the changes in deflection of loaded particleboard beams as relative humidity was being changed. Urea formaldehyde and phenol formaldehyde bonded particleboards having 0.65 g/cm^3 density were tested to determine the effect of moisture content on bending properties as well as creep characteristics. In this study, it was also determined that there was a direct effect of moisture content on both MOE and MOR of particleboard. It was also pointed out that the moisture content and sorption effect are more significant in particleboard than in solid wood.

Halligan et al [26] also reported that higher creep occurs in particleboard than in plywood and solid wood. The findings of this study were also supported by another study by Halligan [27]. One of the possible reasons for lower creep tendency of solid wood as compared to particleboard would be the stronger resistance of chemical bonds in the cell wall of solid wood. It was indicated that the creep tendencies of solid wood, particleboard and hardboard showed an approximate ratio of 1:4:5 [26]. Rheological properties of wood composites as affected by the sorption process are of major importance for

load bearing members [27].

Effect of relative humidity changes on creep properties of particleboard was studied by Halligan and Schniewind [27]. 12-inch by 12-inch specimens mounted in a creep test frame were centrally loaded by a lever system. Deflection of each sample was recorded on a continuos basis by using a dial micrometer for a maximum period of 4 weeks while the samples were subjected to a relative humidity of 97 % .

Creep behaviour of different wood based material were also investigated by Langendorf, Albin, Backmann and Habler [1,4,42,43]. Creep number and modulus of elasticity at creep test were recognized as two important factors for calculating the admissible spans for wood composite panels. As can be seen in Figure 2.15 the creep number (φ) can be defined as a ratio plastic strain to elastic strain.

$$\varphi = \frac{\epsilon_{pl}}{\epsilon_{el}} \qquad (2.39)$$

where ϵ_{pl} and ϵ_{el} are plastic strain and elastic strain in inch/inch, respectively. Based on Hook's law following equation can be written :

$$E_{el} = \frac{\sigma}{\epsilon_{el}} \qquad (2.40)$$

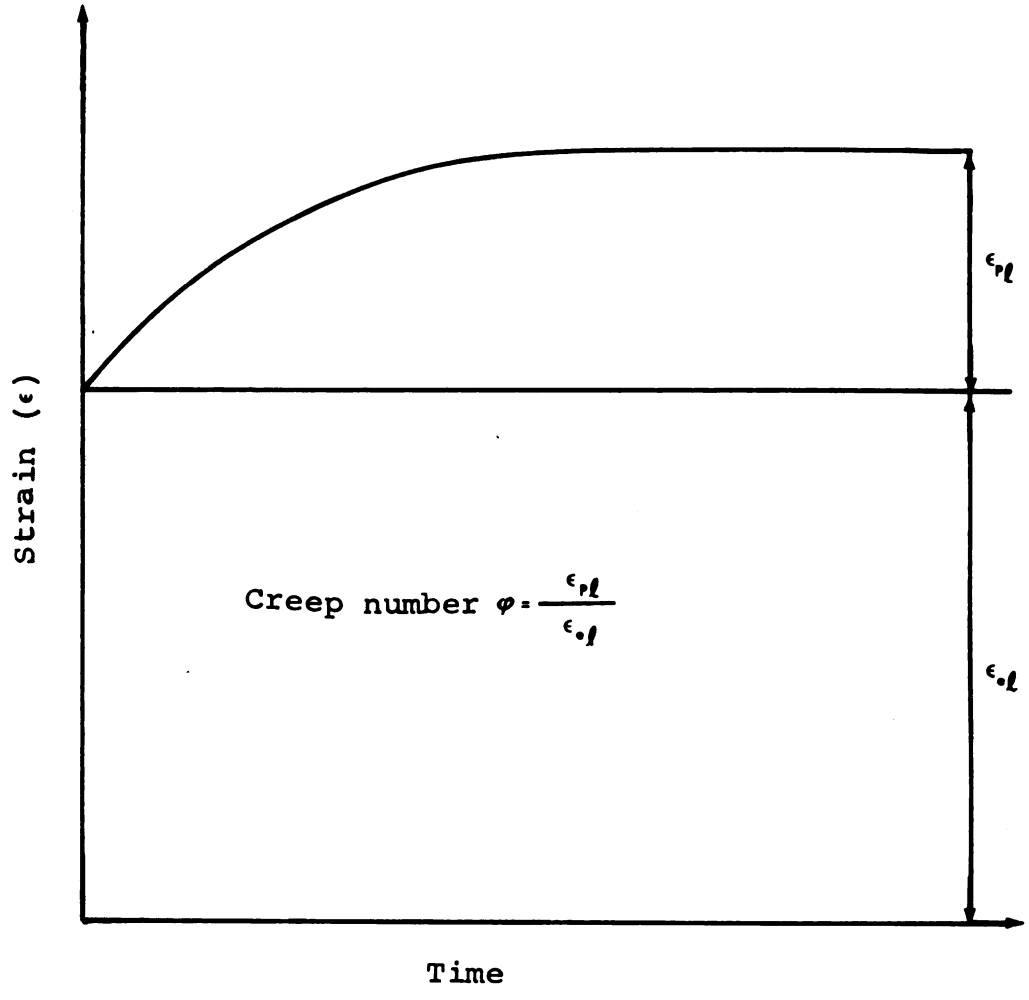

Figure 2.15. Representation of creep number [1].

At the end of a certain period of time , creep will cause reduction in the initial MOE of the wood composite which can be expressed in Eq. (2.41) and (2.42).

$$E_{red} = \frac{\sigma}{\epsilon_{el} + \epsilon_{pl}} \qquad (2.41)$$

$$E_{red} = \frac{\sigma}{\epsilon_{el} + \varphi(\epsilon_{el})} = \frac{\sigma}{\epsilon_{el}\ (1+\varphi)} = \frac{E_{el}}{1+\varphi} \qquad (2.42)$$

where, E_{el} and E_{red} are initial and reduced modulus of elasticity due to creep, respectively.

Albin [1] determined long-term MOE of different types of wood composites and found that particleboard and oriented strandboard exhibited 35 % and 12 % reduction in their initial MOE values as a result of 28 days of loading.

2.5.2. Effect of Thickness and Length of Column on Development of Buckling Deflections

Thickness and column length are two major variables which significantly influence the magnitude of lateral buckling deflection. Based on the theoretical calculations described in section 2.3.2 midpoint deflections of different wood composite columns with various lengths and thicknesses were determined

for fixed ends as a function of moisture content change. Figures 2.16 through 2.20 illustrate the relationships between midpoint deflections of three types of composite columns with different lengths and 0.25-inch, 0.375-inch, 0.437-inch, 0.5-inch and 0.75-inch thicknesses, respectively. As can be seen from the above figures, lateral buckling deflections increase with increasing column length and decrease with increasing thickness. Waferboard resulted in the lowest deflection value among the other panel products due to its low linear expansion. Figure 2.21 shows relationship between critical strain, column length and thickness. It must be noted that these computations are theoretical. However, this approximation could be combined with linear expansion of any wood composites to establish design components of product in structural use with the purpose of prediction of buckling behaviour due to hygroscopicity.

Figure 2.16. Midpoint deflections of restrained samples in different lengths as function of moisture content change. (Thickness is 0.25 inch)

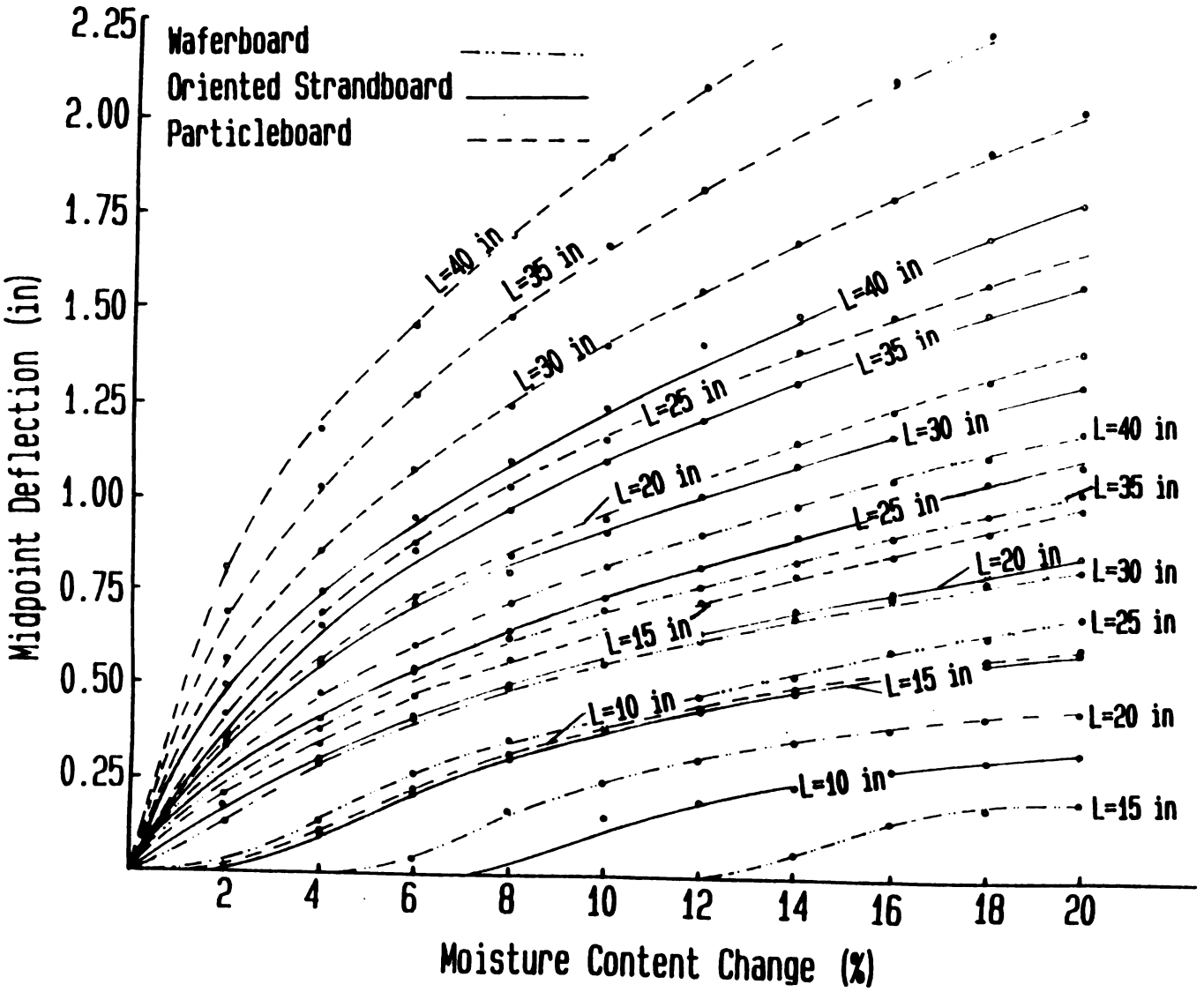
Waferboard
Oriented Strandboard
Particleboard
Midpoint Deflection (in)
2.25
2.00
1.75
1.50
1.25
1.00
0.75
0.50
0.25
L=40 in
L=35 in
L=30 in
L=25 in
L=20 in
L=15 in
L=10 in
2
4
6
8
10
12
14
16
18
20
Moisture Content Change (%)

Figure 2.17. Midpoint deflections of restrained samples in different lengths as function of moisture content change. (Thickness is 0.375 inch)

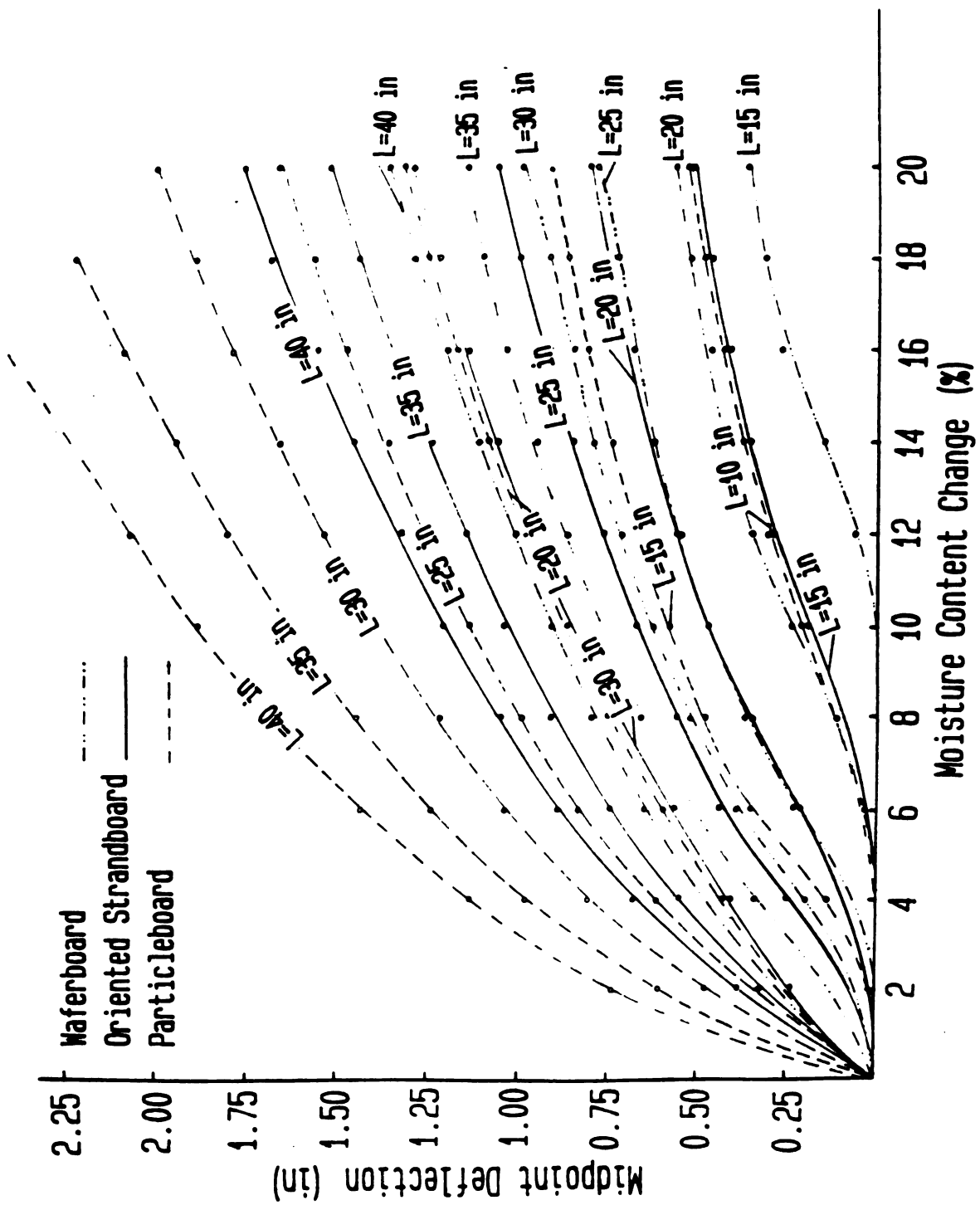
Waferboard
Oriented Strandboard
Particleboard
Midpoint Deflection (in)
Moisture Content Change (%)
2.25
2.00
1.75
1.50
1.25
1.00
0.75
0.50
0.25
2
4
6
8
10
12
14
16
18
20
L=40 in
L=35 in
L=30 in
L=25 in
L=20 in
L=15 in
L=10 in

Figure 2.18. Midpoint deflections of restrained samples in different lengths as function of moisture content change. (Thickness is 0.437 inch)

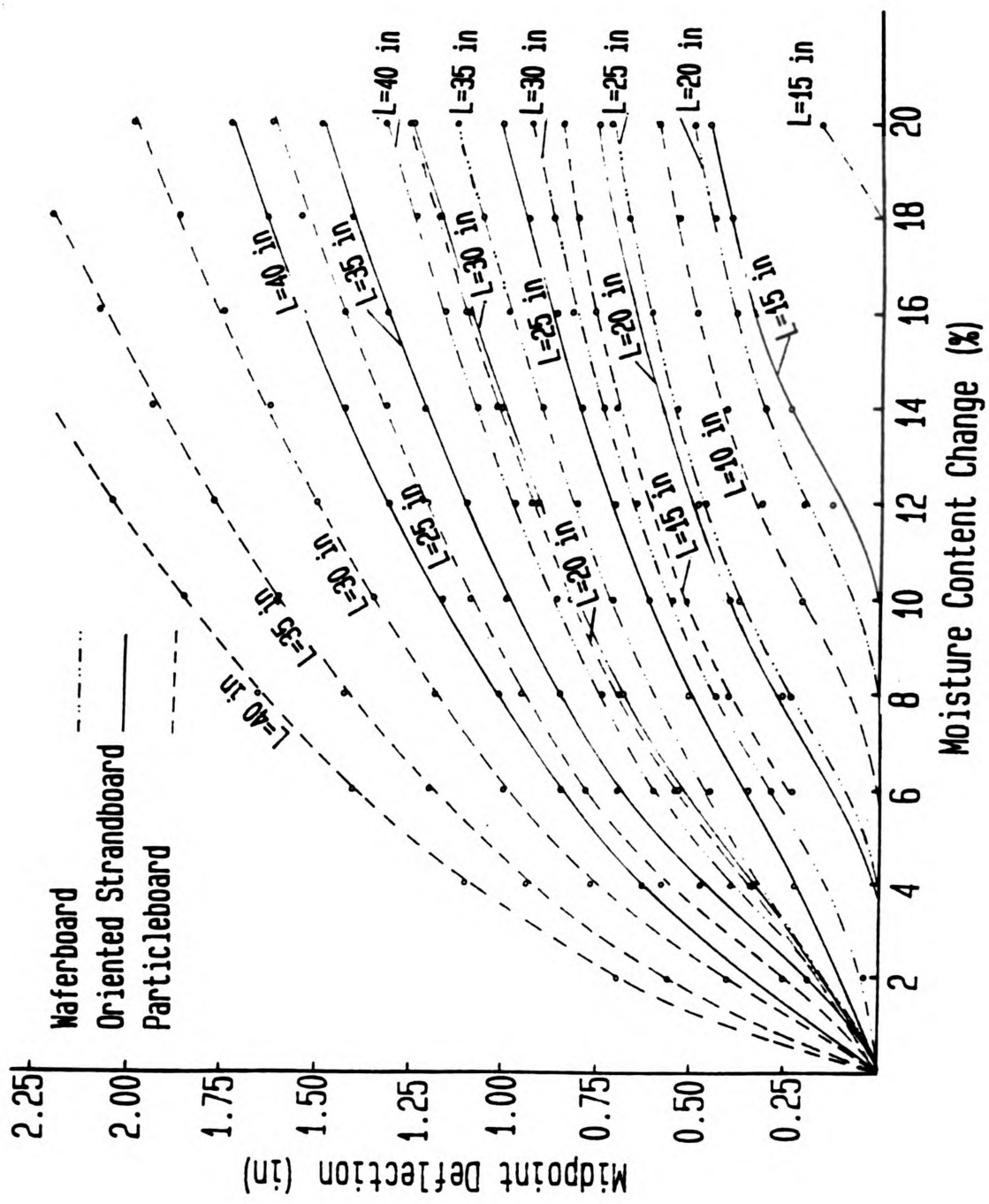
Waferboard
Oriented Strandboard
Particleboard
Midpoint Deflection (in)
Moisture Content Change (%)
2.25
2.00
1.75
1.50
1.25
1.00
0.75
0.50
0.25
2
4
6
8
10
12
14
16
18
20
L=40 in
L=35 in
L=30 in
L=25 in
L=20 in
L=15 in
L=10 in

Figure 2.19. Midpoint deflections of restrained samples in different lengths as function of moisture content change. (Thickness is 0.5 inch)

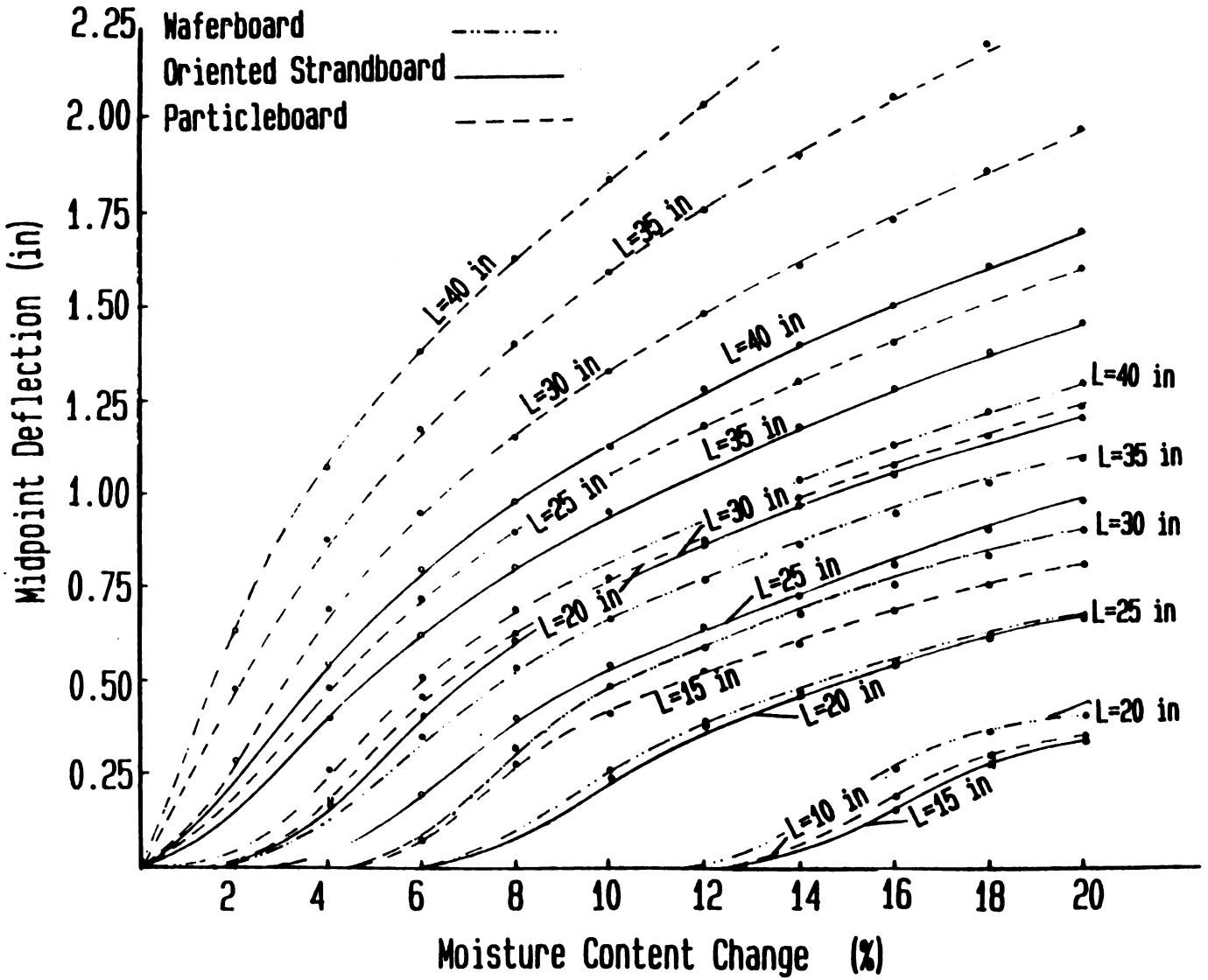
Waferboard
Oriented Strandboard
Particleboard
Midpoint Deflection (in)
2.25
2.00
1.75
1.50
1.25
1.00
0.75
0.50
0.25
L=40 in
L=35 in
L=30 in
L=25 in
L=20 in
L=15 in
L=10 in
2
4
6
8
10
12
14
16
18
20
Moisture Content Change (%)

Figure 2.20. Midpoint deflections of restrained samples in different lengths as function of moisture content change. (Thickness is 0.75 inch)

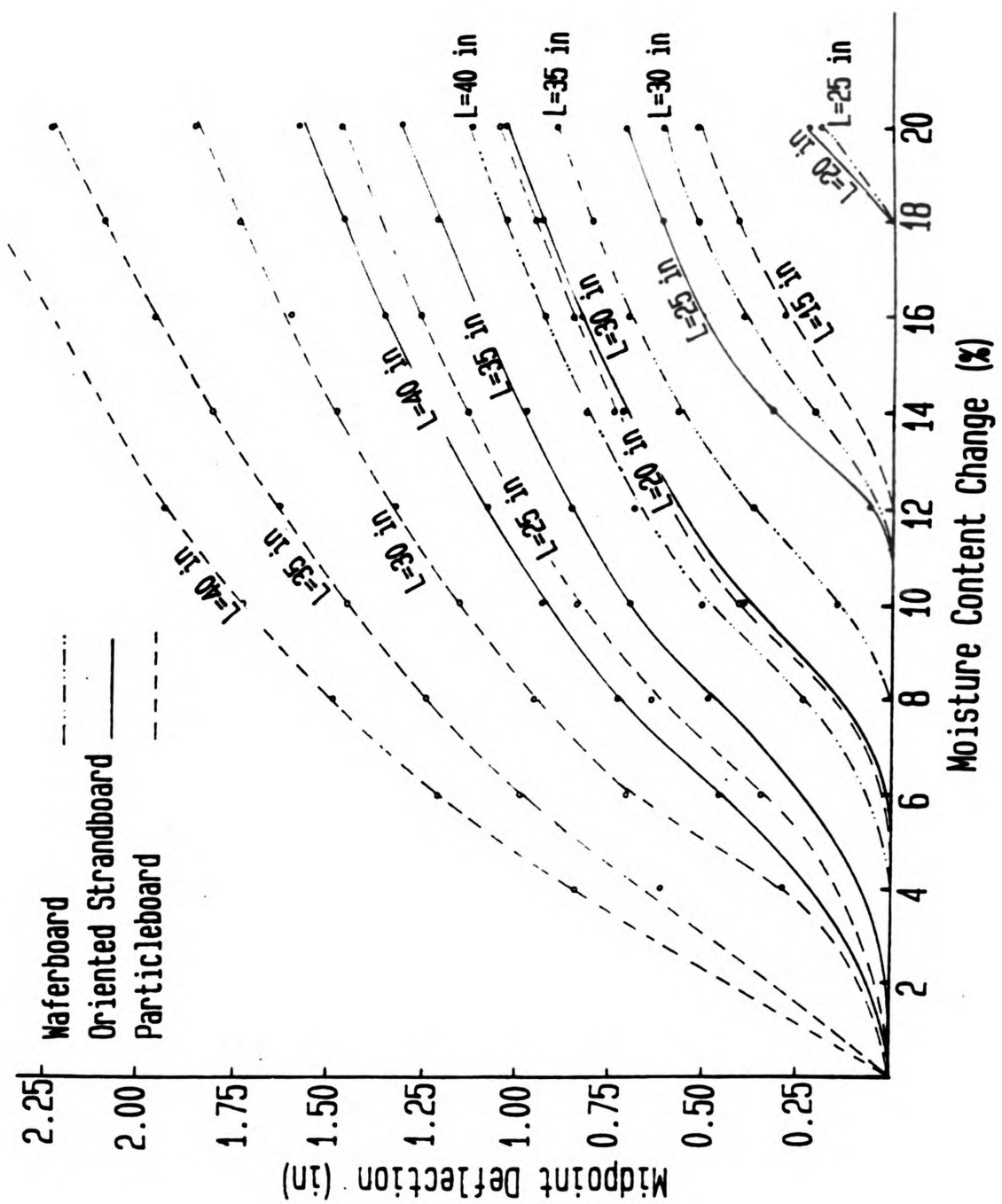
Waferboard
Oriented Strandboard
Particleboard
L=40 in
L=35 in
L=30 in
L=25 in
L=40 in
L=35 in
L=30 in
L=25 in
L=40 in
L=35 in
L=30 in
L=25 in
L=20 in
L=15 in
Midpoint Deflection (in)
Moisture Content Change (%)
0.25
0.50
0.75
1.00
1.25
1.50
1.75
2.00
2.25
2
4
6
8
10
12
14
16
18
20

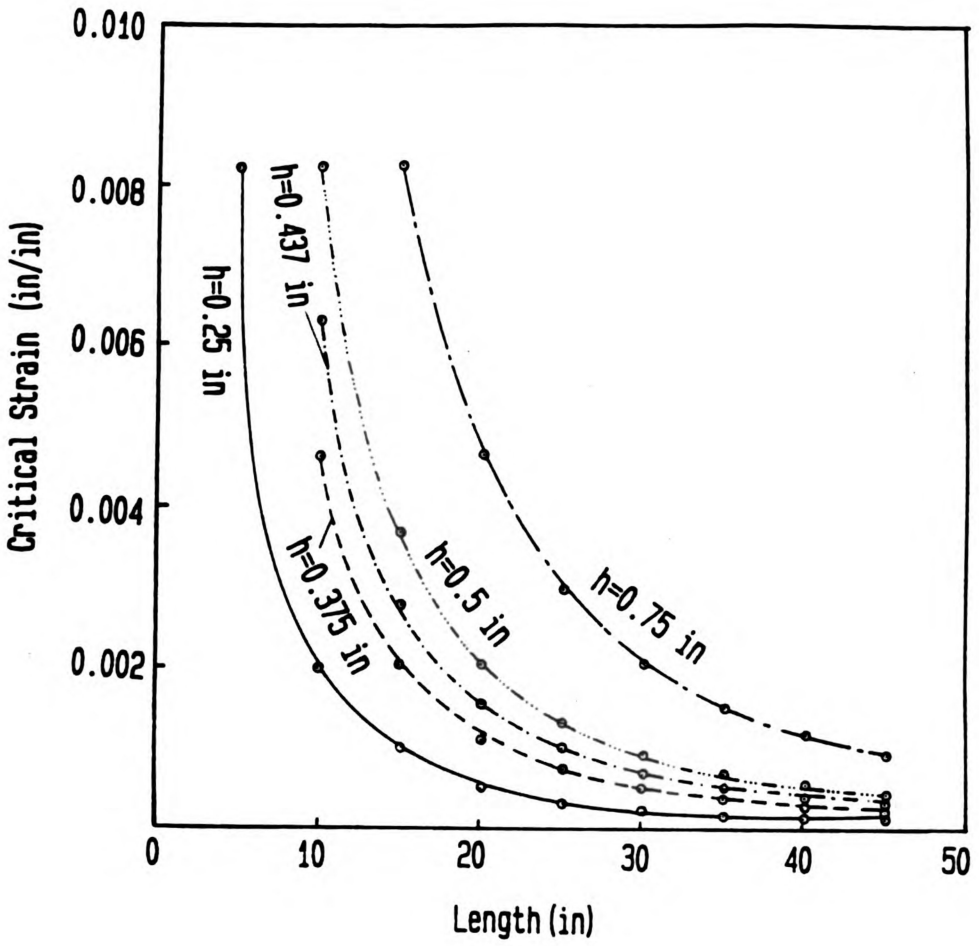

Figure 2.21. Effect of column thickness and length on critical strain.

CHAPTER 3

EXPERIMENTAL SETUP AND TEST PROCEDURES

3.1. General

As described in Chapter 2, three theoretical approaches were used to determine stress development due to various humidity exposures of restrained wood composite columns. Measured linear expansion coefficients, elastic properties and theoretical buckling deflection values were used in the first one. In the second approach, actual buckling deflections from the experiments were used instead of theoretical values in addition to the above measured properties. Finally in the third theoretical approach, elastic deflection values from the experiments were employed for the calculations. Therefore, it was necessary to determine lateral buckling deflection of each type of wood composite column under restrained conditions along with those physical and mechanical properties that were employed in theoretical approaches.

In this chapter, details of the experimental set up and the instrumentation are given, and each type of test procedure is described.

3.2. Material and Sample Design

Three different wood panels produced for commercial

utilization were tested in this study. These wood panels were particleboard (Southern pine underlayment), waferboard and oriented strandboard. Each wood composite was cut into two 4-ft by 4-ft sections from an 8-ft by 4-ft panel in order to prepare the test samples. The thickness of the wood composites were 0.75-inch, 0.5-inch, and 0.473-inch for particleboard, waferboard and oriented strandboard, respectively.

A total of eight strips of each board type with a length of 43-inch and a width of 2-inch were cut from the 4-ft by 4-ft panels to asses the swelling and shrinkage stresses and deformations under four different relative humidity cycles.

In each cycle, two strips were placed in the conditioning chamber. One of them was restrained by a metal frame for the determination of stresses and deformations due to the the change in humidity, while the other one was used to measure free linear expansion caused by the same exposure condition.

Specimens for static bending and tension-parallel-to-surface tests were also obtained from the same panels for the three kinds of wood composite. The cutting schedule is presented in Figure 3.1.

Static bending test specimens (20-inch by 3-inch) and tension test specimens (10-inch by 2-inch) were prepared from each board type with 2 replications at each exposure level. ASTM D1037 [2] was followed in the preparation of the

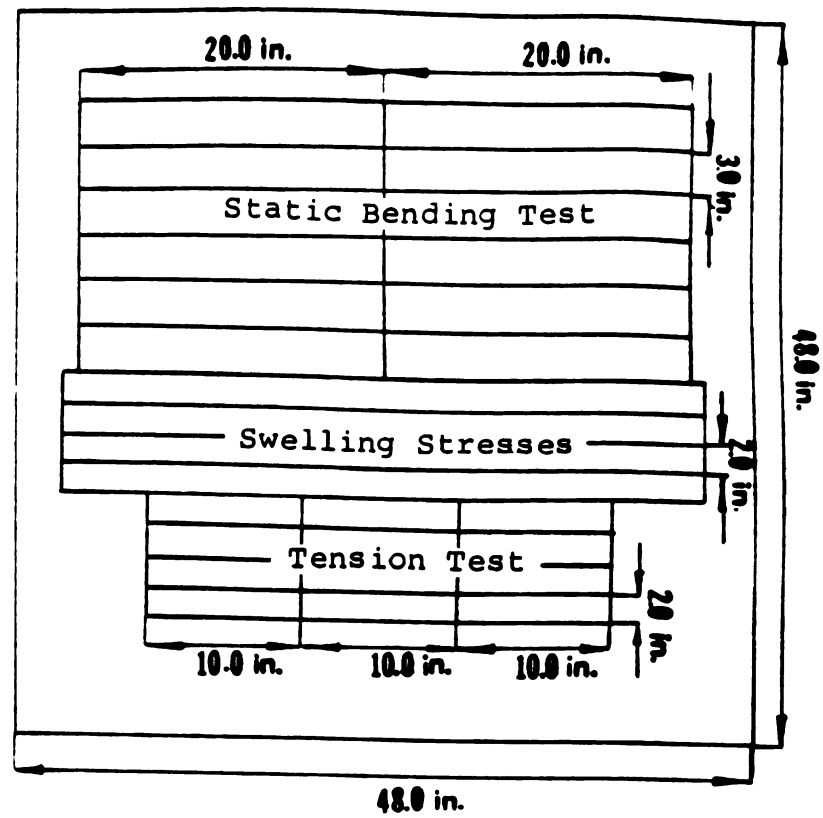

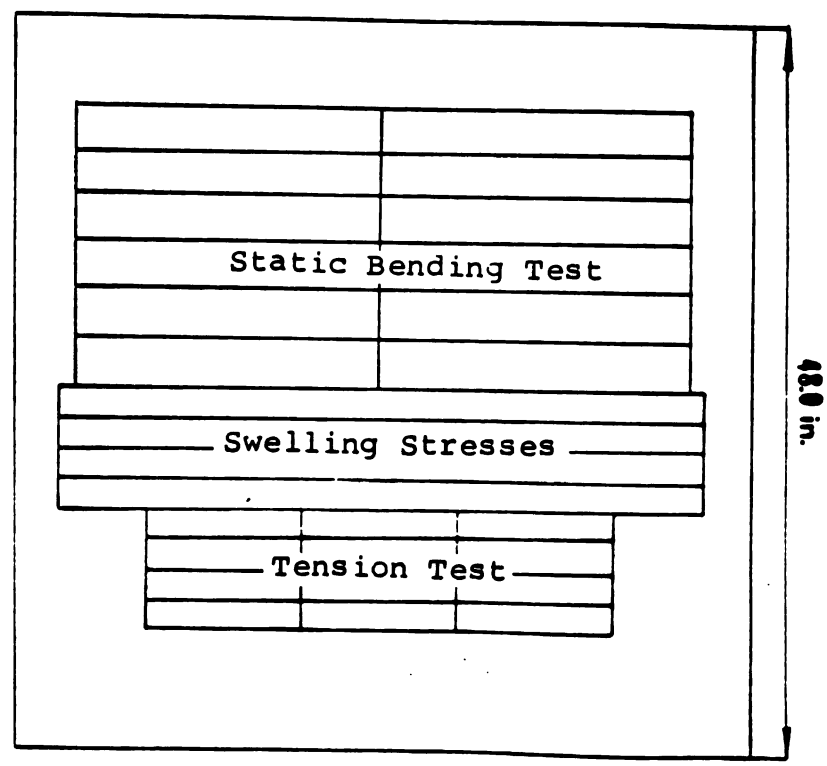

Figure 3.1. Schematic of sampling schedule.

test specimens. Two control samples of the same width as the restrained samples were also included in each cycle to determine equilibrium moisture content.

Finally, 0.75-inch by 0.75-inch square pieces were employed to determine the sorption isotherms and thickness swelling characteristics of all types of wood panels under consideration.

3.3. Swelling and Shrinkage Stresses Test Setup

The setup for determining the swelling and shrinkage stresses and the deformations due to the cycling of relative humidity consisted of four basic units namely, the metal frame, the load cell, the digital strain indicator and the conditioning chamber.

3.3.1. Metal Frame and Load Cell

Two identical metal frames were employed throughout the tests. The swelling stress specimens were mounted in the frame as follows :

Two 5-inch by 2-inch metal plates were secured to each end of the specimen by means of epoxy resin and 2 bolts. A third bolt connected the plate ends and specimens to the frame at one end by means of a threaded rod. Another threaded rod was used to connect the other end of the specimen to the load cell. The load cell was rigidly attached to the frame. Precautions were

also taken to prevent these metal plates from tilting laterally. This mounting procedure was therefore, equilavent to the built in end condition with a free column length between metal plates of 36.5-inch as illustrated in Figure 3.2.

Each frame was also equipped with a dial micrometer with an accuracy of 0.001 inch to determine the midpoint deflection. Figure 3.3 shows the metal frame with specimen and dial micrometer in place.

Two LLC Universal Shear Beam load cells, manufactured by Omega Engineering Company were employed to determine the force created by expansion and contraction of the sample in the metal frame. Technical specifications of the load cell are presented in Appendix A. Each load cell was calibrated using an Instron Test System 4200. A linear relationship between the strain and the load for both tension and compression was obtained as is indicated in Figures 3.4A and 3.4B.

3.3.2. Digital Strain Indicator

A Vishay-Ellis (V/E20) digital strain indicator manufactured by the Instrument Division Measurement Group Company was used to measure the output of the load cell. The strain indicator consists of four basic units :

A) An isolated variable output DC power supply for gauge excitation.

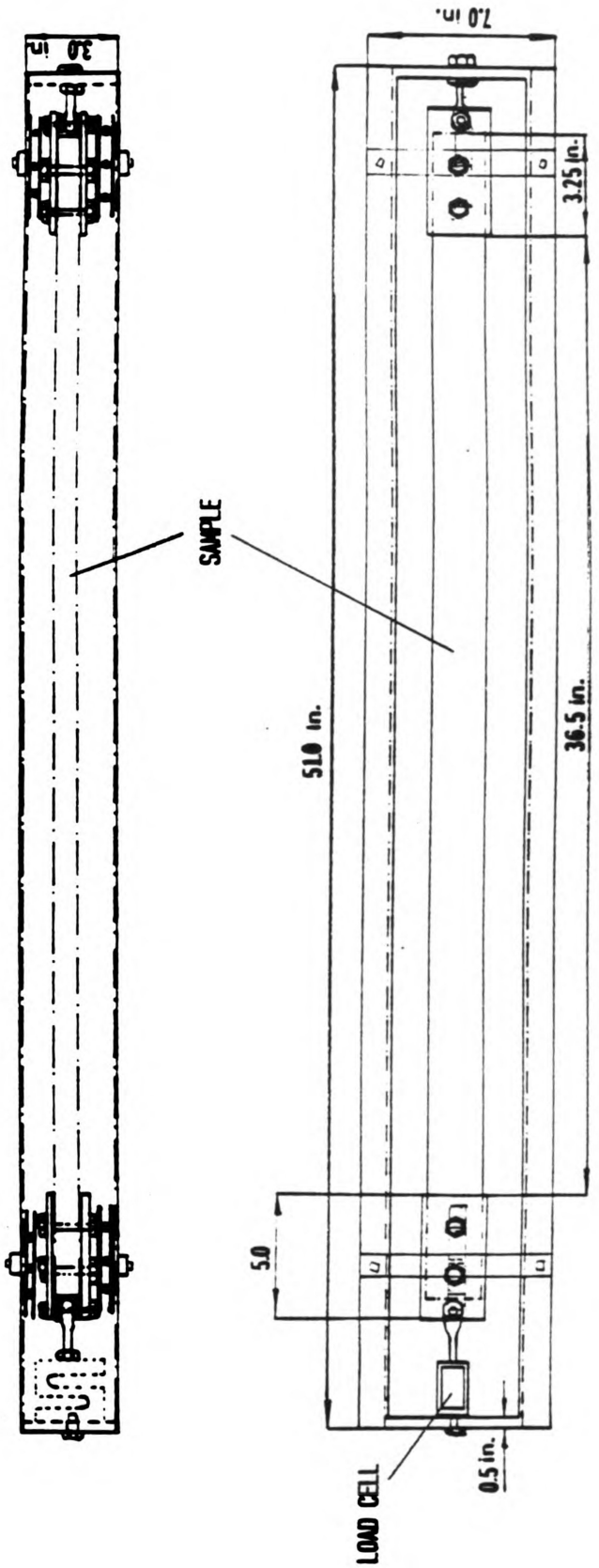

Figure 3.2. Dimensions of the metal frame.

Figure 3.3. Metal frame with specimen installed. Dial gage monitors deflection at center of specimen.

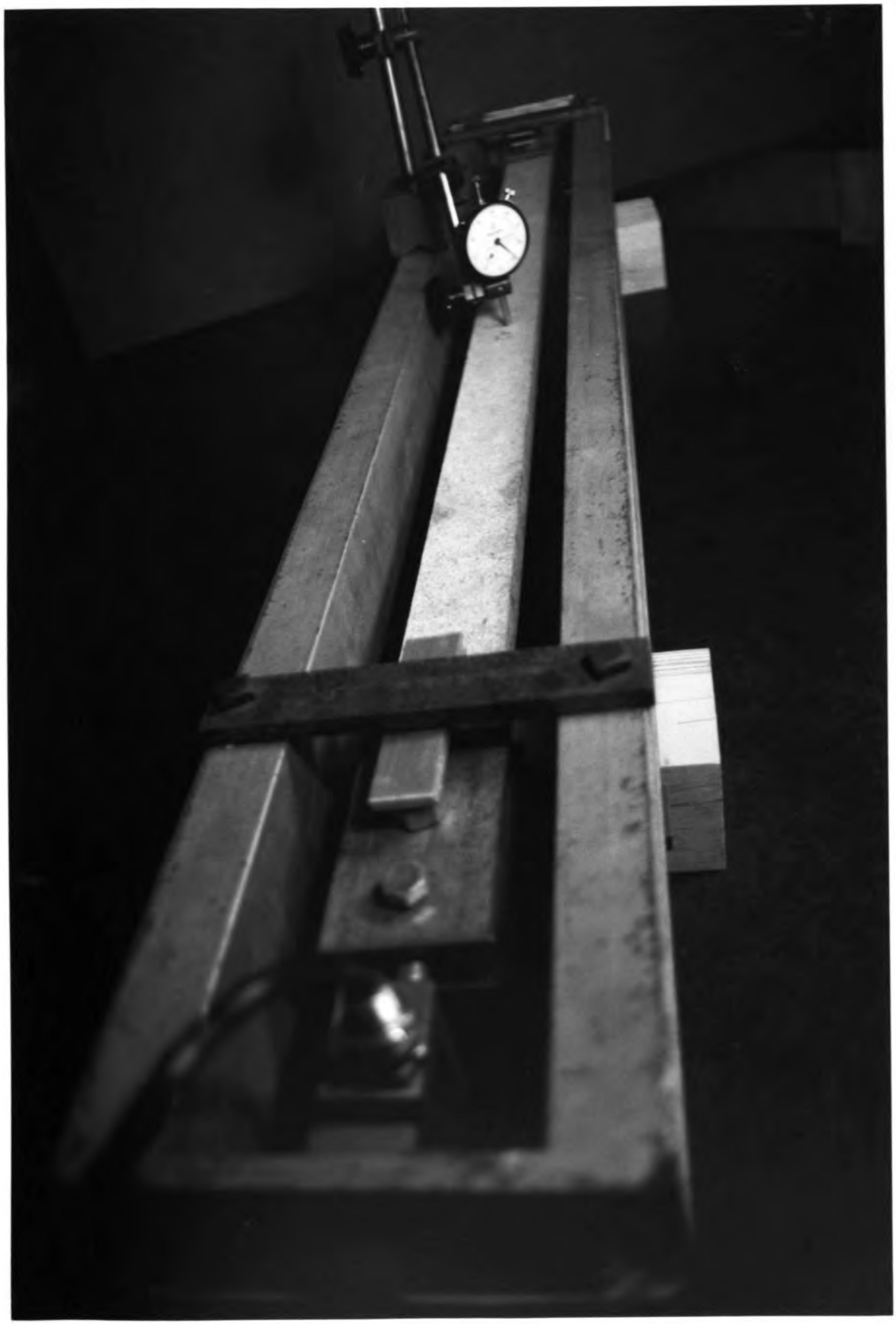

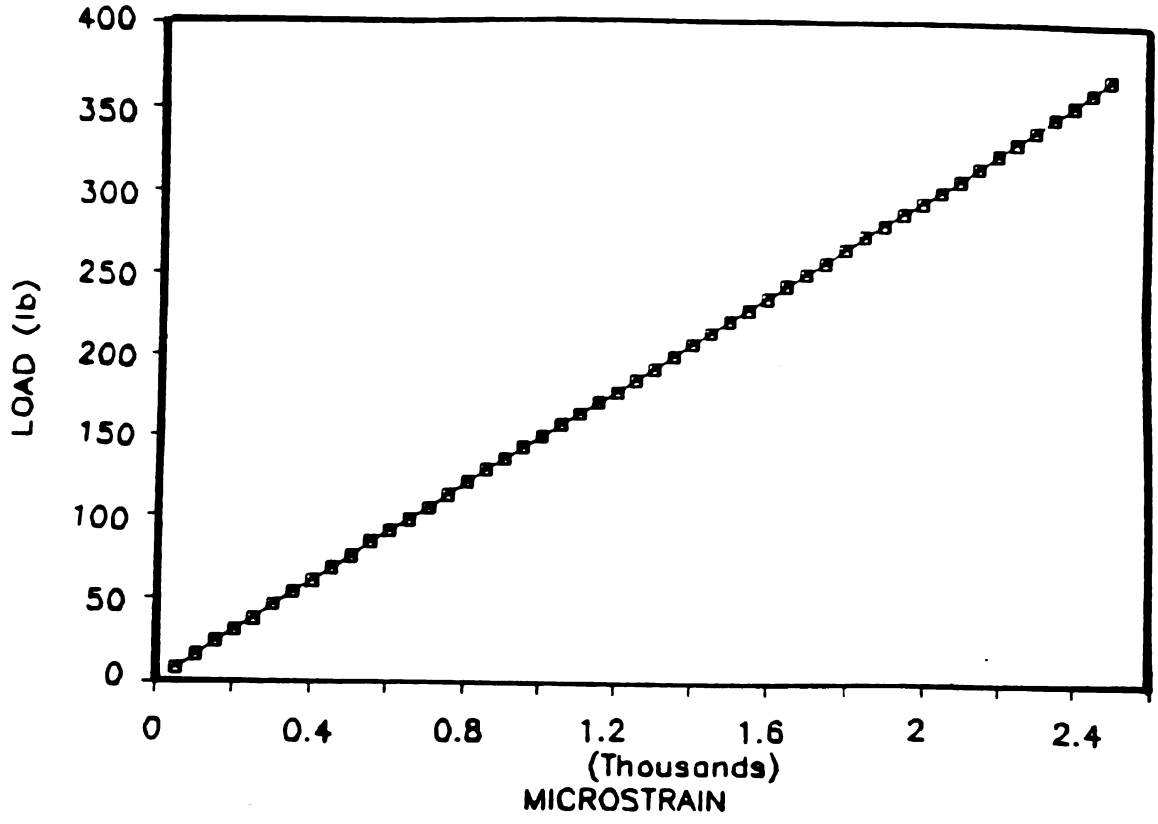

Figure 3.4A. Calibration function of load cell for tension loading.

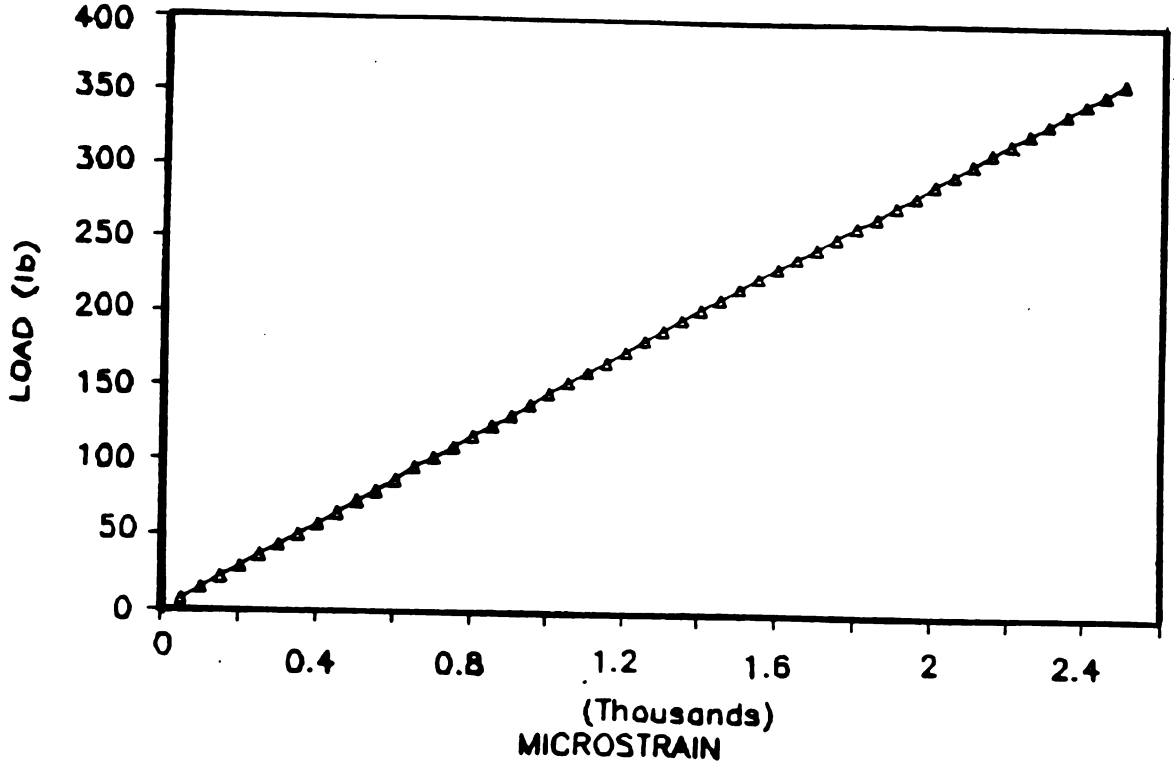

Figure 3.4B Calibration function of load cell for compression loading.

B) Bridge completion and circuit to achive initial bridge balance.

C) A fixed gain DC differential amplifier.

D) A digital voltmeter read out.

The accuracy of the strain indicator is specified by the manufacturer as 0.12 % . The V/E-20 strain indicator can also be used as a central indicator for a multichannel strain gauge data acquisition system with switch balance units. Therefore, load cells from both frames were connected to a SB-10 switch balance unit manufactured by the same company mentioned above. Data from the two load cells were monitored by changing the channel on the switch unit. Detail specifications of the strain indicator are presented in Appendix B.

3.3.3. Conditioning Chamber

A conditioning chamber manufactured by Parameter Generation Company was used in the experiments for the constant relative humidity cycles. The chamber has a volumetric capacity of 20-ft^3 and is equipped with solid-state controls for precise adjustments.

The unit consists of three sections, namely the main test chamber itself and two lower compartments. The lower compartment located on the right-hand side of the chamber includes a conditioning section with a bypass damper, water pump, and a blower motor. The lower compartment located on left

hand side of the chamber contains a refregiration unit and a heat exchanger.

The chamber provides predetermined conditions of dry bulb temperatures and humidity which can be maintained as function of time over temperature and relative humidity ranges of 4° C to 88° C and 10 % to 98 % ,respectively.

In the chamber, water temperature and air temperature are directly sensed and controlled. Basic operating principles of the chamber are as follows :

Air leaves the test chamber through perforated side walls and flows downward to the blower. If the damper is closed, the air will pass through the water spray tank which saturates the air and cools it to the water temperature. It then passes over the dry-bulb heaters and through the perforations, returning to the test chamber. However, if the damper is open, the air bypasses the water spray and goes directly over the dry bulb heaters.

The air is heated to the desired dry-bulb temperature by electric heaters and constantly circulated through the chamber to assure uniformity of humidity and temperature.

Precise control of humidity and temperature is achieved by conditioning the air in the climate section before it enters the test chamber. This also eliminates the main source of humidity and temperature deviations encountered in systems employing sprays, pans, and heaters within the chamber.

Figures 3.5. and 3.6. show the relative humidity test chamber and its operating charateristics, respectively.

3.4. Swelling Stresses and Buckling Deformations Test Procedure

In order to evaluate the swelling stresses and the deformations, four different relative humidity exposures within the maximum range of 93 % and 36 % relative humidity were used, as indicated in Figure 3.7.

A 36 % relative humidity was used as the initial relative humidity level for cycles A1 and A2 while 70 % and 93 % relative humidity were used as initial levels for cycles B and C, respectively. The sample set for each cycle was conditioned at the initial relative humidity until it reached the equilibrium moisture content (EMC). Two 10 inch long samples having the same cross section as the actual swelling stress test samples were employed as control samples. As soon as the control samples reached the equilibrium moisture content the actual test samples were taken out of the test chamber and were glued, then mounted in the metal frame as described previously. The gluing process was carried out in climate controlled rooms with relative humidities of 40 %, 68 %, and 88 % for the different initial humidity levels. The glued and bolted strips were kept for 24 hours in the test chamber before they were mounted into the frames.

Figure 3.5. Conditioning chamber with metal frame and test samples.

Figure 3.6. Chart showing ranges of temperature and humidity available in conditioning chamber.

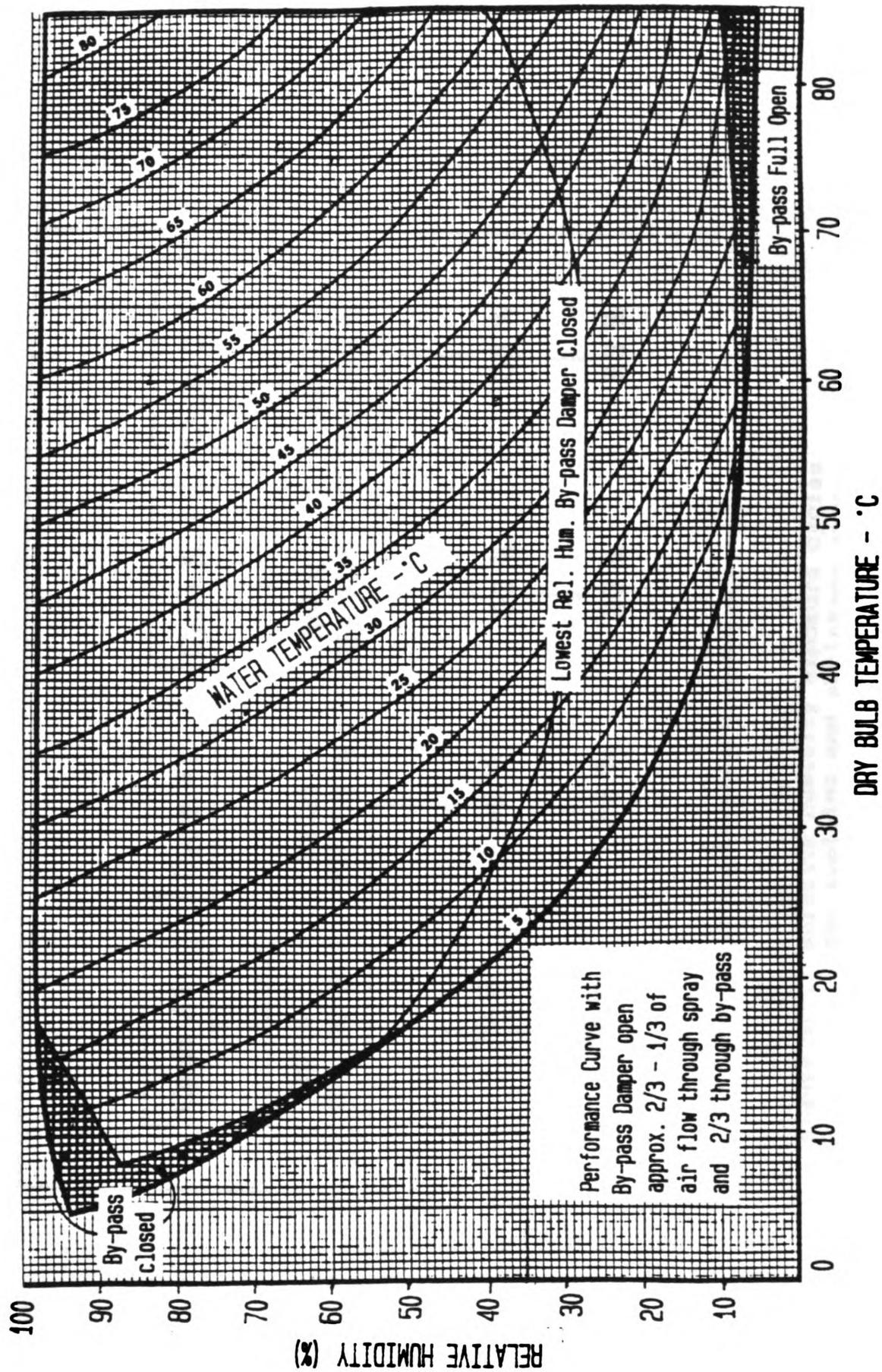
RELATIVE HUMIDITY (%)
DRY BULB TEMPERATURE - °C
WATER TEMPERATURE - °C
Lowest Rel. Hum. By-pass Damper Closed
By-pass Full Open
By-pass closed
Performance Curve with By-pass Damper open approx. 2/3 - 1/3 of air flow through spray and 2/3 through by-pass

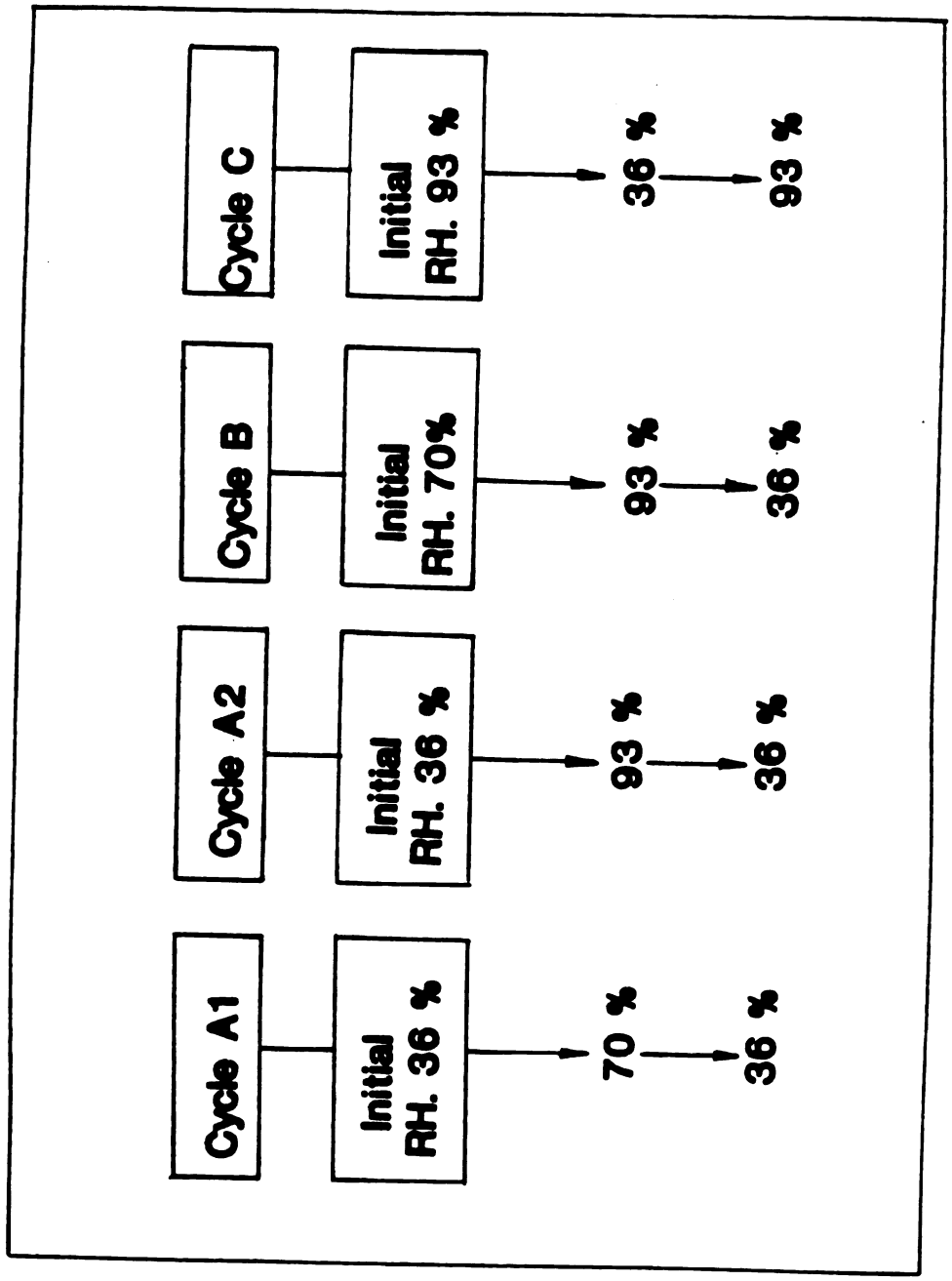

Figure 3.7. Relative humidity exposure cycles for swelling and shrinkage stresses determination.

Next, the steel frames with the test samples were placed in the conditioning chamber with the mechanical test specimens. The conditioning chamber was then adjusted to a temperature of 80 °F and to the required relative humidity.

Each sample was placed into the steel frame making sure that there was no play at any connection points between load cell, specimen, and the steel frame. With the restrained specimens in a stress free condition, the strain indicator was calibrated and set to zero initial position. Two kinds of axial stresses were observed throughout the tests. They were the compressive stress which occured when the relative humidity was increased, and the tensile stress which occured when the relative humidity was reduced.

As mentioned previously, each frame was equipped with a dial micrometer in the center of the test sample to determine the midpoint deflection. Both the magnitude of deflection and stresses were determined and correlated to moisture content change and hygroexpansion of the free matched sample.

As soon as the chamber condition was changed to the second relative humidity level, data from the strain indicator and the dial micrometer were obtained and recorded in certain prespecified time intervals until the new equilibrium moisture content was reached. Control samples were periodically weighed to the nearest of 0.01 gram to monitor moisture adsorption and desorption. Each cycle took approximately 2 months to complete.

All cycles included the conditioning of 6 specimen for static bending as well as for tension tests. Figure 3.8 illustrates the setup.

3.5. Static Bending Test Procedure

Static bending tests were carried out in order to determine MOE and MOR at various moisture content levels corresponding to beginning and end points of the exposure cycles. Samples for the bending test were prepared from particleboard, waferboard and oriented strandboard panels with dimensions of 3-inch by 20-inch, 3-inch by 12-inch in and 3-inch by 12-inch, respectively. Dimensions of each sample were measured to the nearest 0.001 in before the test.

At each humidity level, 2 bending test samples were taken out of the humidity test chamber, and tested on an Instron 4200 Universal Testing Machine following ASTM D-1037 specifications [2]. Samples were wrapped tightly with very thin vinyl sheet during the test to prevent possible adsorption or desorption of water in test room conditions. The bending test fixture is shown in Figure 3.9.

3.6. Tension Strength Parallel to Surface Test Procedure

Tension-strength-parallel-to-surface of wood composite is a difficult test to perform. However, this test is particulary important for design calculations.

Figure 3.8. Swelling and shrinkage stresses and deformations test setup.

Figure 3.9. Static bending test procedure.

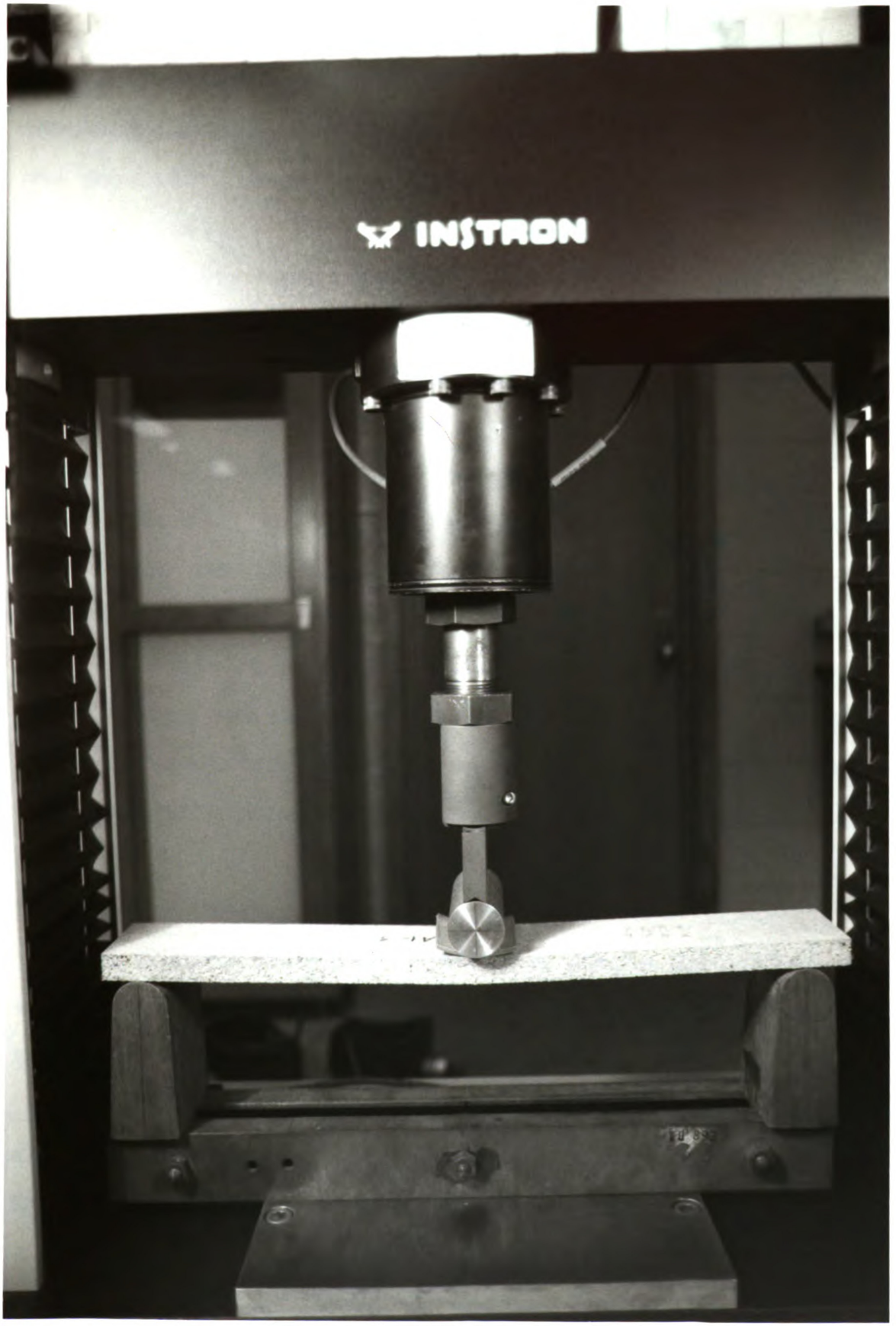
INSTRON

Specimen shape should be prepared according to generally accepted requirements. Uniform state of stress is required in the gage section of the specimen where stress and strain are measured [65].

Two samples were tested for each humidity level to determine effect of cycling condition on tension strength properties. Test samples were bandsawed to shape according to ASTM D-1037 specifications. An Instron Universal Testing Machine 4200 was employed at a crosshead speed of 0.150 inch /min and 0.360 inch/min for flake-type composite panels and particleboard, respectively. A self calibrating Instron 1200 strain gauge extensometer was used to determine elastic strain of each sample. Technical specifications of the extensometer are presented in Appendix D . Tension-strength-parallel-to-surface test fixture and dimensions of the specimen are shown in Figures 3.10. and 3.11.

3.7. Linear Expansion Test Procedure

One 42-inch long and 2-inch wide sample for each type of wood composite was used to determine free linear expansion due to cyclic relative humidity conditions.

An aluminum apparatus with a dial micrometer at its end was employed for this test. Before the sample was located on the linear expansion apparatus, the gage was calibrated by

Figure 3.10. Tension parallel to surface test procedure.

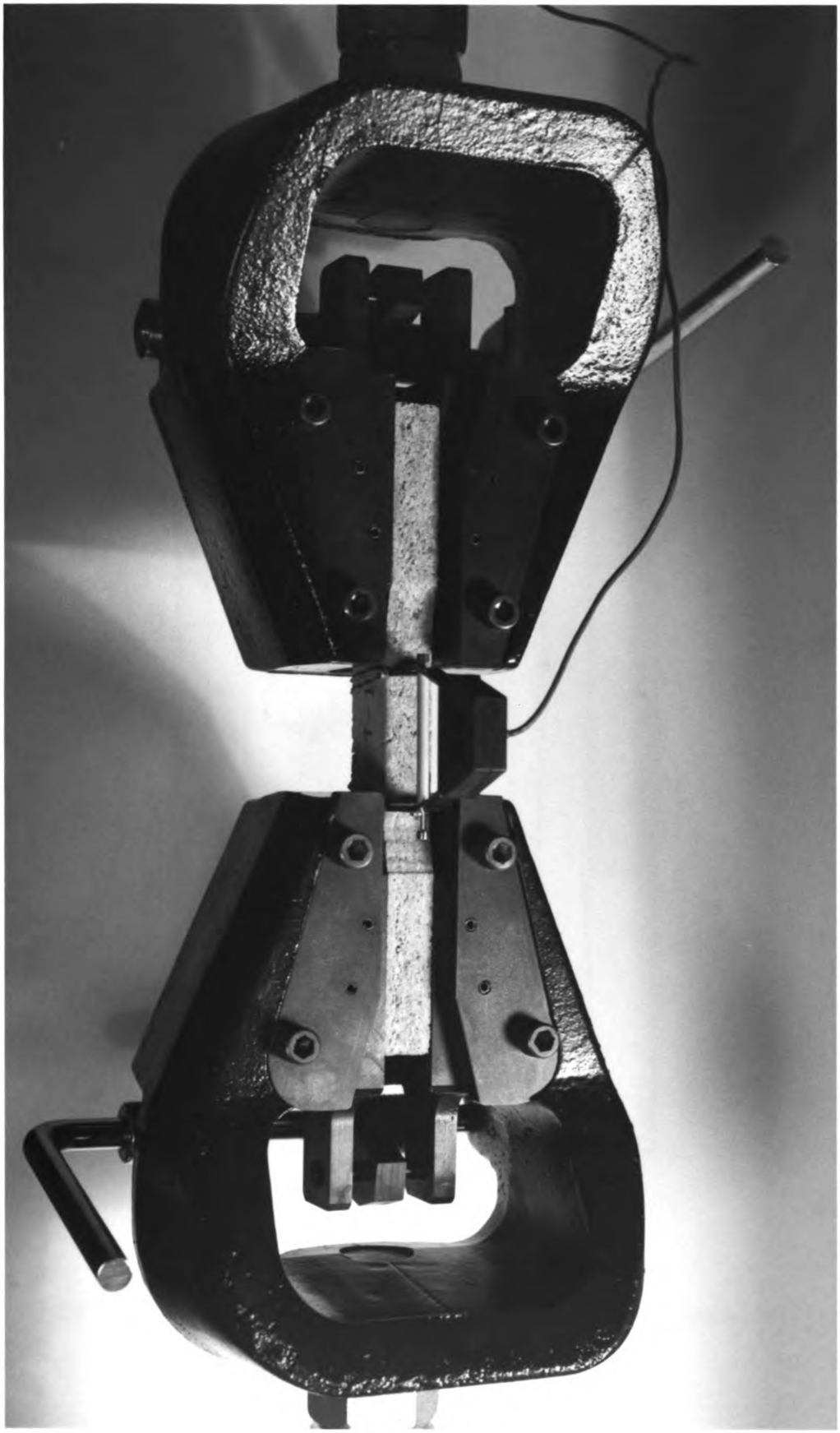

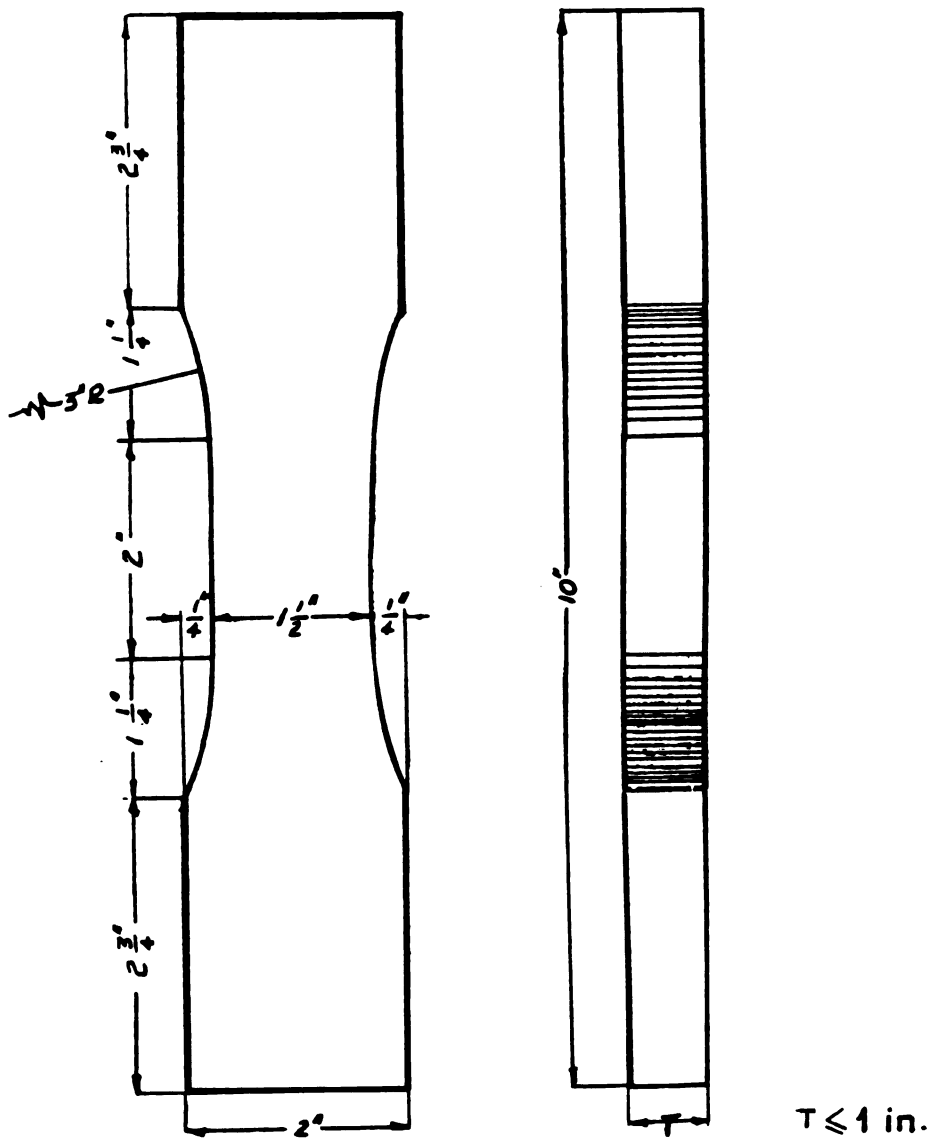

Figure 3.11. Dimensions of tension test specimen.

using a metal bar with 42 inch length. In the next step, initial length of the sample was measured to the nearest 0.001 inch. Linear measurements of the samples were performed at the end of each relative humidity change. Figure 3.12 depicts the linear expansion gage.

3.8. Thickness Swelling Test

Five square samples, 0.75 inch by 0.75 inch from each type of wood composite were used for the determination of thickness swelling. Desiccators charged with chemicals (saturated salt solutions) were employed for the experiments. List of the chemicals used in desiccators and the corresponding relative humidities are presented in Figure 3.13.

Each set of samples was conditioned at 47 % initial relative humidity. The samples were weighed to the nearest 0.001 gram until they reached a constant weight. As soon as equilibrium moisture content was reached, thickness measurements were carried out the nearest 0.001 inch. Samples conditioned at 47 % relative humidity were transferred sequentially to desiccators adjusted to 66 %, 81 % and 93 % relative humidity for the adsorption branch and were returned by the same sequence to 47 % relative humidity.

Figure 3.12. Linear expansion gage with calibration bar.


AMES

3.9. Sorption Isotherms

One sample with dimensions of 0.75 inch by 0.75 inch from each type of wood composite was used for the determination of adsorption and desorption branches of sorption isotherms. A series of 5 desiccators charged with chemical salt solutions was also employed for these experiments. Specimen number 6 through 9 were preconditioned in 47% relative humidity then transferred to desiccators A through D for determining the adsorption isotherm. Specimens 1 through 5 were preconditioned at 93 % relative humidity and then distributed to desiccators A through D to determine the desorption isotherm. As Figure 3.13 illustrated, at the end of each condition, samples were oven dried to determine the moisture content. Figure 3.14 depicts the desiccators charged with chemicals.

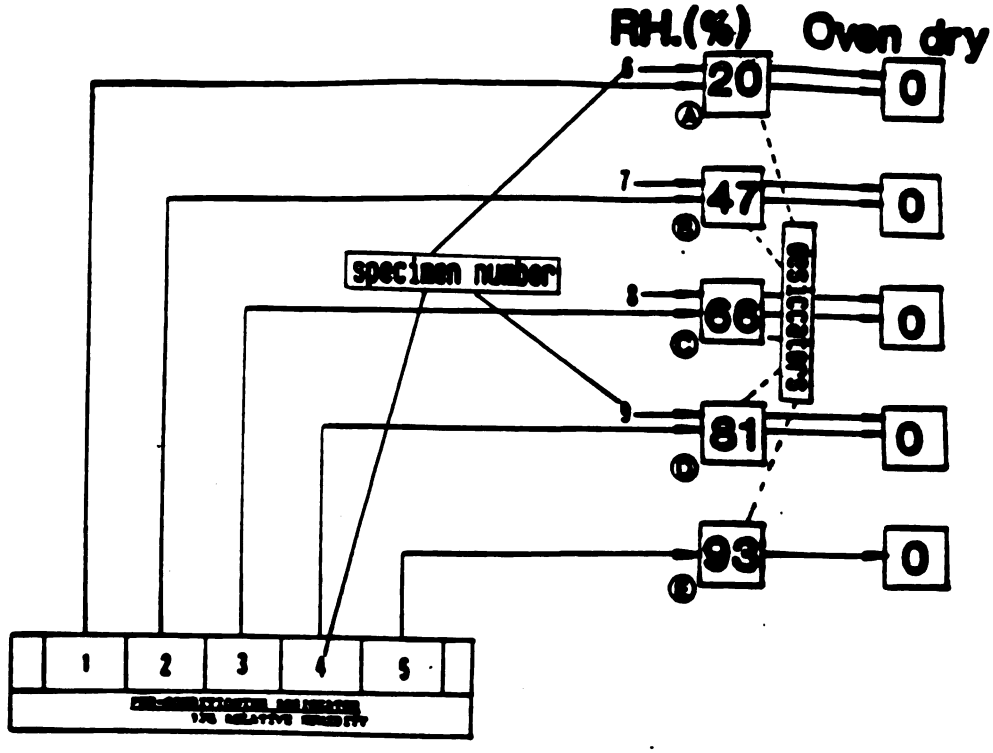

RH.(%)	CHEMICAL
0	Phosphorous pentoxide (P_2O_5)
20	Potassium acetate ($KC_2H_3O_2$)
47	Potassium thiocyanate (KSCN)
66	Sodium nitrite ($NaNO_2$)
81	Ammonium sulfate $(NH_4)_2SO_4$
93	Mono ammonium phosphate(NH_4HPO)

Figure 3.13. Exposure schedule for determination of sorption isotherms and list of chemicals used in desiccators and corresponding relative humidities.

Figure 3.14. Desiccators used for determination of isotherm and of thickness swelling. Desiccators are charged with saturated salt solutions.

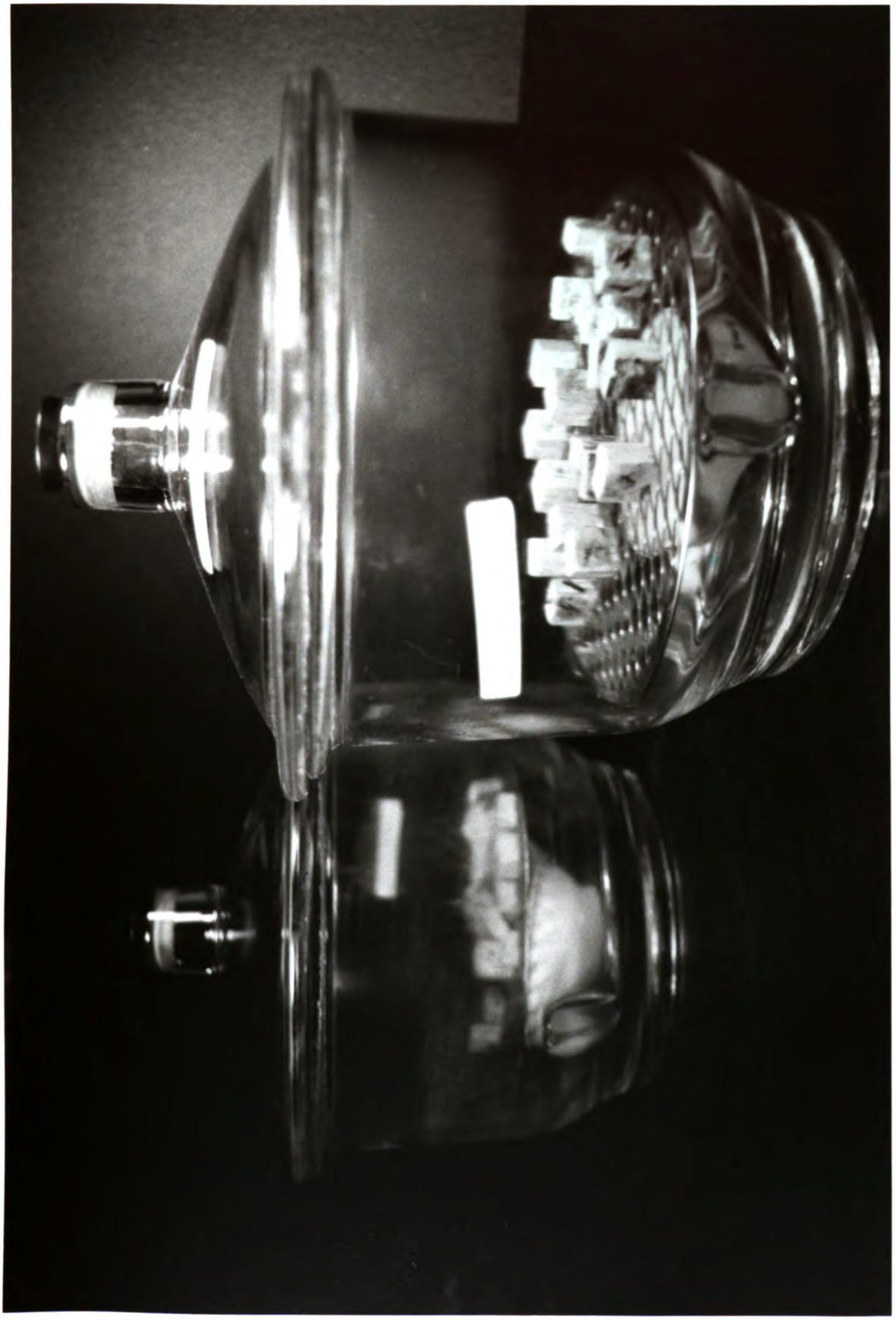

CHAPTER 4

RESULTS AND DISCUSSIONS

4.1. General

In this chapter, experimental results for the determination of axial swelling and shrinkage stresses and buckling deformations of waferboard, oriented strandboard and particleboard are presented and discussed for different relative humidity exposure cycles. Furthermore, since the elastic properties and linear expansion characteristics of each type of product were needed as the input data for the theoretical calculations of the swelling and bending stresses, and deformations, the results of mechanical and physical tests are also presented and discussed.

Finally, calculated theoretical shrinkage and swelling stresses, bending stresess and lateral buckling values are given based on the data from mechanical and physical tests obtained from the experiments.

4.2. Results and Discussions of Experiments

4.2.1. Axial Swelling and Shrinkage Stresses.

The cycles designated as A1 and A2 started with a relative humidity of 36 % . Figures 4.1, 4.2. and 4.3, and Table 4.1 represent the typical measured characteristics of axial

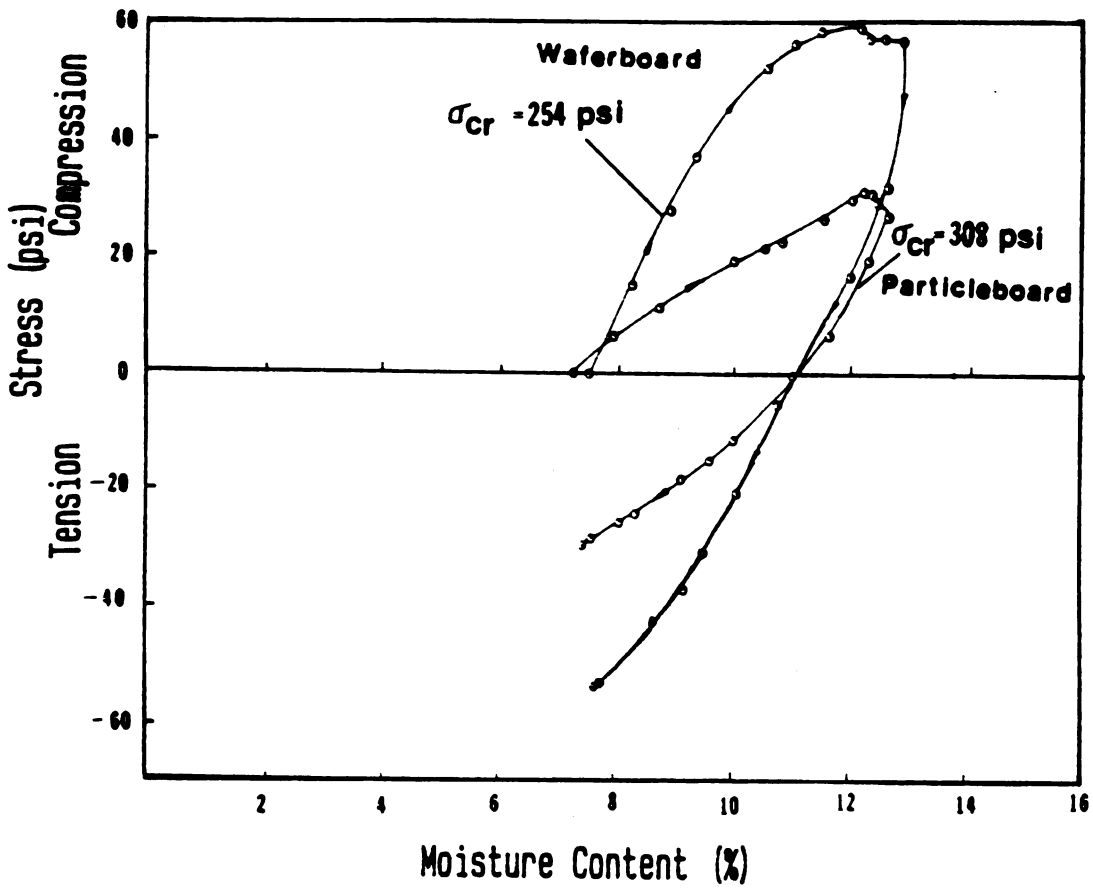

Figure 4.1. Axial swelling and shrinkage stresses as function of average moisture content. Cycle A1, 36 % - 70 % - 36 % relative humidity.

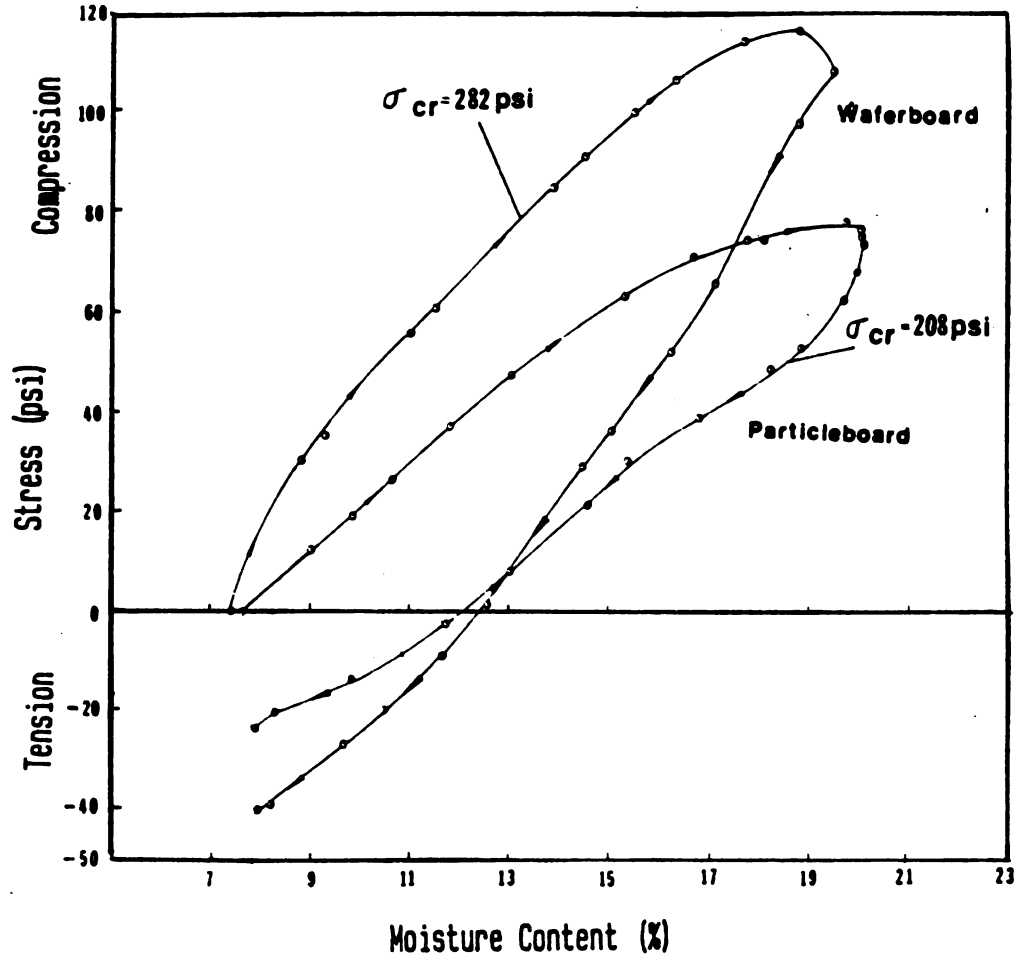

Figure 4.2. Axial swelling and shrinkage stresses as function of average moisture content. Cycle A2, 36 % - 93 % - 36 % relative humidity.

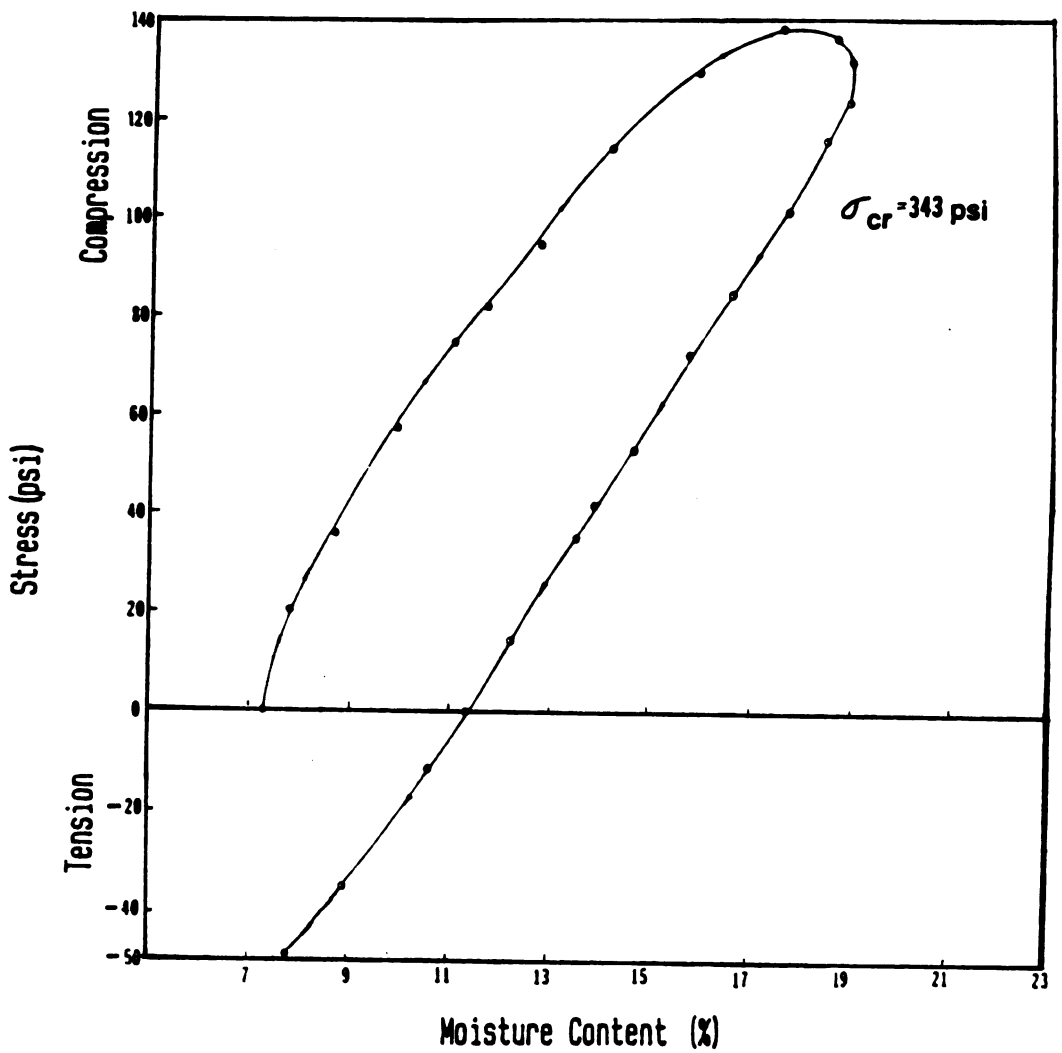

Figure 4.3. Axial swelling and shrinkage stresses of oriented strandboard as function of average moisture content.
Cycle A2, 36 % - 93 % - 36 % relative humidity.

Cycle A1				Cycle A2					
WAFERBOARD		PARTICLEBOARD		WAFERBOARD		PARTICLEBOARD		ORIENTED STRANDBOARD	
Moisture Content (%)	Stress (psi)	Moisture Content (%)	Stress (psi)	Moisture Content (%)	Stress (psi)	Moisture Content (%)	Stress (psi)	Moisture Content (%)	Stress (psi)
7.5	0.0	7.2	0.0	7.4	0.0	7.6	0.0	7.3	0.0
8.2	16.0	7.9	6.5	8.8	30.0	9.0	12.0	7.8	21.0
8.9	28.0	8.7	14.0	9.3	35.0	9.8	19.0	8.7	36.0
9.3	37.2	10.0	20.1	11.0	56.5	10.6	26.0	9.9	57.0
10.5	53.5	10.5	22.0	11.6	61.5	11.8	37.0	11.0	65.0
11.0	57.3	10.8	22.9	13.9	85.3	13.0	48.2	11.7	82.1
11.4	59.0	11.5	27.0	14.5	91.2	15.3	64.1	12.8	95.3
12.1	58.5	12.0	30.1	15.5	100.5	16.7	72.2	14.3	112.0
12.3	58.0	12.2	32.4	17.7	114.2	17.8	74.1	16.0	130.0
12.5	57.5	12.3	30.0	18.8	117.1	18.1	75.0	17.7	139.0
12.8	57.1	12.4	28.5	19.5	107.2	19.8	78.0	18.7	137.5
		12.6	26.8			20.0	72.0	19.0	133.8
12.6	32.0	12.3	20.2	18.8	98.4	19.9	75.0	18.9	125.6
12.0	17.0	11.6	7.0	17.8	74.5	19.8	74.1	18.5	116.5
11.0	0.0	11.1	0.0	17.1	67.3	19.7	63.2	17.8	102.2
10.7	-5.0	10.0	-11.0	16.3	53.1	18.9	54.1	16.6	85.3
10.1	-20.0	9.6	-14.0	15.1	36.0	18.3	40.0	15.8	73.0
9.5	-30.0	9.1	-18.0	14.5	29.0	16.3	39.2	14.7	54.2
9.1	-37.0	8.3	-23.0	13.1	9.2	15.4	30.0	13.9	42.2
8.6	-42.0	8.0	-25.0	12.6	1.2	14.6	22.0	13.5	35.0
7.9	-53.0	7.7	-27.0	11.7	-9.0	12.7	4.0	12.2	15.0
7.8	-54.0	7.5	-30.0	10.5	-20.0	11.8	-2.1	11.3	0.0
				9.7	-27.0	9.8	-14.5	10.6	-12.0
				8.2	-38.1	8.4	-21.1	9.5	-23.0
				8.0	-40.3	8.2	-24.0	8.9	-40.3
				7.9	-44.2			7.7	-49.0

Table 4.1. Compression and tension stress values.

swelling and shrinkage stresses of waferboard, particleboard and oriented strandboard as a function of average moisture content in cycles A1 and A2.

Waferboard indicated a maximum compression stress of 59.0 psi as the relative humidity was increased from an initial value of 36 % to 70 % in cycle A1. Also, in this cycle 11.4 % was found to be the moisture content at the maximum stress level. After the humidity level was reversed from 70 % to 36 % , the sample reached zero stress level at 11.0 % moisture content. Beyond this point, tension stresses developed up to 54.0 psi. At the end of this cycle the moisture content of waferboard was 0.3 % higher than the original value which can be attributed to the hygroscopic hysteresis effect. As discussed in section 2.4 hygroscopic hysteresis is the difference between adsorption and desorption curves which can be related to many types of combinations of physical and chemical phenomena. Additionally, manufacturing variables such as press cycles, heat application, resin content as well as raw wood characteristics are most important factors that control hysteresis of wood composites when they are exposed to change in relative humidity [41,50].

32.4 psi was determined as the maximum compressive stress in particleboard as shown in Table 4.1. 30.0 psi was found to be the maximum tension stress of particleboard which was slightly more than one half of the tension stresses of

waferboard for the same relative humidity cycle. Unlike waferboard, particleboard exhibited much lower compression and tension stresses in the same cycle. This behaviour could be explained by the higher modulus of elasticity of waferboard.

Critical stresses were calculated at the highest moisture content for cycle A1 in order to evaluate the relationship between these stresses and axial swelling stresses. Critical stress calculation were performed based on the discussion given in section 4.3.2. 245 psi and 308 psi were computed as the critical stresses for waferboard and particleboard, respectively in cycle A1. As can be noted from Figures 4.1, 4.2, 4.3, and 4.4 axial stresses were found to be lower than computed critical stresses. This is due mainly to stress relaxation at high moisture content and may also be affected to some extent by the inhomogeneity of the products and the presence at least during part of the cycle of severe moisture content gradients from board surface to board center.

The development of tensile stresses upon redrying is also a clear indication of the significant relaxation of the compressive stresses during the adsorption cycle.

In cycle A2, waferboard exhibited higher compression stress than particleboard as was the case in cycle A1. Corresponding maximum compression stresses for waferboard, particleboard and oriented strandboard were found to be as 117.1 psi, 78.0 psi and 139.0 psi which can be seen in Tables

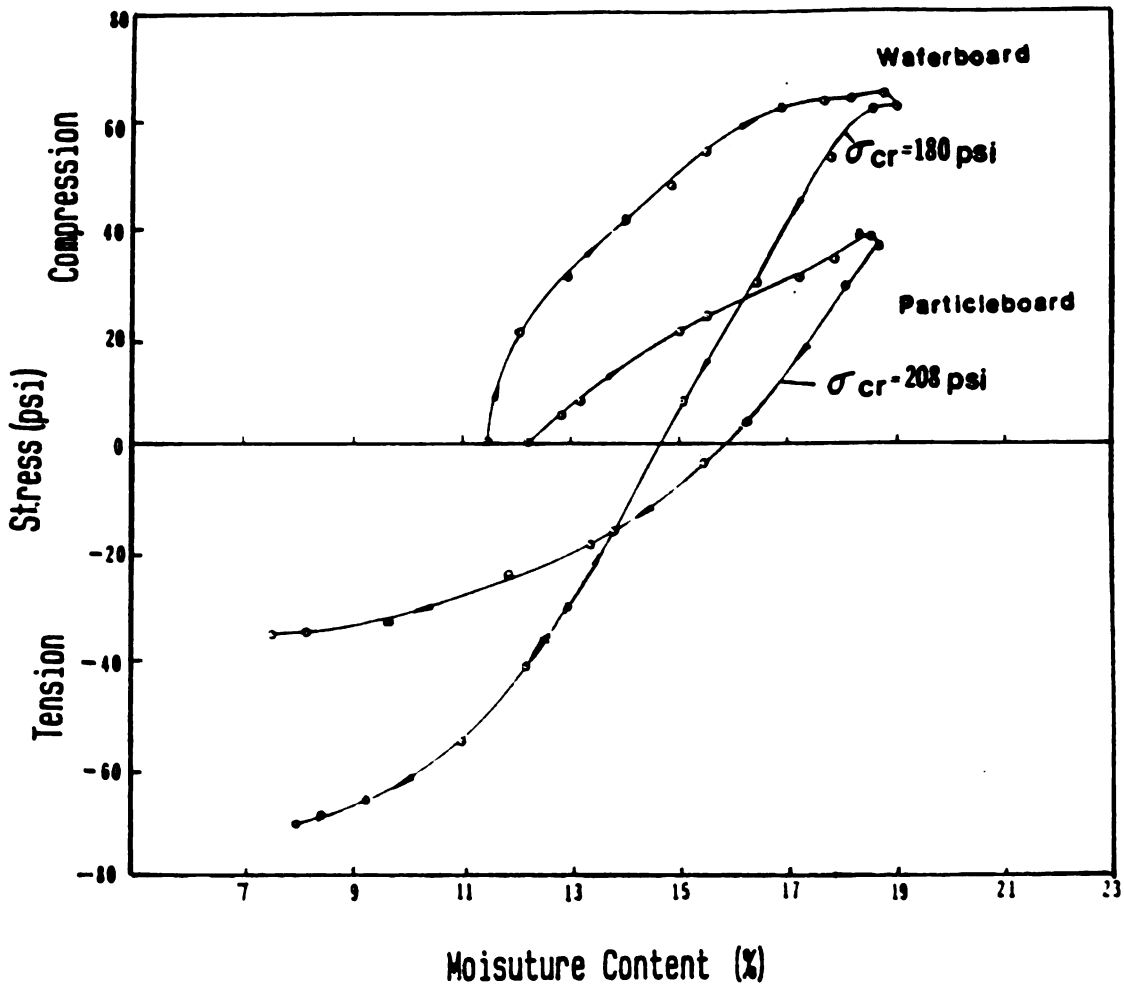

Figure 4.4. Axial swelling and shrinkage stresses as function of average moisture content. Cycle B, 36 % - 70 % - 36 % relative humidity.

4.1 and 4.2 Moreover, it was observed that the general trend of axial compression stresses as a function of average moisture content for the three different types of composites were found to be similar to one another. Both flake-type structural wood composites considered in this study have relatively similar raw material characteristics as well as manufacturing variables. Therefore, similar magnitude of axial stresses of oriented strandboard and waferboard can be related to the similarity in their mechanical and physical properties.

It is also clear that stiffer waferboard and oriented strandboard result in higher level of stresses. The experiments of this study showed that the two flake-type products indicated higher swelling stress characteristics as a function of moisture content than particleboard inspite of their lower expansion values.

In cycle B, 70 % relative humidity was used as initial condition for both waferboard and particleboard. Figure 4.4 represents the axial stress moisture content characteristics of these two wood composites.

Waferboard had 11.5 % equilibrium moisture content while this value was 12.2 % for particleboard at the initial relative humidity level. Development of tension and compression stresses as a function of moisture content for the two composite materials exhibited approximately similar characteristics. However, the stress magnitudes of waferboard were found to be

CYCLE-B				CYCLE-C			
WAFERBOARD		PARTICLEBOARD		WAFERBOARD		PARTICLEBOARD	
MOISTURE CONTENT (%)	STRESS (psi)	MOISTURE CONTENT (%)	STRESS (psi)	MOISTURE CONTENT (%)	STRESS (psi)	MOISTURE CONTENT (%)	STRESS (psi)
11.5	0.0	12.2	0.0	18.0	0.0	18.5	0.0
12.5	21.0	12.9	6.5	17.3	-44.1	18.0	-26.0
13.0	31.8	13.2	8.1	16.3	-77.0	17.7	-37.8
14.0	42.7	15.1	21.4	12.7	-150.0	17.1	-58.5
15.6	54.2	15.6	24.0	12.3	-155.0	16.2	-89.1
16.9	61.0	17.3	31.4	11.7	-164.0	15.5	-106.2
17.8	63.0	17.9	35.0	11.0	-170.6	13.4	-131.0
18.3	64.0	18.4	39.1	9.9	-176.0	11.3	-146.0
18.8	64.9	18.6	38.2	9.0	-180.0	9.5	-150.0
19.1	63.5	18.8	36.0	7.6	-182.0	8.2	-147.5
				7.3	-180.0	8.1	-148.0
						7.5	-145.2
18.6	62.1	18.1	29.2	8.9	-146.0	8.0	-131.5
17.9	53.2	16.4	4.0	9.5	-125.2	9.2	-126.3
16.5	30.1	15.5	-4.5	9.9	-116.3	9.9	-108.3
15.1	8.2	13.4	-19.0	10.4	-100.1	10.6	-96.5
13.7	-16.0	11.9	-24.0	11.4	-69.0	12.3	-63.2
13.0	-30.0	9.7	-33.1	12.9	-35.0	13.0	-42.0
12.2	-22.2	8.7	-35.2	15.5	16.0	14.0	-3.0
11.0	-35.2	7.5	-36.1	16.3	25.0	16.2	18.2
9.2	-66.1			16.9	32.0	17.0	23.0
8.4	-69.0			17.0	34.3	17.2	25.0
8.0	-71.0			17.3	37.0	17.8	27.0
						17.9	26.1

Table 4.2. Compression and tension stress values.

higher than those of particleboard. As can be seen from Figure 4.4 maximum compression stresses were 64.9 psi for waferboard and 39.1 psi for particleboard. When equilibrium moisture content was obtained for the samples at 93 % relative humidity, the relative humidity of the conditioning chamber was reduced to 36 %. Waferboard reached zero stress at approximately 12.0% moisture content before it exhibited a maximum of 71.0 psi tension stress. Zero stress moisture content was found to be nearly 13 % for particleboard and it gave the maximum tension stress of 36.1 psi which was nearly one half that of waferboard. This illustrates the greater plasticity of particleboard which would be expected to develop higher stresses because of its larger linear expansion. Moreover, it can be noted that the slope of the stress-moisture content characteristics of waferboard is significantly higher than the slope of particleboard as was also pointed out for cycles A1 and A2. Again higher MOE of waferboard could be considered as major factor for these results. Equilibrium moisture contents were calculated as 8.0 % and 7.5 % at the final point of 36 % relative humidity for waferboard and particleboard, respectively.

Figure 4.5 illustrates axial swelling stress moisture content characteristics of waferboard and particleboard in cycle C. 18.0 % and 18.5 % equilibrium moisture content were observed at initial relative humidity of 93 % in cycle C for

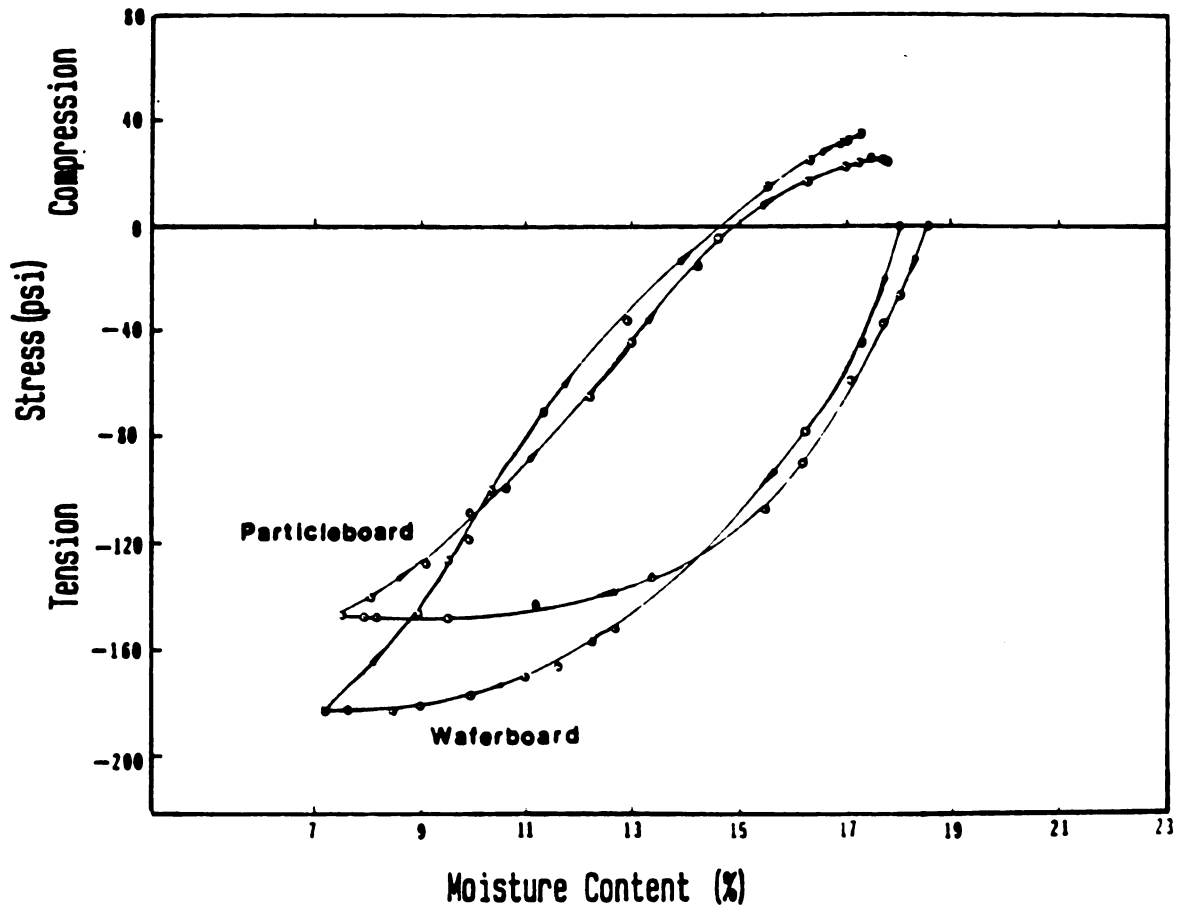

Figure 4.5. Axial swelling and shrinkage stresses as function of average moisture content. Cycle C, 93 % - 36 % - 93 % relative humidity.

waferboard and particleboard correspondingly.

Both types of wood composites did not indicate any significant differences in development of tension and compression stresses due to the change in relative humidity from 93 % to 36 % . However, similar to the results of the previous cycles, again waferboard presented higher stresses than those of particleboard as can be seen from Table 4.2. 182.0 psi and 150.0 psi were determined as maximum tension stresses for waferboard and particleboard, respectively. Corresponding values for compression stress for the above wood composites were 37.0 psi and 26.1 psi. Table 4.2 presents the results of cycles B and C.

As can be seen from Figures 4.1, 4.2, 4.3, and 4.4 none of the wood composites considered in the experiments showed complete relaxation of compressive stresses as found in hardboard strips with a 1 inch by 0.25 inch cross section by Suchsland (Figure 2.5) [76]. Most hardboards are not highly elastic material[53]. Particleboard and flakeboards like waferboard and oriented strandboard are therefore more elastic than hardboard. The greater relaxation in hardboard is probably related to the smaller size of the elements and to different types of bonding.

4.2.2. Lateral Buckling Deflections

As was pointed out in section 3.3 each frame was equipped with a dial micrometer to determine the midpoint deflection of the restrained sample for varying relative humidities. Residual deflection values of each sample was also detected at the end of each cycle. Reduction in the midpoint deflections was only recorded for cycle A2 when the relative humidity decreased from 93 % to 36 % .

Maximum of 0.436 inch deflection at midpoint of particleboard was determined due to the increase in relative humidity from 36 % to 70 % for cycle A1. Waferboard presented 1.9 times lower deflection than that of particleboard, 0.227 in for the same cycle. Figures 4.6 and 4.7 depict the midpoint deflections of two composite materials for cycle A1. After the relative humidity was reversed from 70 % to 36% , tension stresses developed in the sample. 0.108 inch and 0.054 inch residual midpoint deflections were measured for particleboard and waferboard, respectively, as can be seen from Table 4.3.

As was mentioned previously, oriented strandboard was also included in cycle A2 in addition to waferboard and particleboard. In this cycle particleboard again resulted in the highest midpoint deflection value of 1.018 inch due to its large linear expansion coefficients. Corresponding values for waferboard and oriented strandboard were found to be 0.582 inch and 0.885 inch, respectively. Figures 4.8, 4.9, and 4.10

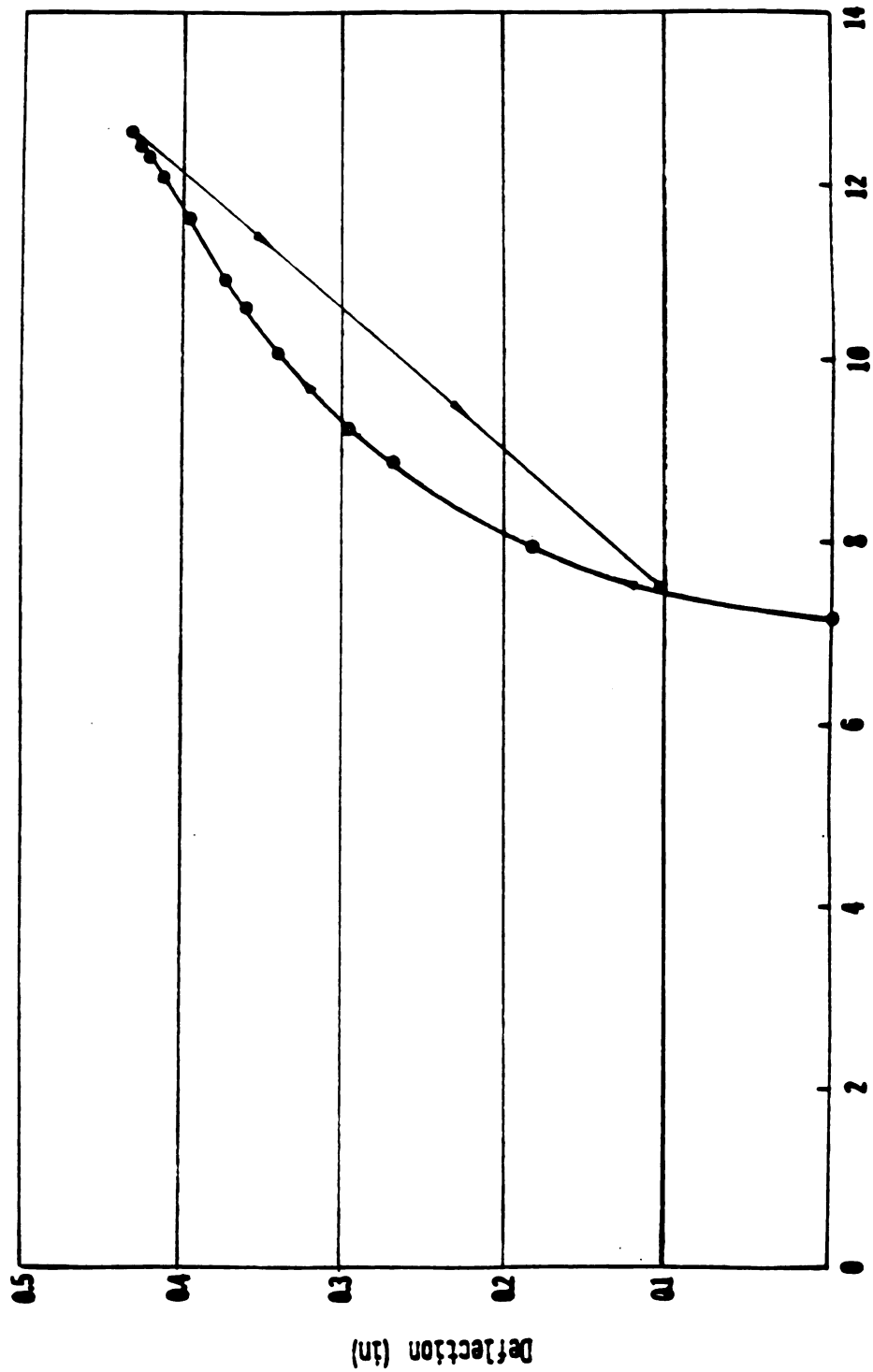

Figure 4.6. Midpoint deflections of particleboard as function of moisture content. Cycle A1, 36 % - 70 % - 36 % relative humidity.

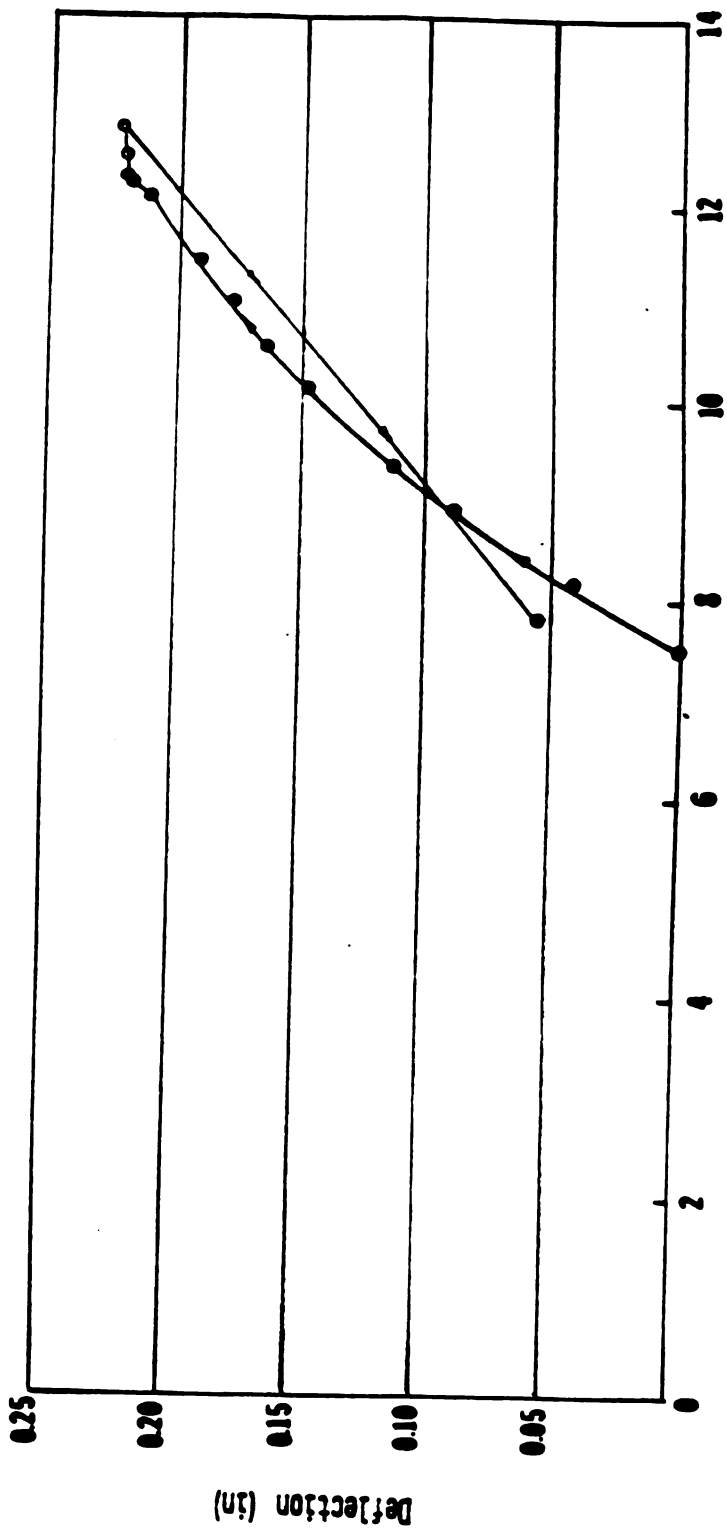

Figure 4.7. Midpoint deflections of waferboard as function of moisture content. Cycle A1, 36 % - 70 % -36 % relative humidity.

Cycle A1				Cycle A2							
PARTICLEBOARD		WAFERBOARD		PARTICLEBOARD				WAFERBOARD			
36→70		36→70		36→93		93→36		36→93		93→36	
MC (%)	Y (in)	MC (%)	Y (in)	MC (%)	Y (in)	MC (%)	Y (in)	MC (%)	Y (in)	MC (%)	Y (in)
7.2	0.0	7.4	0.0	7.6	0.0	20.0	1.018	7.4	0.0	19.5	0.582
7.9	0.185	8.9	0.042	9.7	0.260	19.5	0.943	9.3	0.108	18.8	0.560
8.7	0.273	9.3	0.091	10.8	0.335	18.8	0.856	11.5	0.238	17.6	0.480
9.2	0.292	10.1	0.149	12.3	0.401	16.8	0.695	12.1	0.324	16.1	0.408
9.9	0.346	10.5	0.168	13.3	0.457	13.4	0.618	13.9	0.422	15.5	0.376
10.5	0.365	10.9	0.181	15.4	0.650	10.7	0.540	14.4	0.453	14.6	0.320
10.9	0.379	11.4	0.179	16.1	0.725	9.4	0.513	15.3	0.490	13.8	0.291
11.4	0.398	12.0	0.218	16.5	0.808	8.2	0.504	16.4	0.522	10.8	0.215
12.0	0.419	12.1	0.225	17.4	0.916			17.7	0.552	9.4	0.211
12.2	0.423	12.2	0.226	18.9	0.956			18.7	0.573	8.7	0.204
12.4	0.431	12.5	0.226	19.3	0.995			19.5	0.582	7.9	0.201
12.8	0.436	12.8	0.227	20.0	1.018						
7.5	*0.108	7.8	*0.054								

Y : Midpoint Deflection (in)
MC : Moisture Content (%)
(*) : Residual Deflection (in)

Table 4.3. Midpoint deflection values for cycles A1 and A2.

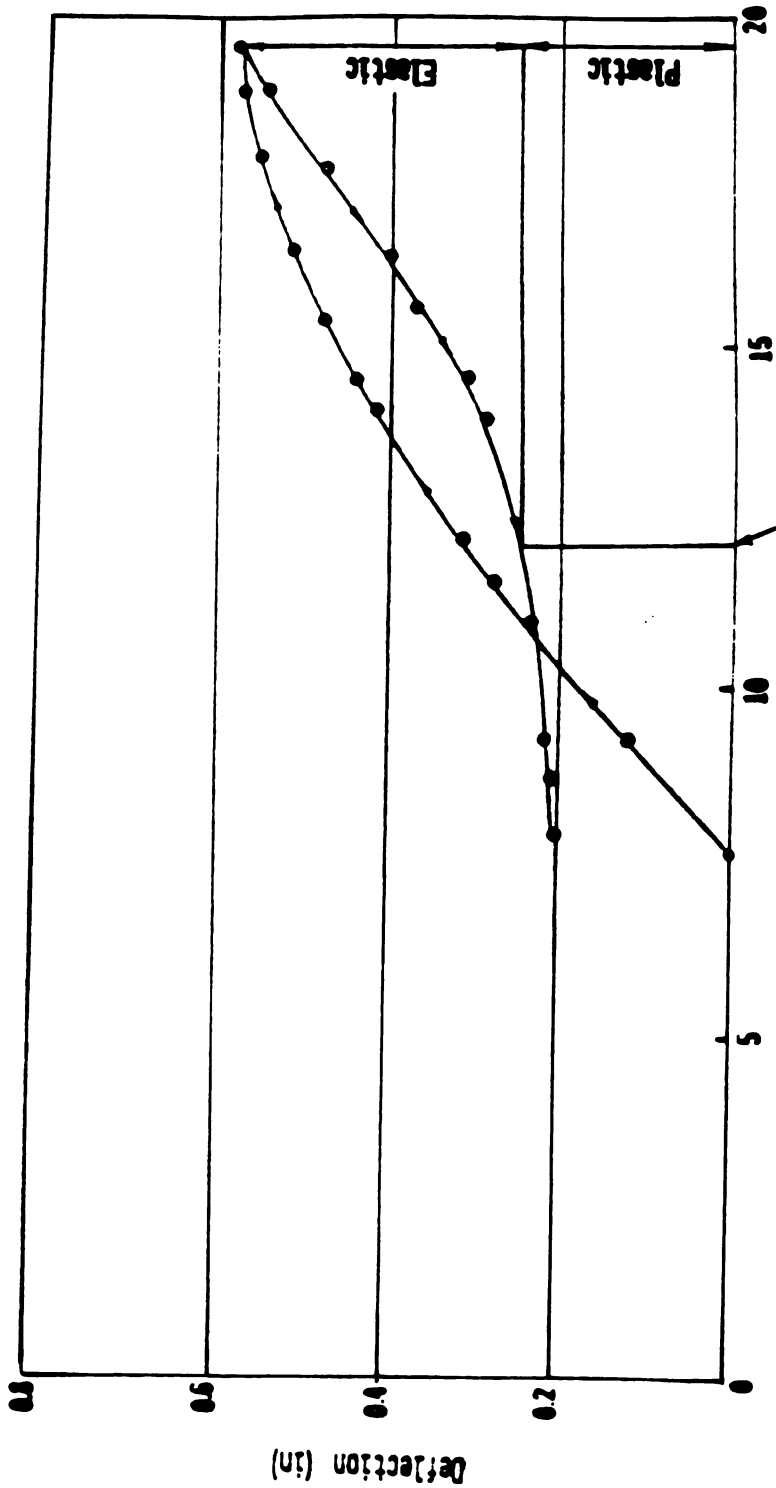

Figure 4.8. Midpoint deflections of waferboard as function of moisture content. Cycle A2, 36 % - 93 % -36 % relative humidity.

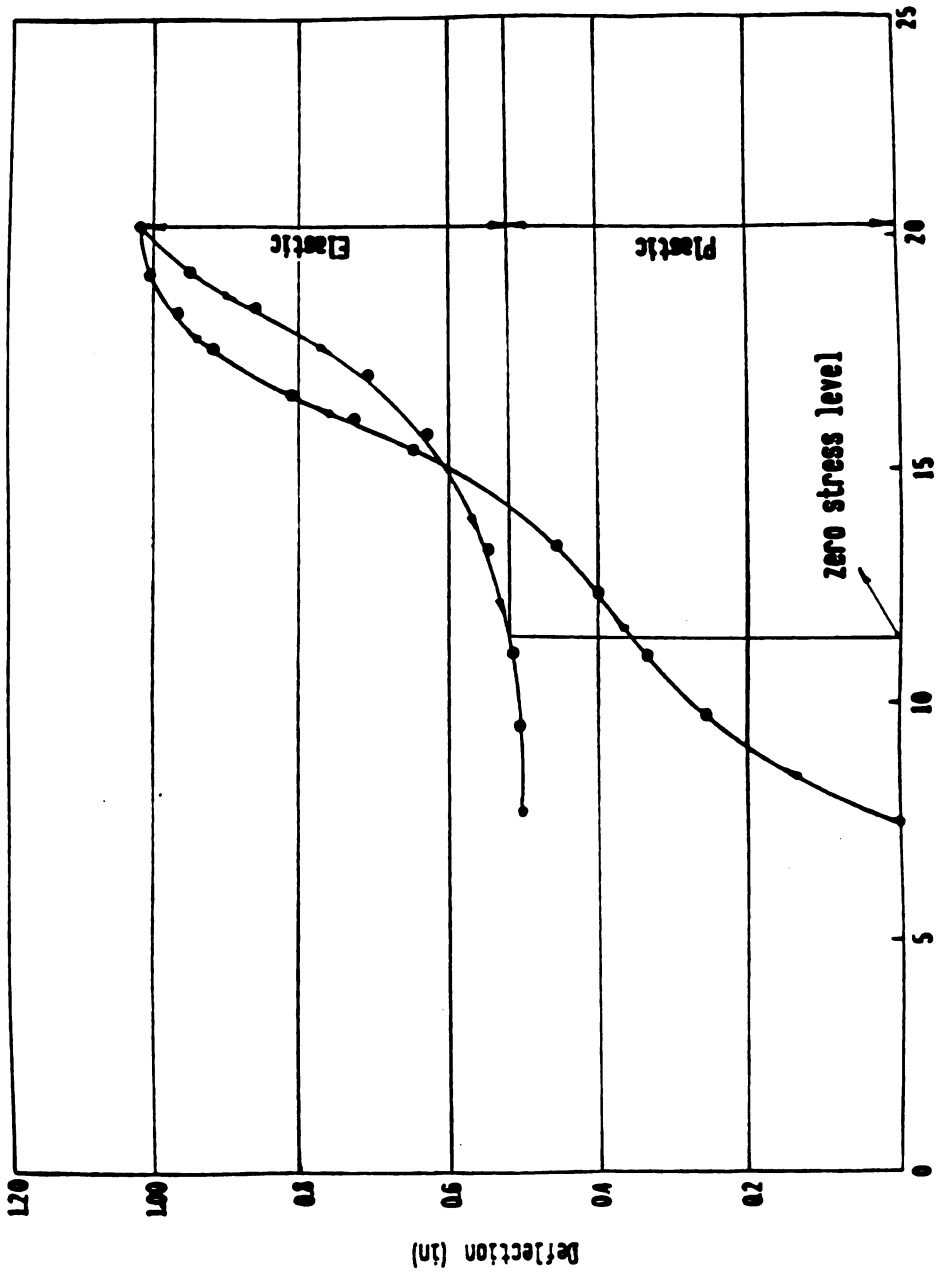

Figure 4.9. Midpoint deflections of particleboard as function of moisture content. Cycle A2, 36 % - 93 % - 36 % relative humidity.

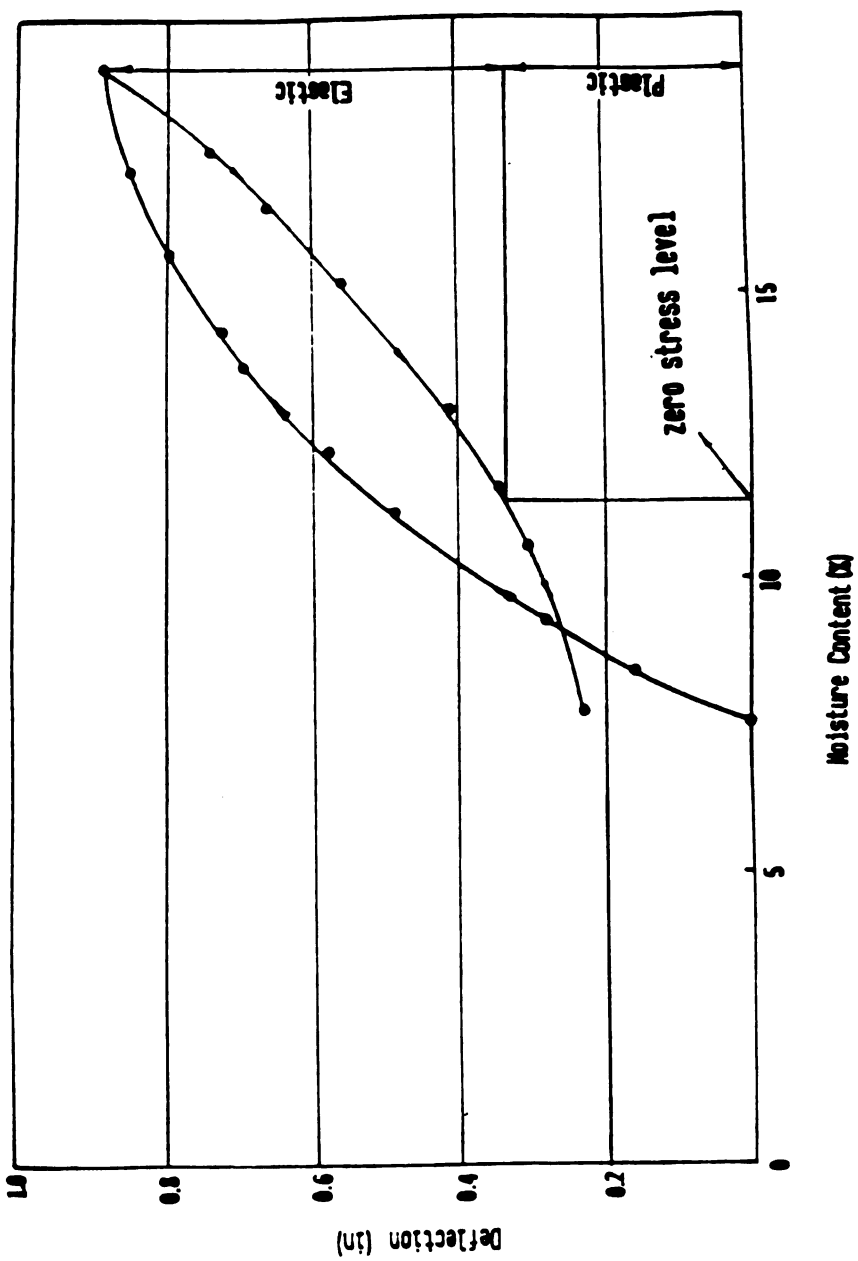

Figure 4.10. Midpoint deflection of oriented strandboard as function of moisture content. Cycle A2, 36 % - 93 % - 36 % relative humidity.

illustrate midpoint deflection of waferboard, particleboard and oriented strandboard in cycle A2. No significant difference was observed between residual deflection of waferboard and oriented strandboard. 0.201 inch residual deflection was determined for waferboard while this value was 0.221 inch for oriented strandboard. The highest residual deflection was measured for particleboard as 0.504 inch.

Similar to cycles A1 and A2, also in cycle B, particleboard resulted in a higher midpoint deflection value of 0.818 inch than waferboard. Waferboard exhibited only 0.345 inch deflection due to the increase in relative humidity from 70 % to 93 % . Figures 4.11 and 4.12 represent the midpoint deflections for waferboard and particleboard as functions of moisture content for cycle B. Table 4.4 also presents the midpoint deflection values of the three types of wood composites in cycles A2 and B.

All three types of wood composites considered in this work resulted in residual deflections at the end of humidity exposure cycles of A1, A2 and B. These residual deflection values were determined as percentage of the maximum deflections and they were found to be 49.5 %, 34.5 % and 24.9 % for particleboard, waferboard and oriented strandboard, respectively, in cycle A2. In cycle A1, 24.8 % and 23.8 % of the maximum deflection of particleboard and waferboard were retained in the specimens when they were released.

CYCLE - A2				CYCLE - B			
ORIENTED STRANDBOARD				PARTICLEBOARD		WAFERBOARD	
36→93		93→36		70→93		70→93	
MC(%)	Y(in)	MC(%)	Y(in)	MC(%)	Y(in)	MC(%)	Y(in)
7.3	0.0	19.0	0.885	12.2	0.0	11.5	0.0
8.5	0.147	17.5	0.730	12.6	0.093	11.8	0.089
9.4	0.278	16.4	0.652	12.9	0.200	12.1	0.313
11.1	0.468	15.2	0.552	15.1	0.484	12.7	0.185
12.2	0.574	12.8	0.404	15.5	0.581	14.2	0.260
13.3	0.684	11.6	0.399	15.9	0.624	14.8	0.281
14.2	0.721	10.5	0.301	17.3	0.757	15.5	0.304
15.7	0.793	7.8	0.221	18.8	0.818	16.2	0.321
17.2	0.852					17.5	0.337
19.0	0.885					18.2	0.344
						19.1	0.345
				7.5	*0.202	8.0	*0.080

Y: Midpoint Deflection (in)
MC : Moisture Content (%)
(*): Residual Deflection (in)

Table 4.4. Midpoint deflection values for cycles A2 and B.

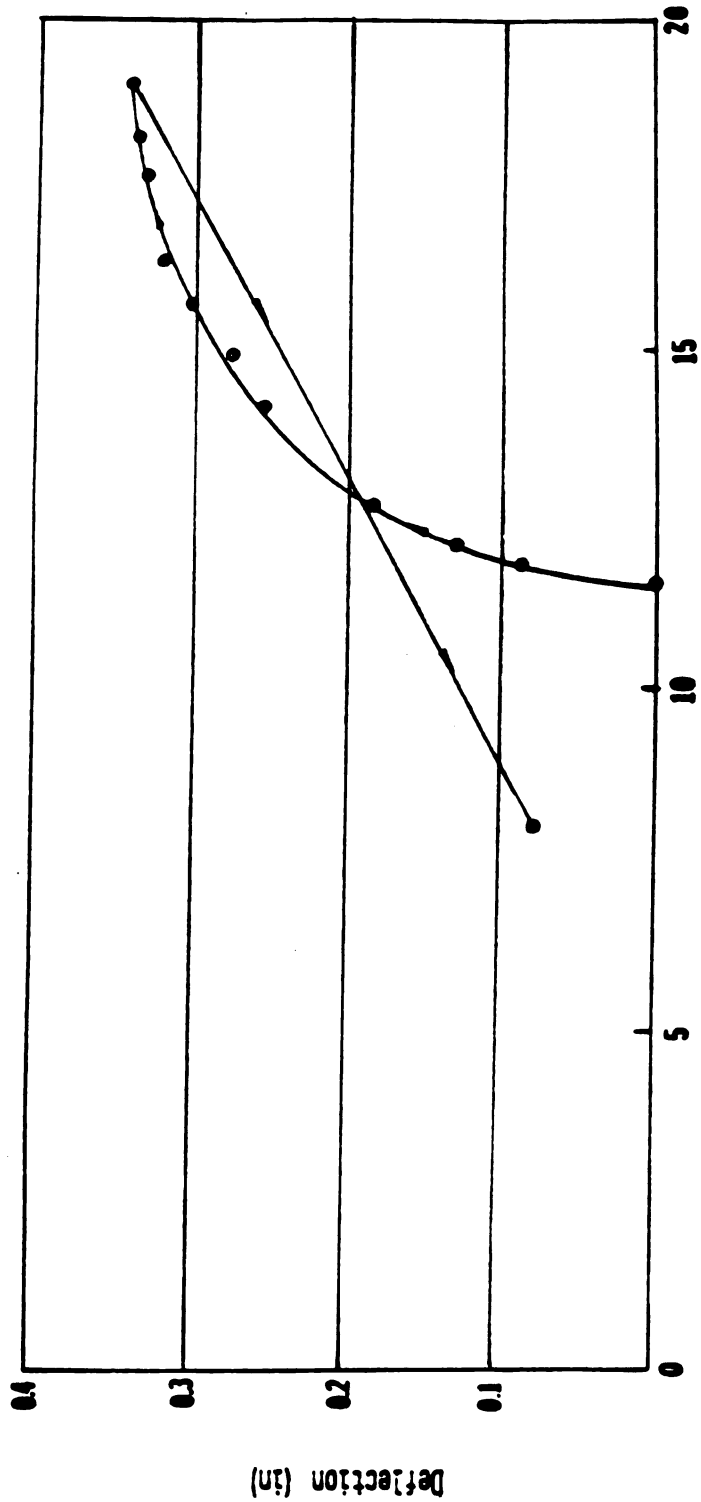

Figure 4.11. Midpoint deflection of waferboard as function of moisture content. Cycle B, 70 % - 93 % - 36 % relative humidity.

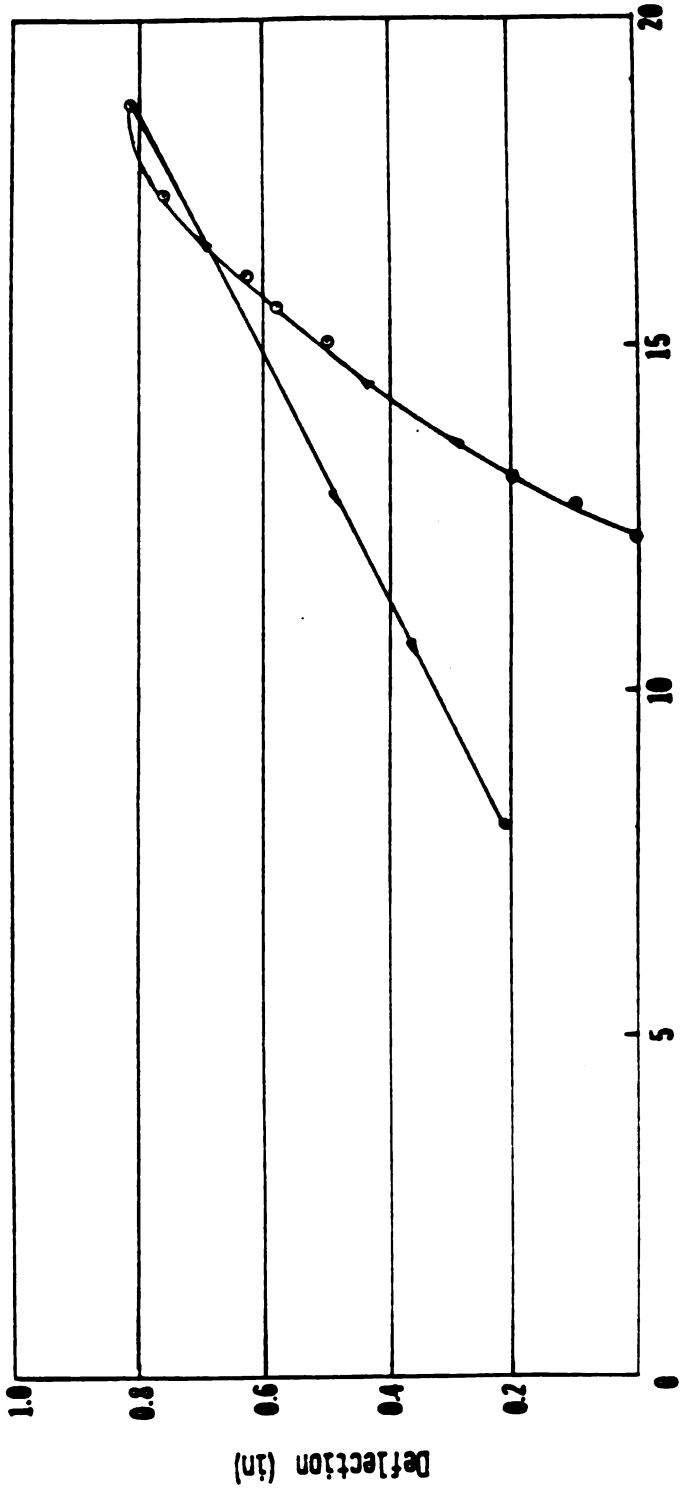

Figure 4.12. Midpoint deflection of particleboard as function of moisture content. Cycle B, 70 % - 93 % - 36 % relative humidity.

Corresponding values for cycle B were observed as 24.7 % and 23.2 % for particleboard and waferboard. Particleboard had the highest percentage of residual deflection in cycle A2. It could be concluded from the above results that particleboard presented more plasticity than waferboard and oriented strandboard. In cycles A1 and B, both waferboard and particleboard did not show any significant difference in terms of residual percentage values which could be related to less extreme humidity levels of that cycle. Less plasticity of waferboard and oriented strandboard could be attributed to their larger particle size and higher slenderness ratio. Moreover, improved continuity of the glue line between flakes of both oriented strandboard and waferboard could be considered to be another factor for their more elastic behaviour [5,26].

4.2.3. Mechanical and Physical Tests

4.2.3.1. Static Bending and Tension Parallel to Surface Tests

The effect of cyclic humidity on static bending properties of the three wood composites were investigated for MOE and MOR. Table 4.5 shows the results of the static bending tests.

It was experimentally observed that change in relative humidity considerably affected bending properties of particleboard, waferboard and oriented strandboard. Furthermore, this influence was more pronounced when the samples were exposed to extreme conditions such as raising

Relative Humidity (%)	STATIC BENDING TEST				TENSION TEST			
	PARTICLEBOARD		WAFERBOARD		PARTICLEBOARD		WAFERBOARD	
	MOE (psi)	MOR (psi)	MOE (psi)	MOR (psi)	MOE (psi)	Tension Strength (psi)	MOE (psi)	Tension Strength (psi)
Cycle A1								
36	259,821	2,023	554,141	3,260	225,953	592	769,670	1,720
70	223,432	1,620	413,150	2,939	179,974	545	612,256	1,240
36	235,132	1,812	485,639	2,991	220,850	577	712,693	1,358
Cycle A2								
36	237,441	1,993	550,400	2,400	282,734	677	601,351	1,555
93	151,077	1,102	195,916	1,190	135,622	240	209,201	784
36	173,619	1,350	308,999	1,651	241,588	526	442,624	894
Cycle B								
70	226,881	1,500	503,141	3,246	301,565	594	580,975	1,796
93	128,534	980	297,765	1,871	117,731	285	282,542	913
36	169,689	1,270	445,964	2,925	244,362	482	510,500	1,579
Cycle C								
93	142,600	1,012	279,184	1,906	149,996	268	300,818	955
36	236,771	1,400	441,781	3,289	335,681	523	435,085	1,517
93	106,124	821	233,819	1,635	109,859	201	247,191	851
Cycle A2	ORIENTED STRANDBOARD							
36	944,412	6,305			498,885	1,219		
93	384,065	2,965			152,879	1,029		
36	675,016	5,065			332,915	783		

Table 4.5. Static bending and tension test results for cyclic relative humidity exposures.

relative humidity from 36 % to 93 % . Table 4.6 shows the average bending test results at the initial relative humidity. Also, in the same table percentage reductions in MOE and MOR are indicated after the samples were exposed to different relative humidity levels during each cycle. As can be seen from Table 4.5 changes in MOE and MOR due to cyclic relative humidity levels of 30 % ,70 %, 36 % were relatively small. Moreover, both MOE and MOR values generally recovered with insignificant amount of permanent loss when the samples were reconditioned to the initial relative humidity of 36 % . Reductions of 32.2 % and 26.7 % in MOE and MOR of particleboard were found due to the cyclic relative humidity exposure in cycle A2. Corresponding values for the same materials as in cycle A1 were determined to 9.5 % and 10.4 % which were lower than those for cycle A1.

The highest MOE and MOR values of particleboard without the consideration of cyclic condition at 36 % relative humidity in cycle A1 were measured as 259,821 psi and 2,023 psi, respectively. The lowest values were found to be 128,534 psi and 980 psi at 93 % relative humidity in cycle B. Figures 4.13 through 4.20 depict MOE and MOR values for different exposure cycles.

Modulus of elasticity in tension and tension strength parallel to the surface of each material were also determined. Results and reductions in tension modulus and tension strength

	PARTICLEBOARD				WAFERBOARD			
	STATIC BENDING TEST		TENSION TEST		STATIC BENDING TEST		TENSION TEST	
	MOE (psi)	MOR (psi)	MOE (psi)	Tension Strength (psi)	MOE (psi)	MOR (psi)	MOE (psi)	Tension Strength (psi)
Cycle-A1								
36% 70% 36%								
Initial Condition	259,821	2,023	225,953	592	554,141	3,260	769,670	1,720
After Cycling	235,132	1,812	220,850	577	485,639	2,940	712,683	1,358
Reduction (%)	9.5	10.4	2.2	2.5	12.3	9.8	7.4	21.0
Cycle-A2								
36% 93% 36%	237,441	1,993	282,724	667	550,400	2,400	601,351	1,555
Initial Condition	237,441	1,993	282,724	667	390,401	2,400	601,351	1,555
After Cycling	173,619	1,350	241,558	526	308,999	1,651	442,624	894
Reduction (%)	26.7	32 2	14.5	21.1	43.6	31.2	26.4	42.5
Cycle-B								
70% 93% 36%								
Initial Condition	226,881	1,500	301,565	594	503,141	3,246	580,975	1,796
After Cycling	169,689	1,275	244,362	482	445,964	2,925	510,500	1,597
Reduction (%)	25.2	15.0	18.8	18.8	11.3	9.8	12.1	12.0
Cycle-C								
93% 36% 93%								
Initial Condition	142,600	1,012	149,996	268	279,184	1,906	300,818	995
After Cycling	106,124	740	109,859	201	233,819	1,635	247,191	851
Reduction (%)	25,5	26.8	26.7	25.0	19.4	14.2	17.8	14.4
	ORIENTED STRANDBOARD							
Cycle-A2								
36% 93% 36%								
Initial Condition	994,412	6,513	489,855	1,219				
After Cycling	675,016	5,065	332,915	783				
Reduction (%)	28.5	19.6	33.2	33.2				

Table 4.6. Effect of relative humidity on mechanical properties of structural wood composites.

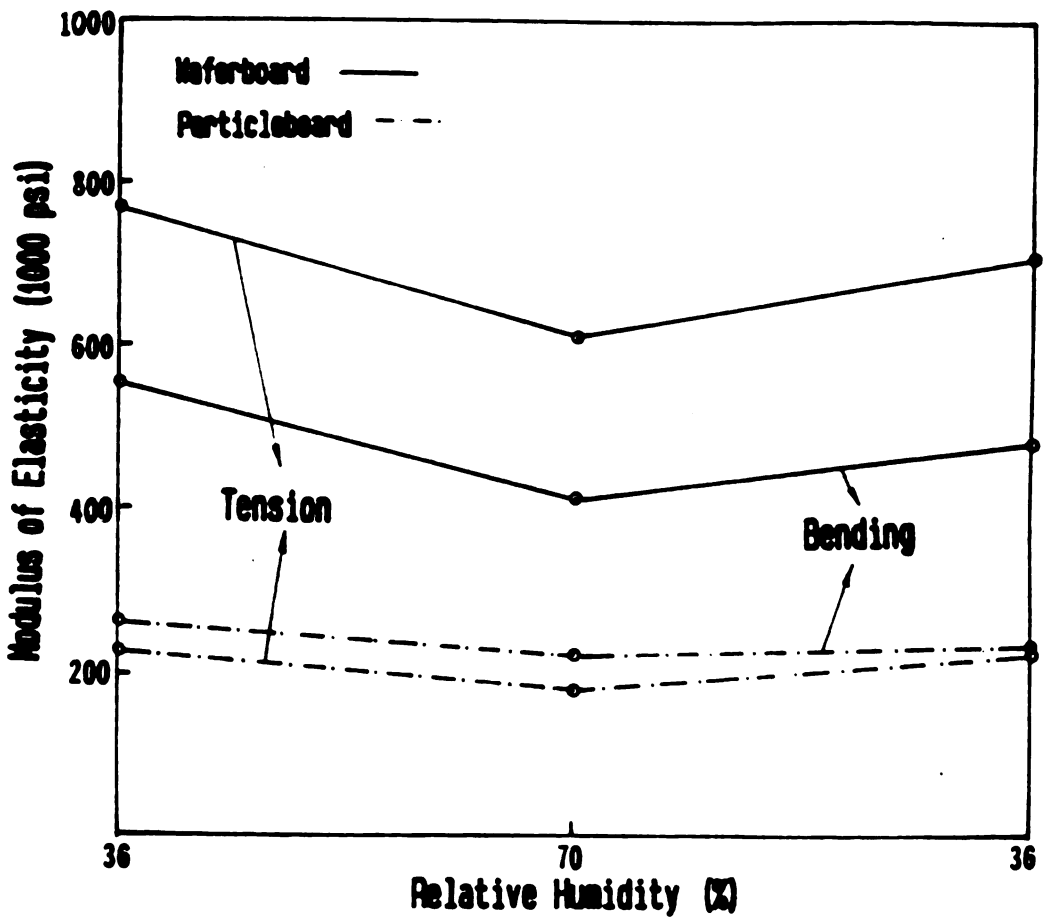

Figure 4.13. Effect of relative humidity on modulus of elasticity in cycle A1.

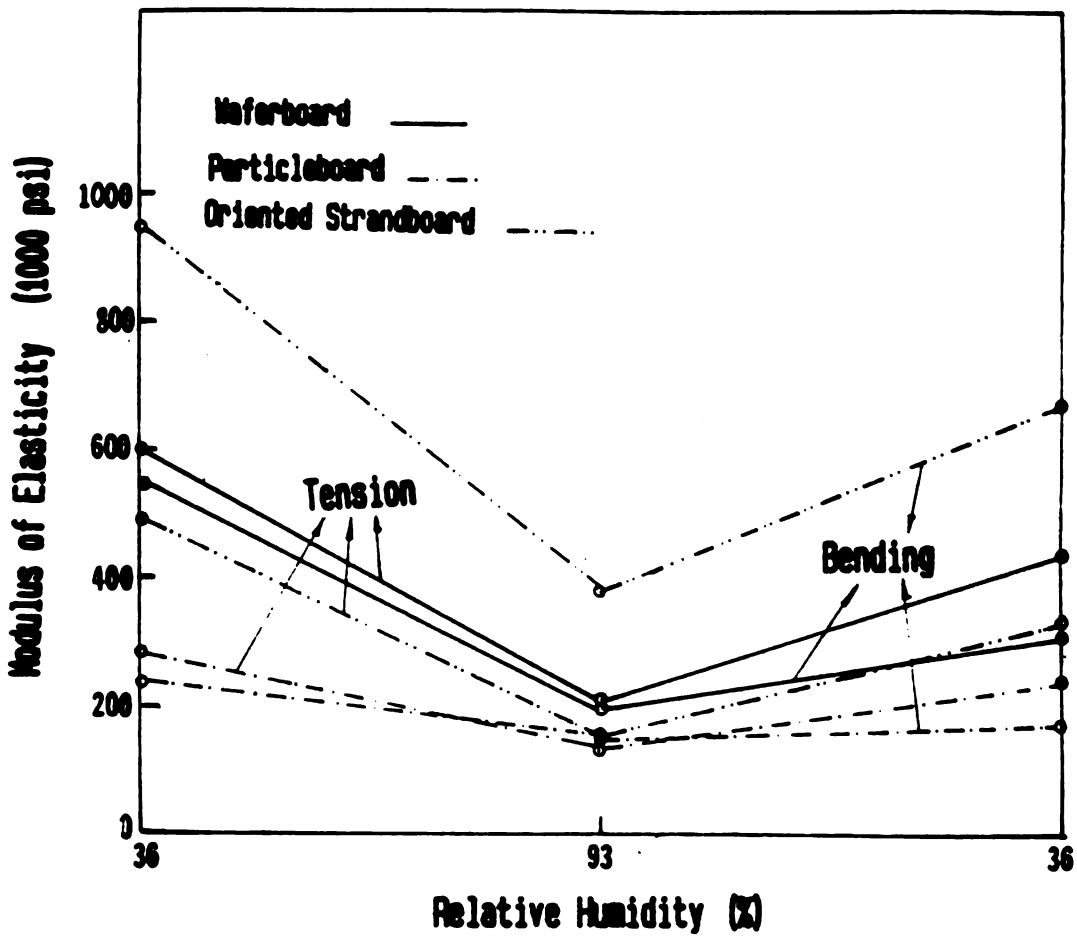

Figure 4.14. Effect of relative humidity on modulus of elasticity in cycle A2.

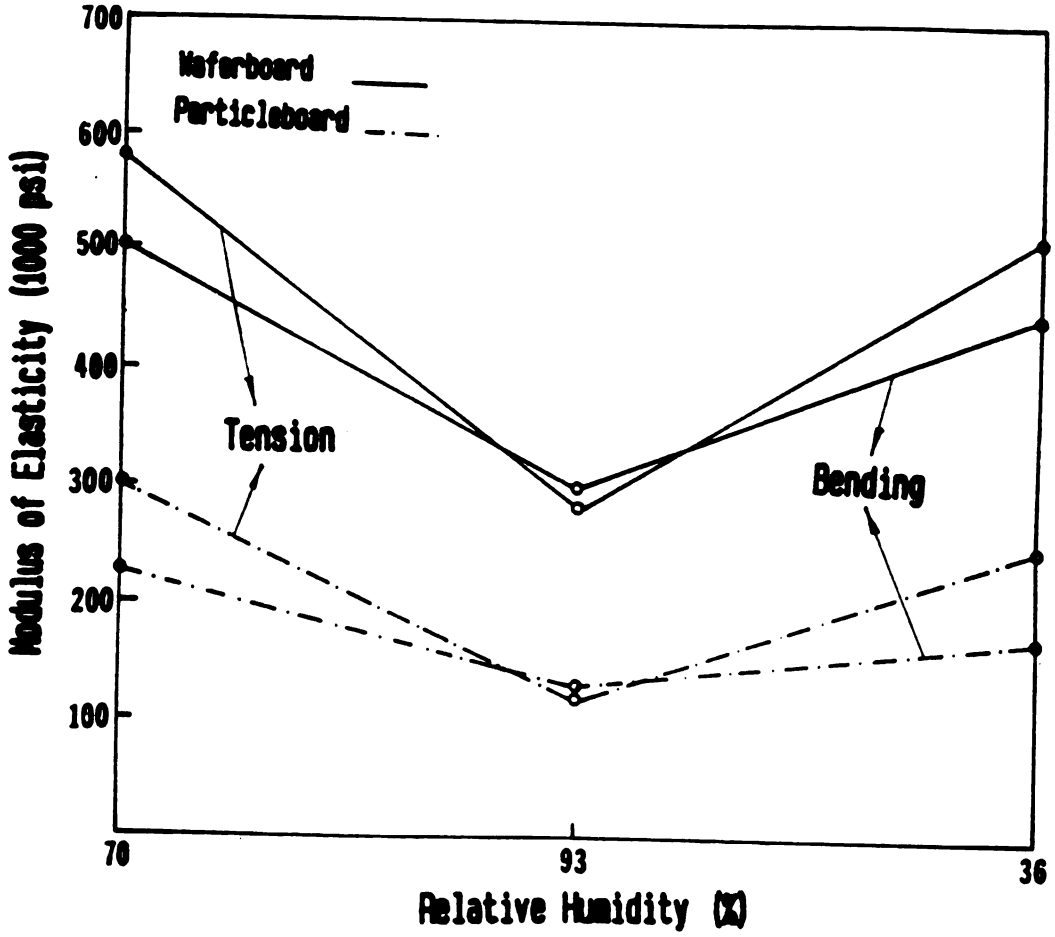

Figure 4.15. Effect of relative humidity on modulus of elasticity in cycle B.

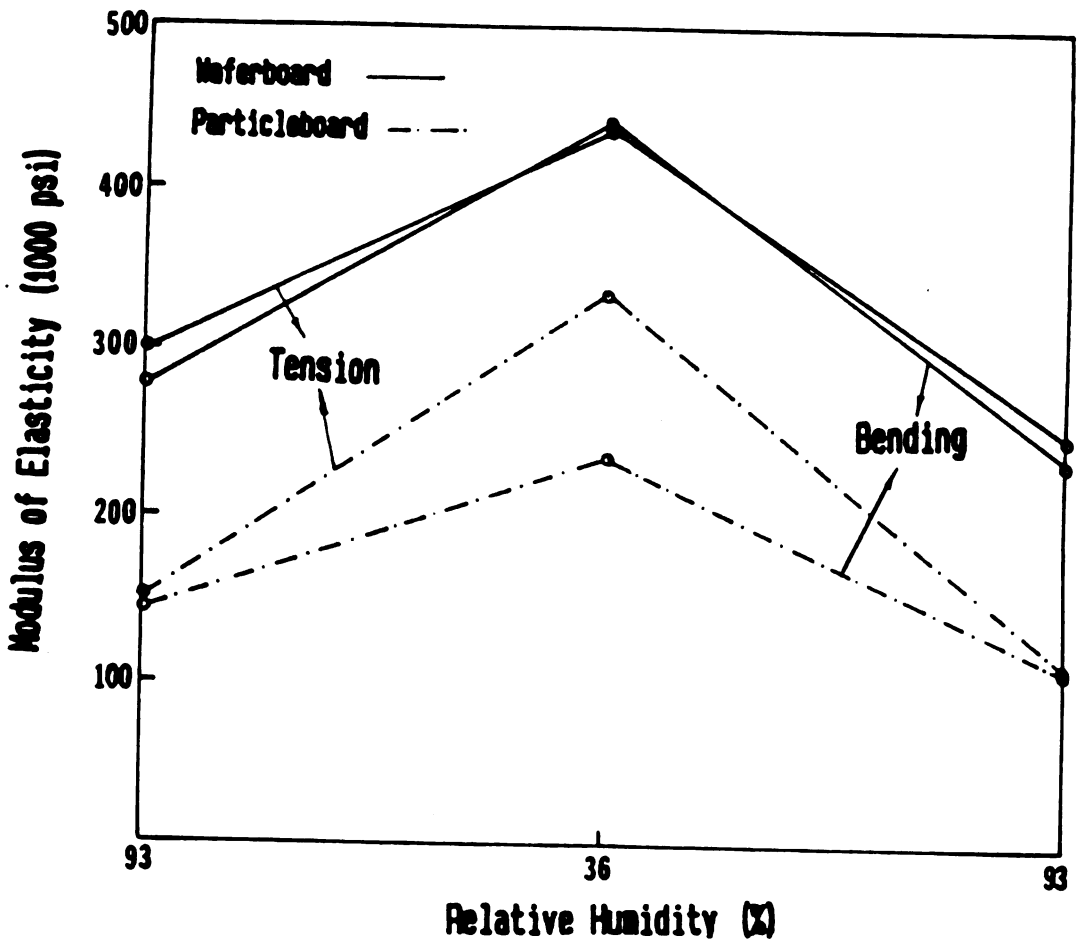

Figure 4.16. Effect of relative humidity on modulus of elasticity in cycle C.

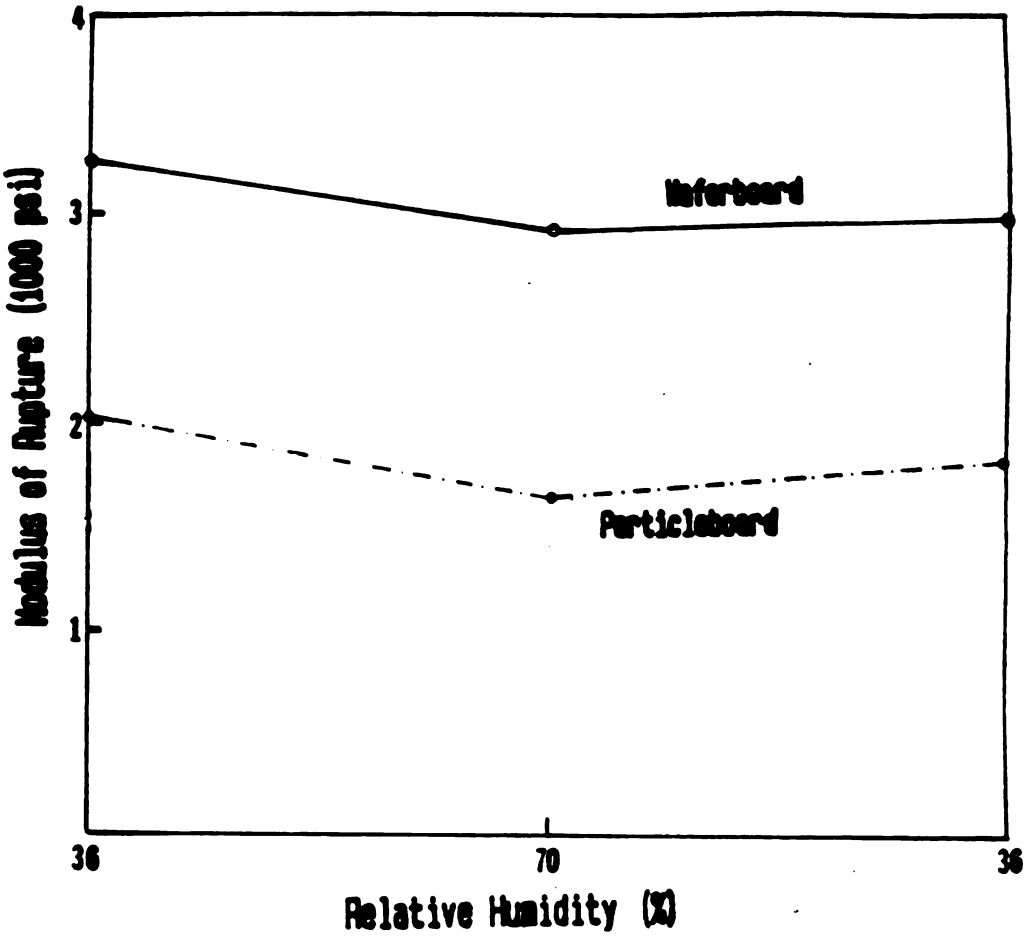

Figure 4.17. Effect of relative humidity on modulus of rupture in cycle A1.

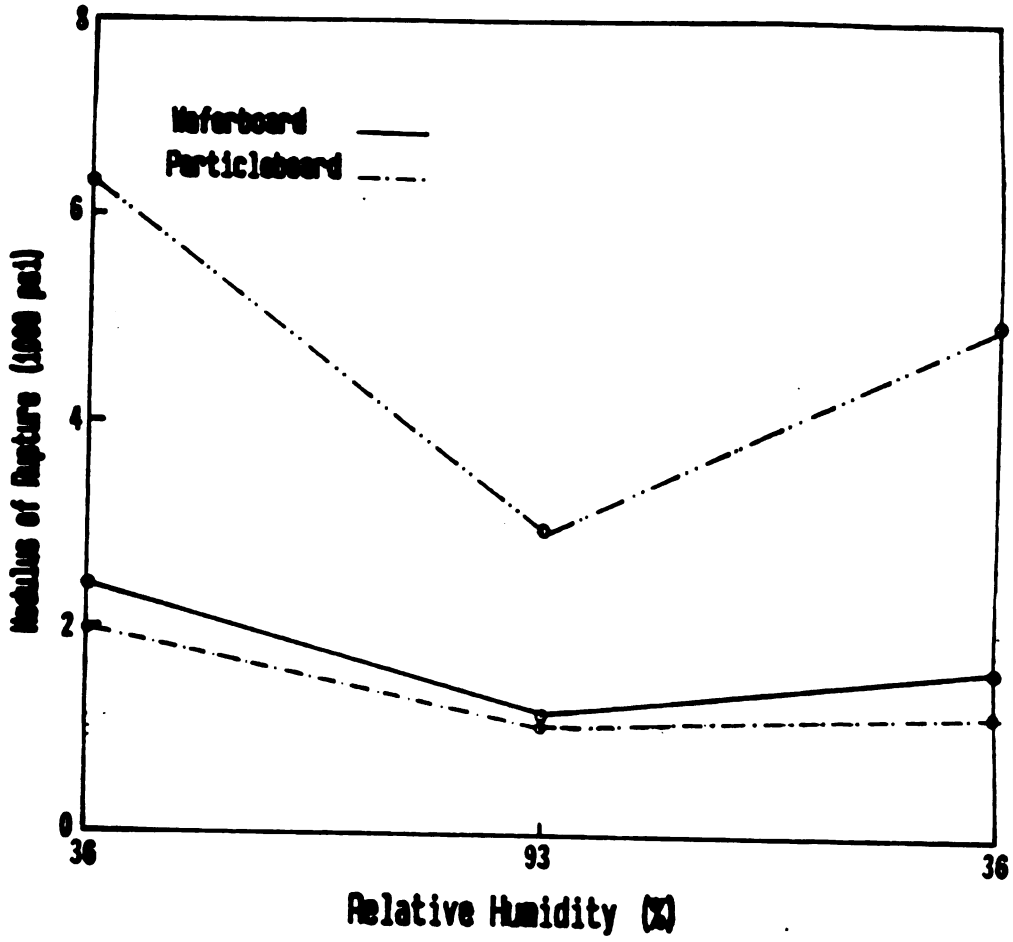

Figure 4.18. Effect of relative humidity on modulus of rupture in cycle A2.

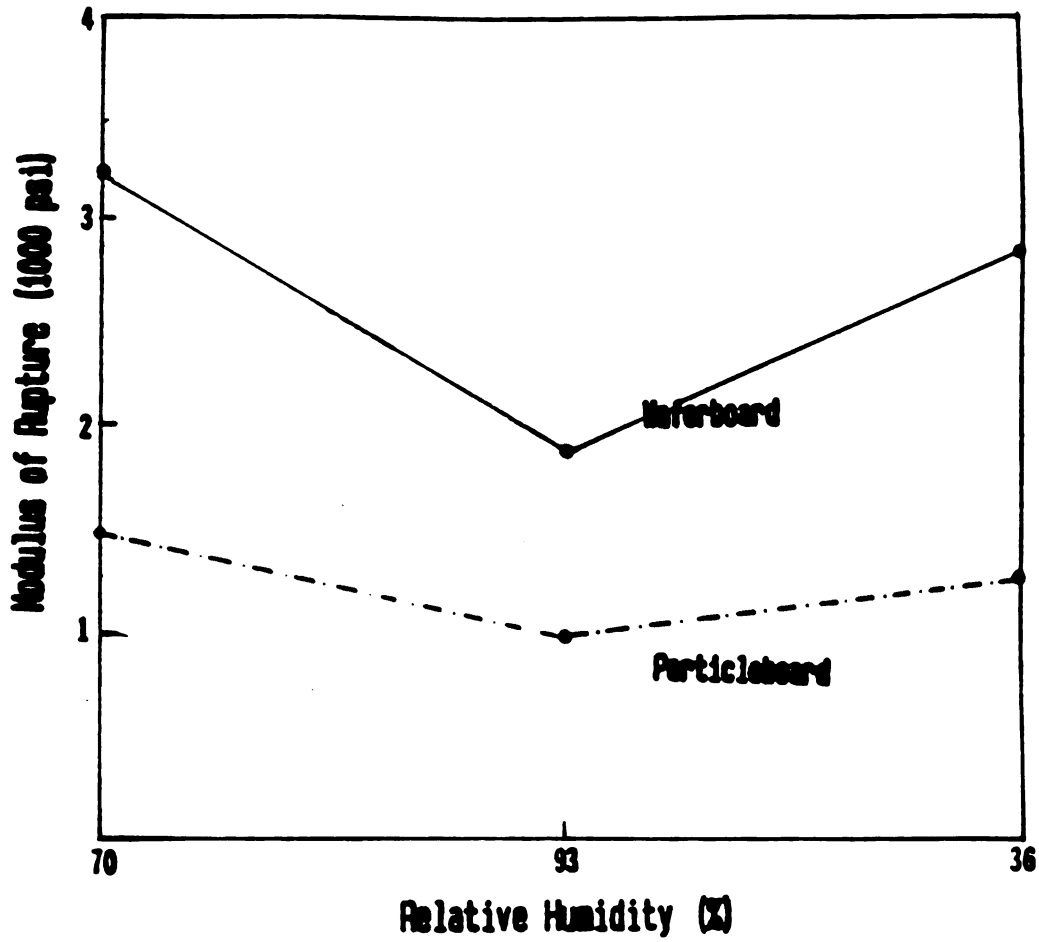

Figure 4.19. Effect of relative humidity on modulus of rupture in cycle B.

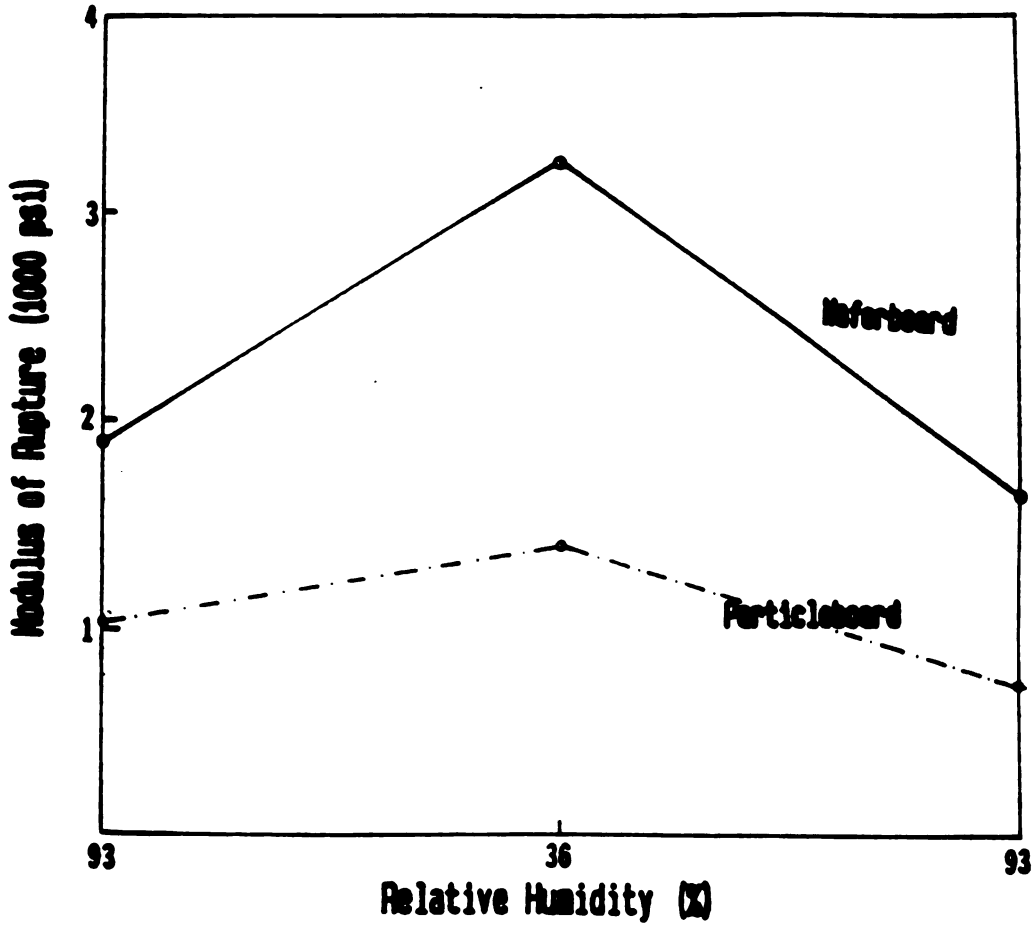

Figure 4.20. Effect of relative humidity on modulus of rupture in cycle C.

due to cyclic relative humidity exposure are given in Tables 4.5, and 4.6.

All of the tension modulus values for waferboard and particleboard were found to be higher than those from bending tests with the exception of particleboard at 36 % relative humidity in cycle A1. Bending modulus of elasticity was determined as 258,821 psi while tension modulus of elasticity was 225,953 psi for this particular case. Higher modulus of elasticity values from tension test can be attributed to elimination of shear forces in the test.

Similarly to the static bending test, tension properties of all types of wood composites considered in this study were also impaired by cyclic humidity exposures. Moreover, higher exposure levels such as in cycles A2 and C resulted in higher reduction in tension characteristics of these wood composite as can be seen from Table 4.6.

Particleboard retained 73 % and 68 % of its original MOE and MOR values due to the exposures in cycle A2 . Corresponding values for waferboard were found to be 79 % for MOE and 69 % for MOR which were slightly higher than those of particleboard in the same cycle. Oriented strandboard also presented similar reductions in percentages of MOE and MOR to the above as given in Table 4.6. Furthermore, cycle A1 presented results similar to the finding of cycle A2 for waferboard and particleboard.

McNatt [51] also pointed out that no significant difference was observed between reduction in MOE and MOR of urea formaldehyde bonded particleboard and phenol formaldehyde bonded waferboard due to exposure of 30 % and 90 % relative humidity cycles. Lee and Biblis [44] reported that retention in MOE and MOR of particleboard were found to be 76 % and 83 % , respectively due to the exposure of the specimen to one cycle of 65-30-65-90 % relative humidity levels. These results are relativly close to the findings of this study.

Cyclic relative humidity exposure had important influence on MOE and MOR properties of all types of wood composites tested in this study [49,51]. Noticible trend towards reduced valus of both static bending and tension properties as relative humidity increased can also be related to deterioration of the internal structure of the wood composites. Cyclic shrinkage and swelling of the panel may result in loosening of the structure and may cause further deterioration which might influence the mechanical strength of the wood composites [45].

4.2.3.2. Linear Expansion and Thickness Swelling Tests

As mentioned previously linear expansion is the most significant factor that affects the development of buckling. Overall linear expansion results were found to be greater for the particleboard than for the other two flake-type products. In panels made from flakes, the grain direction of the wood

lies essentially in the plane of the panel , whereas in particleboard the grain direction of small particles can deviate substantially from the plane of the panel [50,51]. Moreover, random distribution of overlapping wafers restricts linear movement in much the way as cross alignment of veneers in plywood. In addition to particle orientation resin content and particle geometry are also important factors for both improved mechanical and physical properties of structural wood composites [19,21].

Resin content is one of the most important manufacturing variables which affects properties of structural wood composites [23,31,34,36,37,47,48,58]. However, resin content cannot be increased beyond a certain extend due to high cost. As a raw material characteristic, particle geometry can be considered as a significant factor from the linear expansion view point. As presented in section 2.4, particles with higher slenderness ratio result in lower linear expansion than boards made from particles with lower thickness-length ratio [9,58].

Linear expansion of particleboard was from 3.4 to 3.8 times higher than that of waferboard in four humidity cycles. This difference was also reflected as higher buckling deflection values of particleboard in comparison to waferboard and oriented strandboard for all exposure cycles. Moreover, Table 4.7 shows that linear expansion values of waferboard and particleboard in cycle A2 (relative humidity range 36 % - 93%)

Cycle	Relative Humidity (%)	WAFERBOARD				PARTICLEBOARD			
		Moisture Content (%)		Linear Expansion (%)	Linear Expansion Coefficient (1/%)	Moisture Content (%)		Linear Expansion (%)	Linear Expansion Coefficient (1/%)
A1	36 → 70	7.5	12.8	0.088	0.000166	7.2	12.6	0.300	0.000556
	70 → 36	12.8	7.8	-0.076	0.000152	12.6	7.5	-0.280	0.000545
A2	36 → 93	7.4	19.5	0.184	0.000152	7.6	20.0	0.669	0.000540
	93 → 36	19.5	7.9	-0.174	0.000150	20.0	8.2	-0.608	0.000515
B	70 → 93	11.5	19.1	0.116	0.000153	12.2	18.8	0.405	0.000613
	93 → 36	19.1	8.0	-0.172	0.000155	18.8	7.5	-0.700	0.000619
C	93 → 36	18.0	7.3	-0.172	0.000161	18.5	7.5	-0.656	0.000637
	36 → 93	7.3	17.3	0.154	0.000154	7.3	17.9	0.555	0.000556
		ORIENTED STRANDBOARD		$\bar{x}$ = 0.000155				$\bar{x}$ = 0.000572	
A2	36 → 93	7.3	19.0	0.297	0.000254				
	93 → 36	19.0	7.7	0.273	0.000242				
				$\bar{x}$ = 0.000248					

Table 4.7. Linear expansion tests results.

were almost twice as large as in cycle A1. This increase in linear expansion caused the buckling deflection to increase in these materials.

Therefore, it is necessary to improve dimensional stability of wood composites in order to reduce the magnitude of buckling under the restraint conditions. Flake alignment, optimization of resin content, and improved particle geometry are at least partial solutions to the buckling problem.

Thickness swelling is not one of the most important properties of wood composites when they are utilized as structural materials except when one considers the deterioration effect of thickness swelling on bonds between particles.

Based on the experimental findings of this study, oriented strandboard and waferboard exhibited higher thickness swelling values than particleboard. Higher thickness swelling of oriented strandboard and waferboard can be attributed to their large particle size.

Maximum thickness swelling for oriented strandboard, waferboard and particleboard were measured to be 15.71 % , 15.13 %, 9.55 % , respectively as a result of exposures from 47 % to 93 % relative humidities. Samples did not return to their original thicknesses at the end of humidity exposures. This behaviour is defined as irreversible or permanent

thickness swelling which was found to be 7.99 % , 7.68 % and 3.41% for oriented strandboard, waferboard and particleboard, respectively. Thickness swelling test results are given in Table 4.8.

Figure 4.21 illustrates the thickness swelling of the three types of wood composite products as functions of cyclic relative humidity exposures ranging from 47 % to 93 % .

In general the thickness swelling results are in good agreement with earlier findings of Suchsland [75] and, Price and Lehmann [61]. Since wood swells and shrinks more across the grain orientation rather than along the grain, orientation of large flakes in the plane of waferboard and oriented strandboard caused high thickness swelling values. Thickness swelling is also affected by flake thickness, particularly in connection with springback which occurs when equilibrium moisture content exceeds 15 % for most wood composites [29].

4.2.3.3. Sorption Isotherm Test Results

Sorption isotherm characteristics were obtained for all three types of wood products. Table 4.9 presents the average values of isotherm test results for each type of material considered in this study. As can be seen from Figures 4.22, 4.23, and 4.24 no significant differences were found between the isotherm characteristics of waferboard, oriented

THICKNESS SWELLING (%).							
Relative Humidity (%)	Sample #1	Sample #2	Sample #3	Sample #4	Sample #5	Average Value	Standart Deviation
			WAFERBOARD				
66	2.28	2.09	1.44	2.10	1.66	1.91	0.312
81	7.06	7.53	6.81	9.03	7.91	7.66	0.779
93	15.60	15.27	14.25	15.96	14.58	15.13	0.633
81	12.68	14.01	11.57	13.86	13.33	13.09	0.891
66	11.43	11.08	10.12	12.18	11.48	11.25	0.613
47	6.96	8.42	6.92	8.63	7.51	7.68	0.717
			PARTICLEBOARD				
66	1.07	1.00	1.04	1.02	1.03	1.03	0.023
81	3.60	3.64	3.65	2.58	3.63	3.42	0.420
93	9.37	9.30	10.17	9.09	9.86	9.55	0.396
81	9.10	9.04	8.83	8.82	8.80	8.91	0.125
66	6.96	7.44	6.55	6.28	6.53	6.75	0.407
47	3.48	2.65	4.14	3.74	3.06	3.41	0.518
			ORIENTED STRANDBOARD				
66	2.81	1.72	3.39	1.29	1.72	2.18	0.784
81	7.14	6.88	6.67	7.54	6.04	6.85	0.499
93	14.71	13.54	16.37	16.66	17.27	15.71	1.250
81	14.50	14.91	15.06	14.53	13.32	14.46	0.611
66	10.60	11.18	12.00	13.14	11.66	11.51	0.565
47	7.30	7.74	8.73	7.59	8.42	7.95	0.534

Table 4.8. Thickness swelling test results.

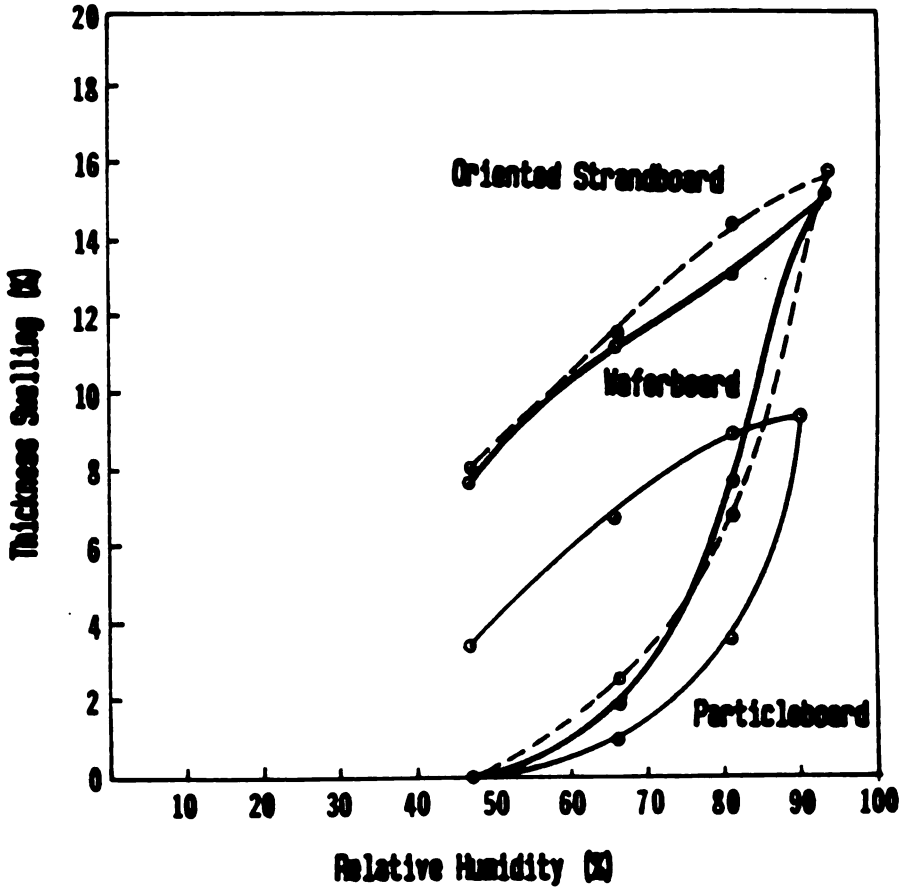

Figure 4.21. Thickness swelling values as function of relative humidity.

Relative Humidity (%)	Moisture Content (%)		
	Waferboard	Particleboard	Oriented Strandboard
20	5.3	4.7	4.2
47	7.9	7.8	7.3
66	10.1	9.8	9.8
81	13.8	13.6	13.9
93	18.7	18.4	18.8
81	16.1	15.3	17.1
66	12.6	12.8	13.8
47	9.7	10.1	9.7
20	6.3	5.7	5.5

Table 4.9. Sorption isotherm results.

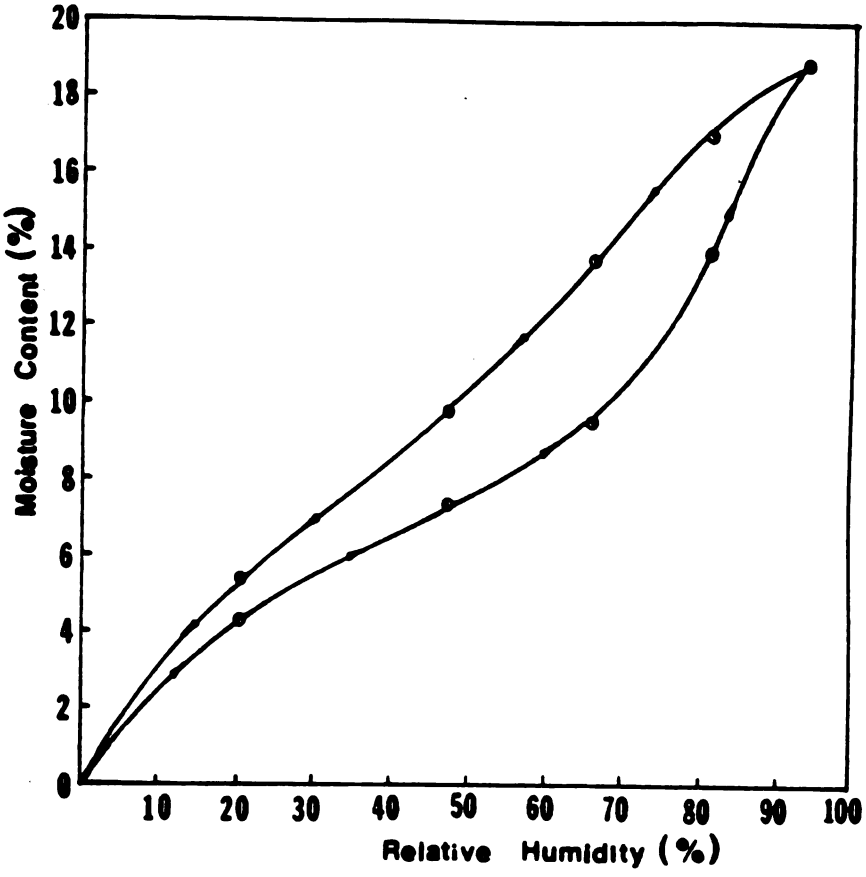

Figure 4.22. Isotherm characteristics of oriented strandboard.

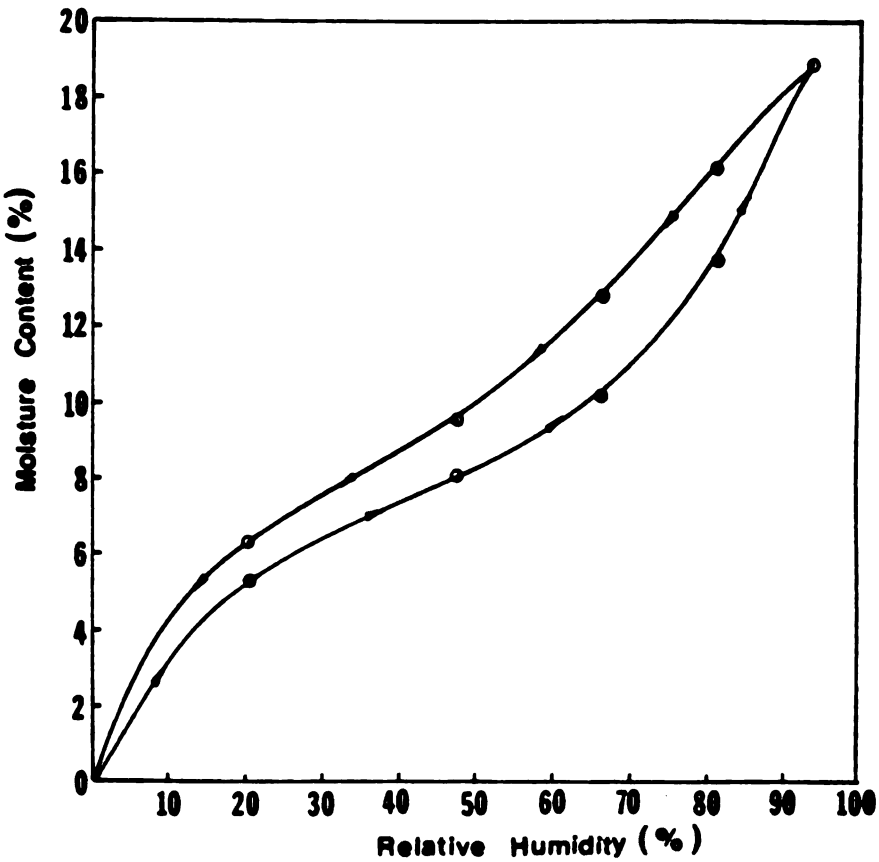

Figure 4.23. Isotherm characteristics of particleboard.

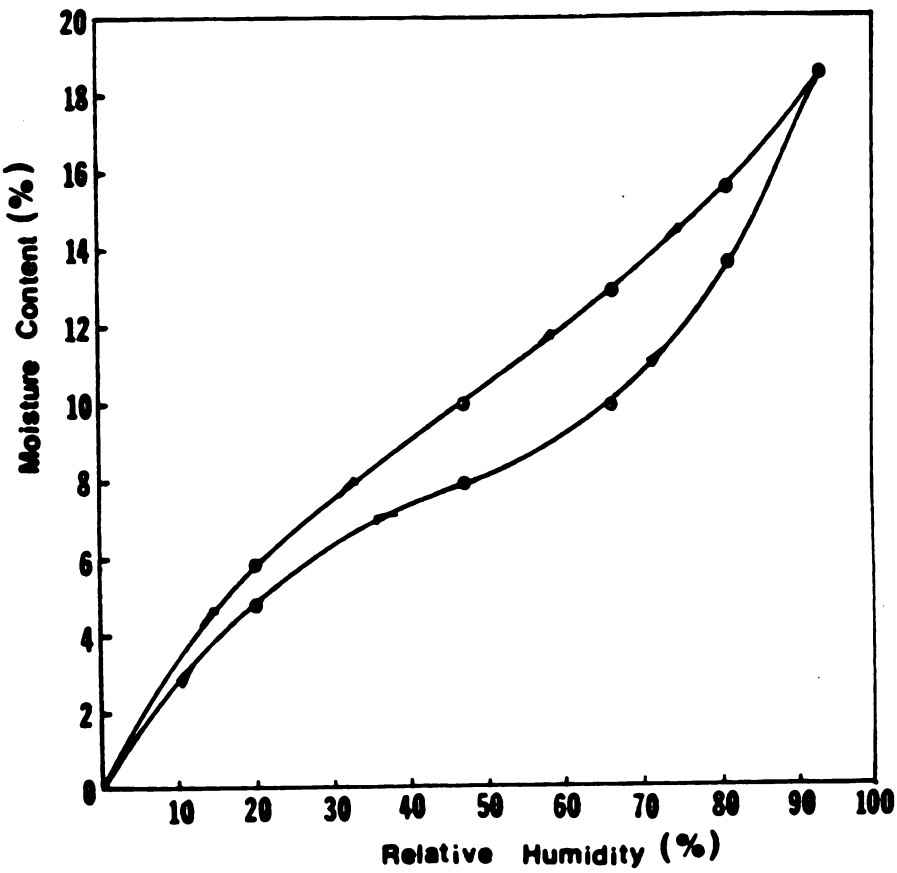

Figure 4.24. Isotherm characterics of waferboard.

strandboard and particleboard. However, particleboard exhibited slightly lower equilibrium moisture content values in the desorption phase. Additionally, equilibrium moisture content values of the cycled test specimens were very close to those obtained from the isotherm curves.

4.3. Results and Discussions of Theoretical Stresses and Deformations.

4.3.1. Theoretical Bending Deformations.

According to calculations which were described in section 2.3.2, theoretical deflections of waferboard, particleboard and oriented strandboard strips with fixed ends were determined as can be seen in Figures 4.25, 4.26, and 4.27. 0 % , 7 % and 12 % of initial moisture contents were used in calculations of the theoretical deflections. As indicated previously, 36.5 inch effective length of each type of material was employed for computations. However, in most applications 4 ft by 8 ft structural panels are restrained at their center by nailing on a base which results in about 24 inch of span with fixed ends. Therefore, deflection behaviour of a 24 inch long columns for three different kinds of wood composites was also determined theoretically as illustrated in Figures 4.25, 4.26 and 4.27.

In this study, deflections were estimated theoretically based on elasticity. Also assumed throughout the calculations

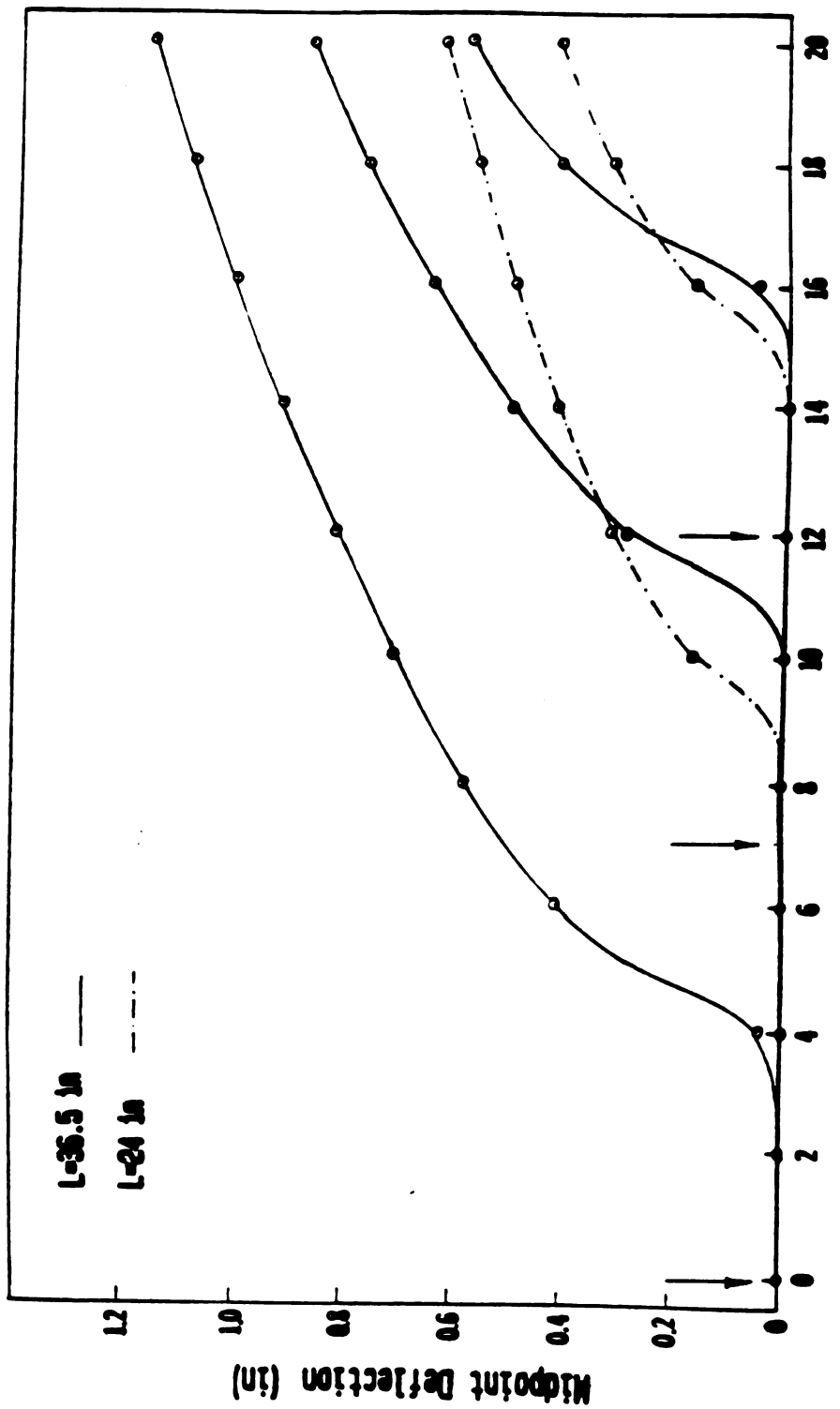

Figure 4.25. Theoretical midpoint deflections of restrained waferboard strips.

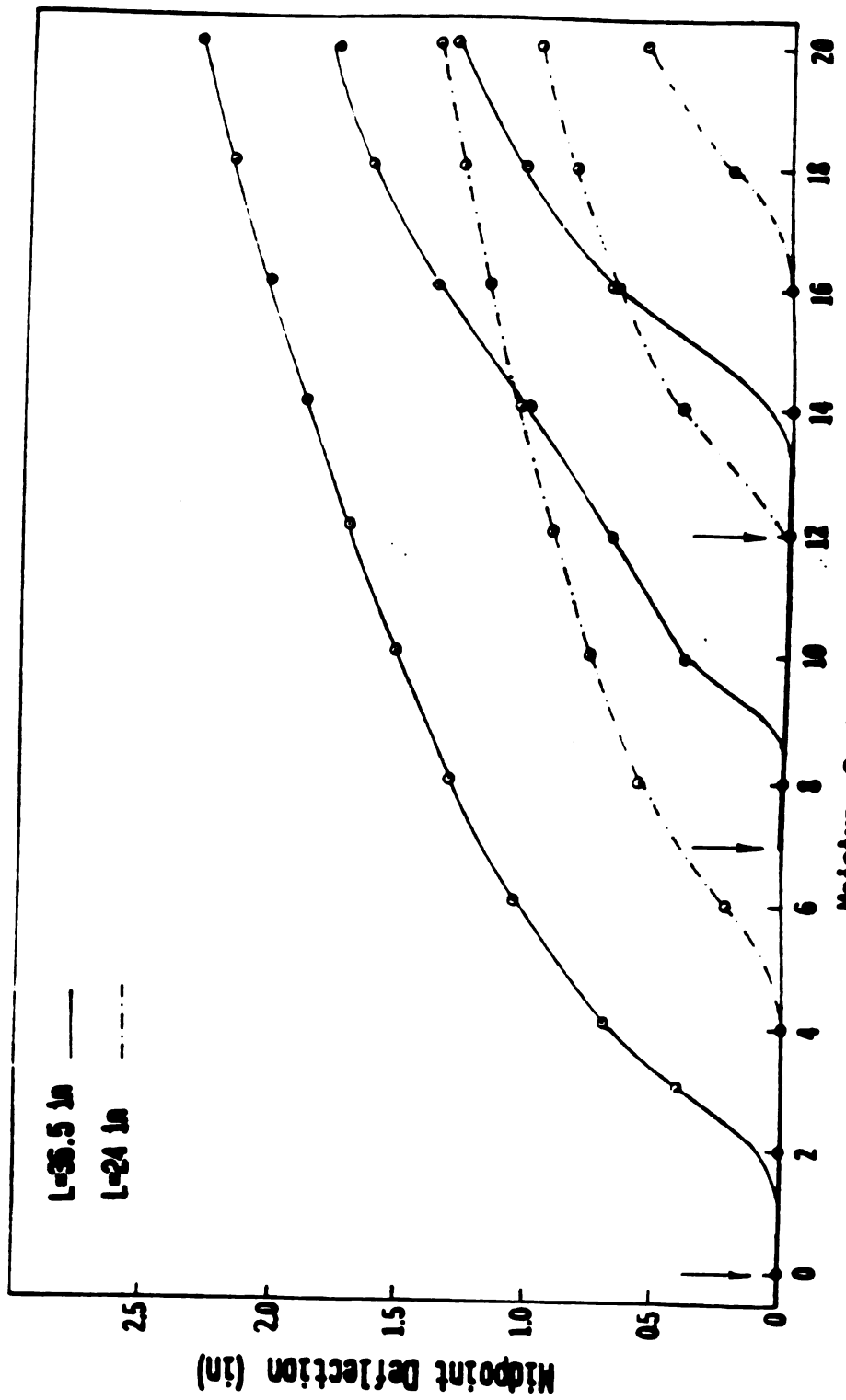

Figure 4.26. Theoretical midpoint deflections of restrained particleboard strips.

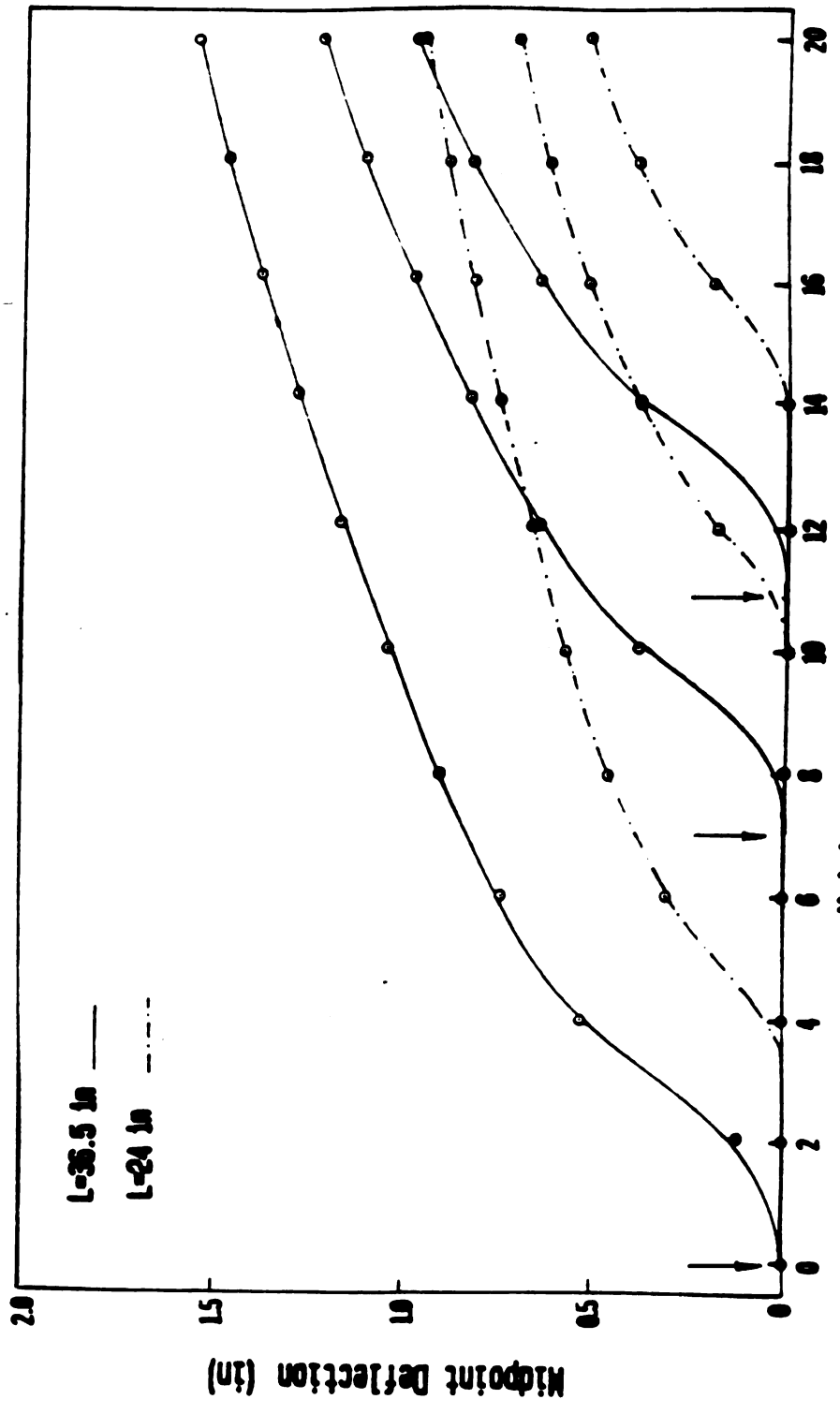

Figure 4.27. Theoretical midpoint deflections of restrained oriented strandboard strips.

was that the moisture content was uniformly distributed over the cross section of the wood composite and that the initial deflection was zero. Average linear expansion coefficients obtained from the experiments for each type of product were used for the theoretical computations.

Particleboard exhibited the highest deflection values as compared to those of waferboard and oriented strandboard (see Figures 4.26, 4.27, 4.28). Waferboard resulted in the lowest values of deflection as a function of moisture content change.

It was determined that theoretical deflection values were found to be higher than the experimental deflections for all types of wood composites considered in this study.

The difference in theoretical and experimental deflection values may be due to a less than uniform moisture content distribution in the test specimens.

Columns with 24 inch length showed smaller deflections than the longer columns as expected (Figure 2.2) . Suchsland [76] reported that theoretical deflection of hardboard with fixed ends were quite similar to those obtained from the experiments. More uniform material structure of hardboard and smaller cross section of the test samples can be the reasons for the similarity between experimental and theoretical deflection values in Suchsland's study.

However, differences between theoretical and experimental

values from the result of this investigation can be related to two major factors. Thickness of particleboard, oriented strandboard and waferboard specimen is greater than that of hardboard specimens in Suchsland's study. As discussed in section 4.2.1, thickness of wood composite may be one of the major factors on the uniformity of moisture content distribution over the cross section.

4.3.2. Theoretical Bending Stresses from Theoretical Buckling Deformations

Equation (2.38) was employed to calculate maximum theoretical compressive bending stresses in restrained wood composite columns due to change in moisture content. These stresses are presented in Figures 4.28, 4.29, and 4.30.

Again, 0% ,7 % and 12 % initial moisture content were also used to determine development of theoretical stresses. 24 inch and 36.5 inch spans for each type of wood composite were considered throughout the stress calculations. Tables 4.10 and 4.11 present the results of theoretical stresses and MOE values at different relative humidity levels used for the calculations, respectively. Also shown in Figures 4.28, 4.29, and 4.30 are the ultimate bending strength values, determined by means of static bending tests at various humidities. The figures indicate that under the exposure conditions the bending stresses caused by buckling exceed the bending strength in

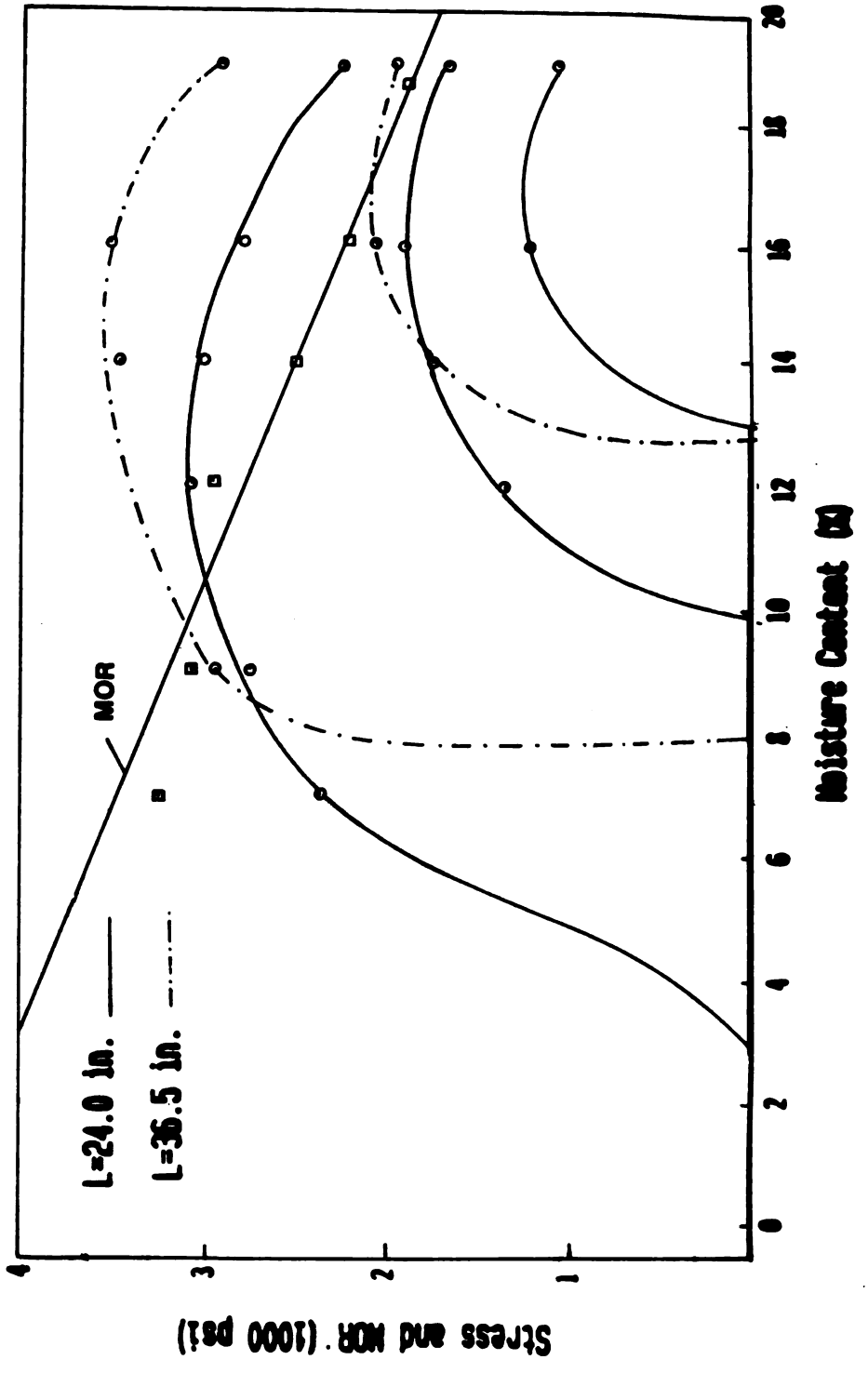

Figure 4.28. Theoretical bending stresses of restrained waferboard strips as function of moisture content.

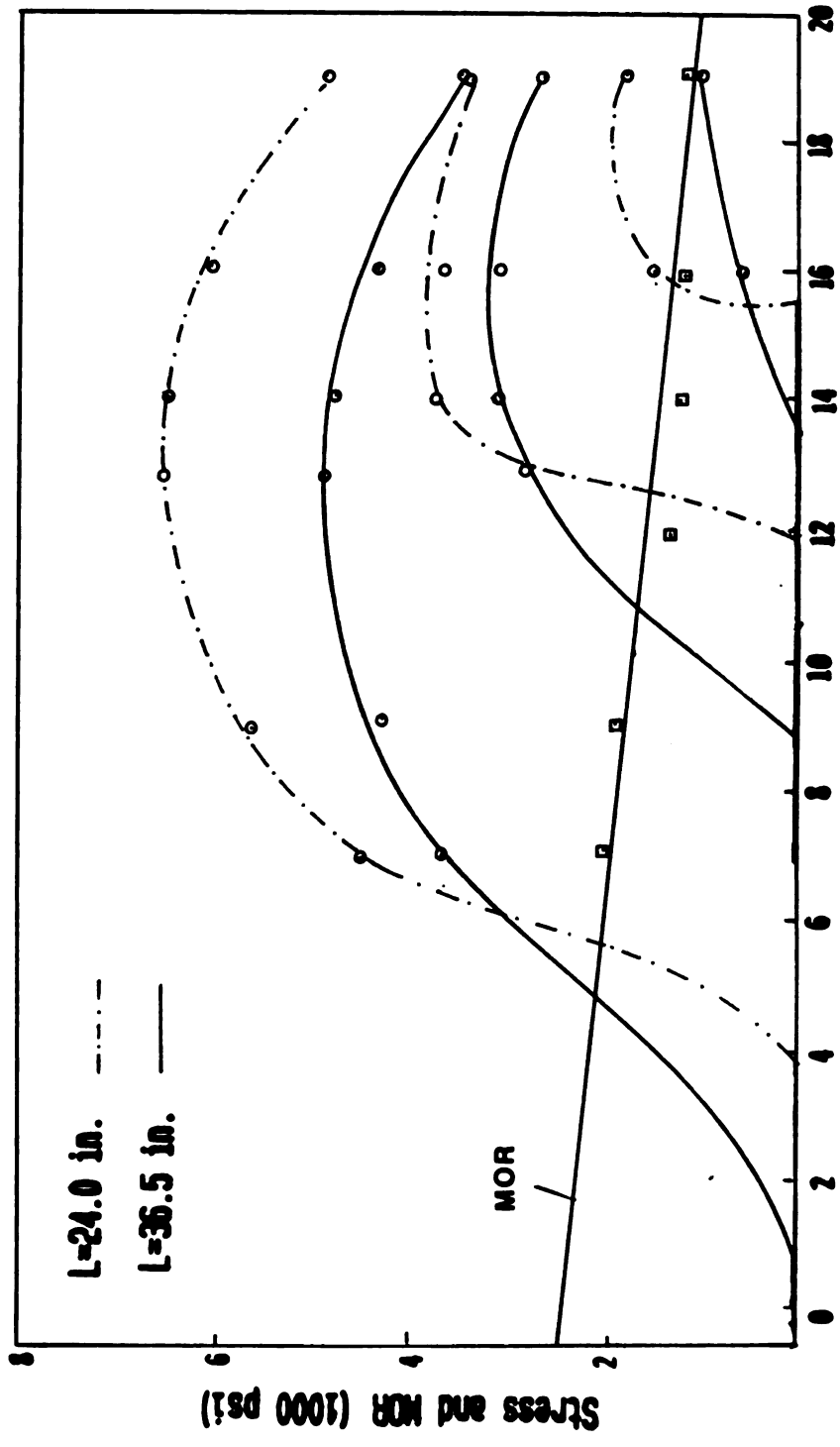

Figure 4.29. Theoretical bending stresses of restrained particleboard strips as function of moisture content.

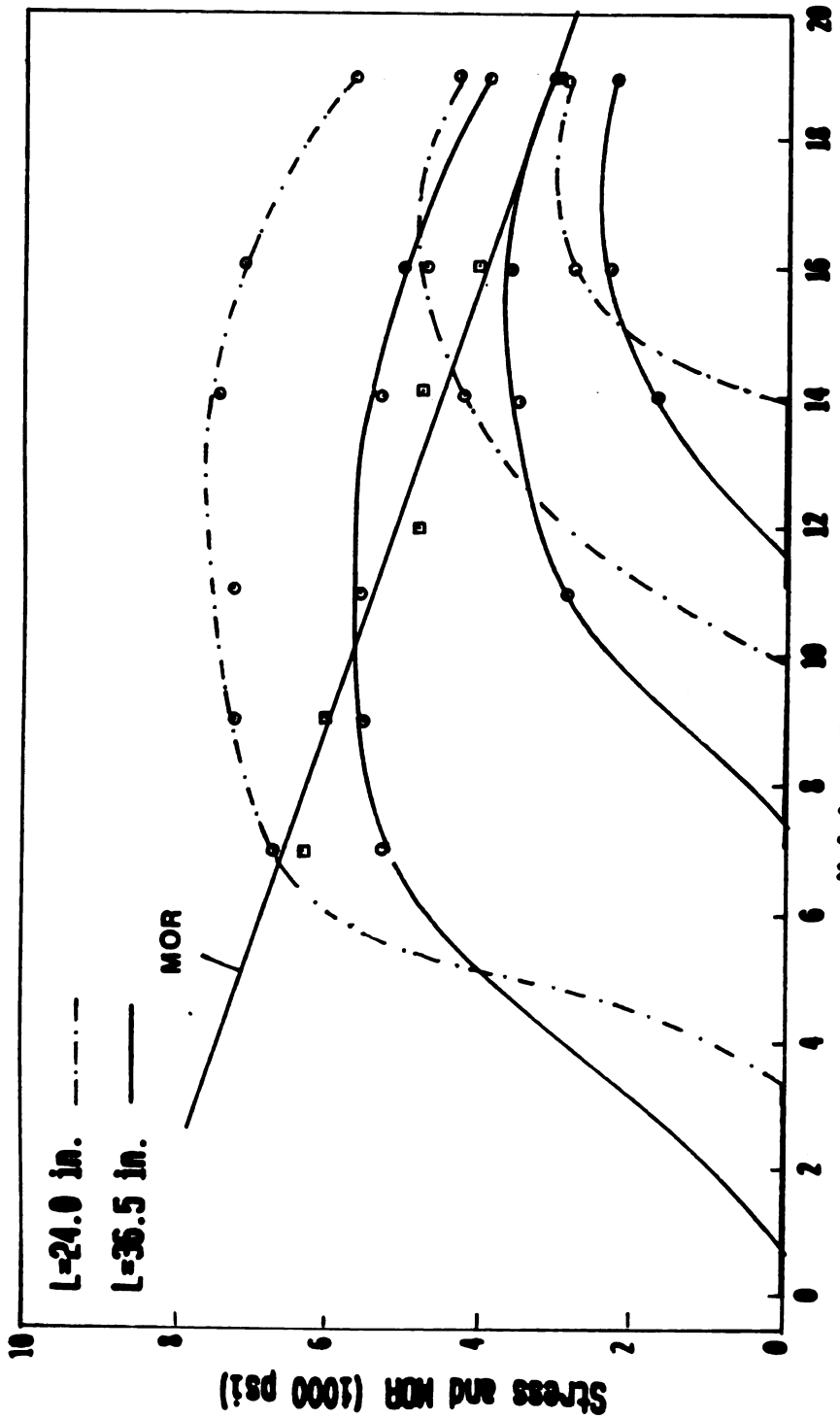

Figure 4.30. Theoretical bending stresses of restrained oriented strandboard strips as function of moisture content.

MC (%)	STRESS (psi)																	
	PARTICLEBOARD						WAFERBOARD						ORIENTED STRANDBOARD					
	L=24 in			L=36.5 in			L=24 in			L=36.5 in			in L=24 in			L=36.5 in		
0	0			0			0			0			0			0		
1																		
2																		
3																		
4																		
5																		
6																		
7	4399	0		3626	0		2938			2389			6263	0		5274	0	
8																		
9	5617			4232				726		2750			7190			5531		
10																		
11													7541		0	5550	2843	0
12	6457	3753	0						0	3043								
13				4824	2932	0						0				5295	3537	1738
14				4739	3090		3456			3001			7443					
15																4999	3620	2476
16	5910	3619	1880	4259	3038		3512	2053		2780		1229	7124	4707	2371			
17																		
18																3935	3066	2230
19	4818	4818	1920	3400	2627	1871	2909	1943		2234	1672	1085	5703	4233	3044			
20																		

Table 4.10. Theoretical bending stresses of restrained strips as function of moisture content.

Relative Humidity (%)	WAFERBOARD		PARTICLEBOARD		ORIENTED STRANDBOARD	
	MOE (psi)	MOR (psi)	MOE (psi)	MOR (psi)	MOE (psi)	MOR (psi)
36	554,273	3,246	248,631	1,724	944,912	6,300
55	509,140	3,114	245,955	1,600	814,796	6,003
70	458,145	2,991	225,156	1,041	728,658	4,780
80	405,366	3,240	212,117	980	602,544	4,402
86	356,150	3,485	176,665	1,005	564,510	4,012
93	251,621	1,906	128,534	788	384,065	2,905

Table 4.11. Static bending test results at different relative humidities.

most cases, resulting in failure of the board.

The practical evidence is, of course, that does not happen. The theoretical calculations based on the assumption of elasticity, therefore, overestimate the bending stresses. The reason for the discrepancy is as indicated earlier, the less than elastic behaviour of these materials. This is illustrated by relatively low axial stresses (the only stress that can be measured) and by substantial residual bending deformations. The discrepancy is the largest in the case of particleboard, because it has the largest linear expansion coefficient leading to larger theoretical bending deformations.

4.3.3. Theoretical Bending Stresses from Measured Buckling Deflections

To allow for the visco-elastic behaviour of the tested materials, the theoretical calculations were modified, first by using the actual measured bending deflections as input into Eq. (2.38) and secondly by idendifying an " elastic " portion of the measured bending deflection and using it as an input into Eq. (2.38). The "elastic" portion of the measured bending deflection was idendified as that portion that was recovered upon redrying as the axial stresses reached zero (Figure 4.31).

Both results are shown in Figures 4.32, 4.33, and 4.34. There is a considerable reduction in the estimated bending

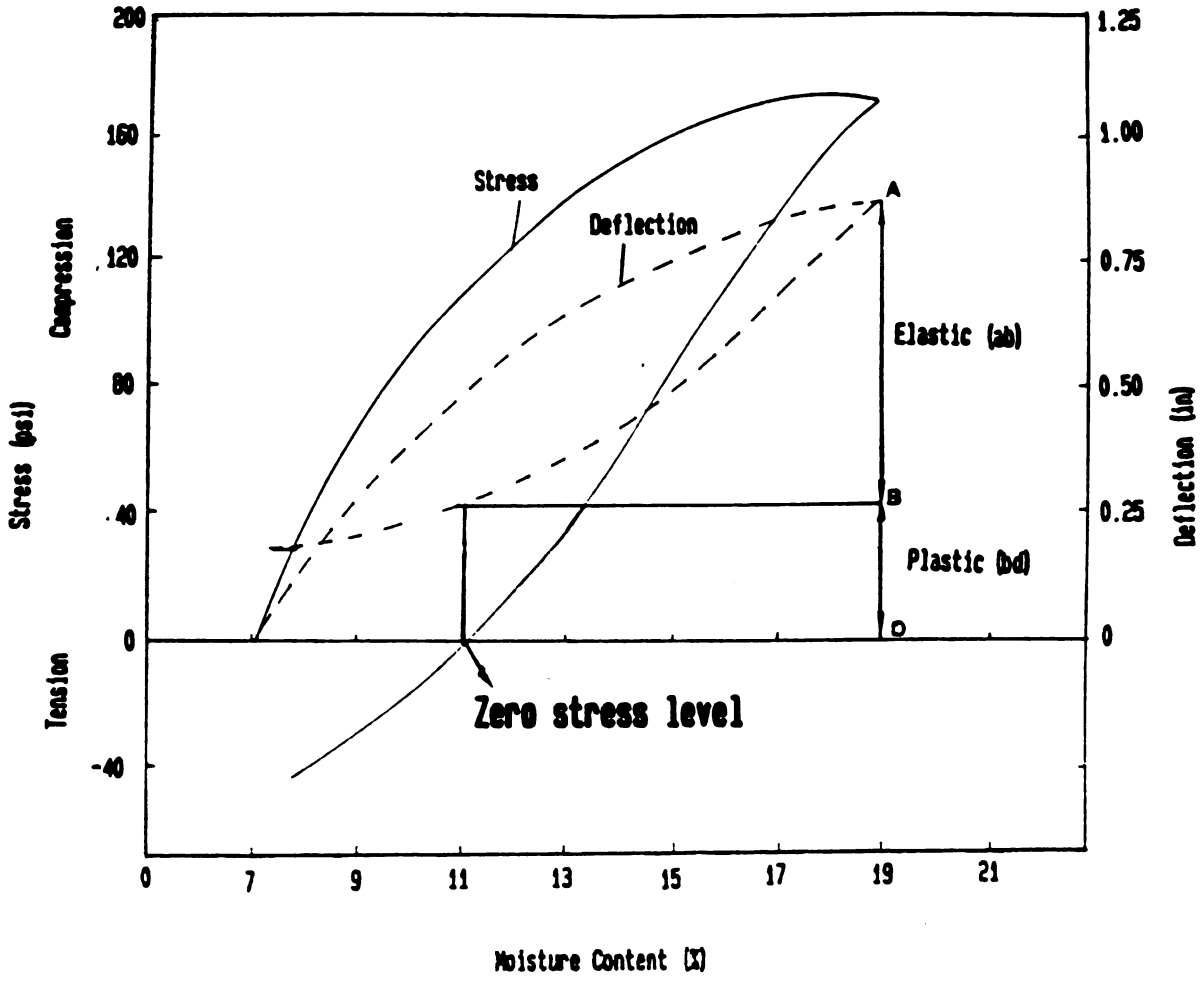

Figure 4.31. Illustration of elastic buckling deflection from experiments.

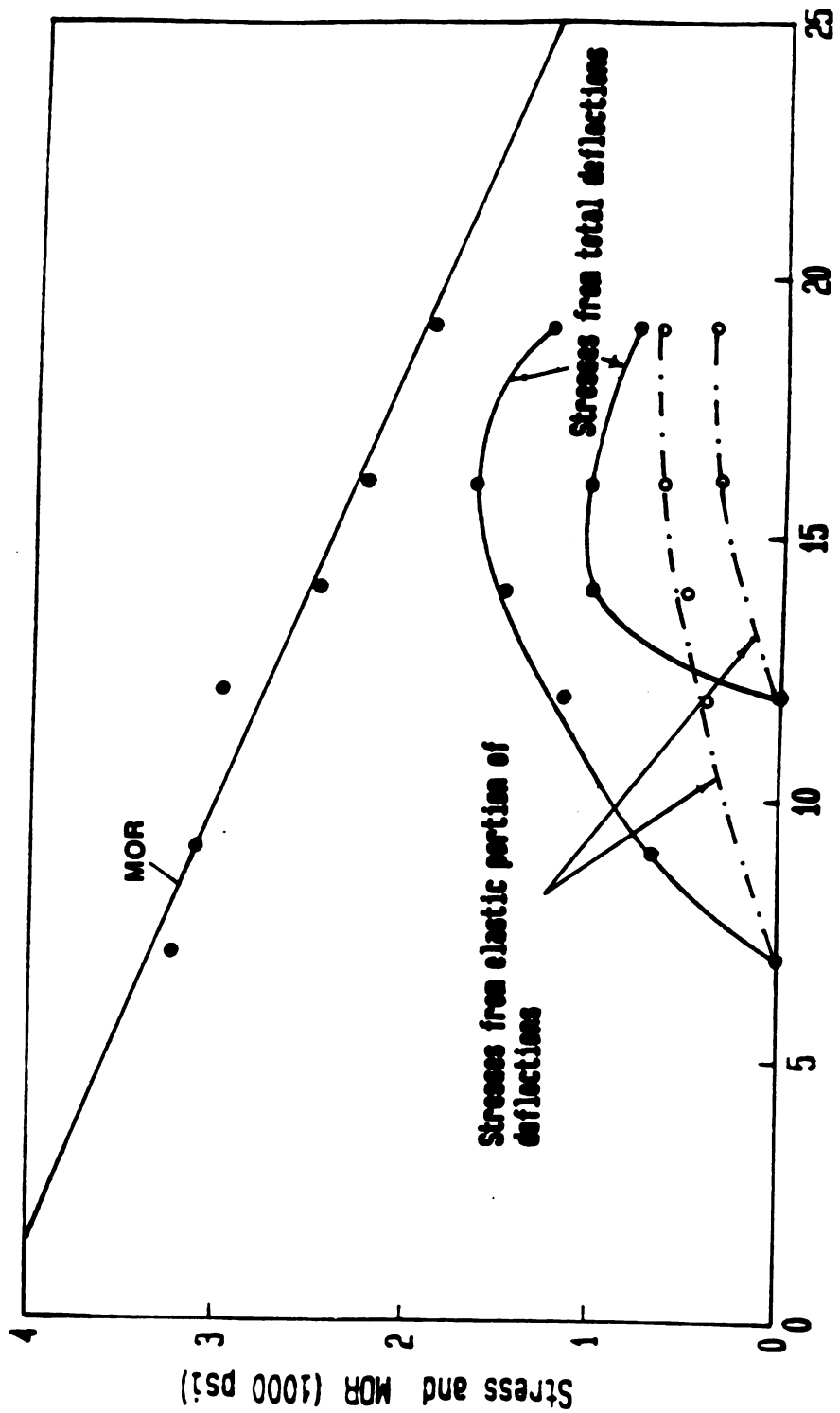

Figure 4.32. Theoretical bending stresses of restrained waferboard strips by using experimental buckling deflections.

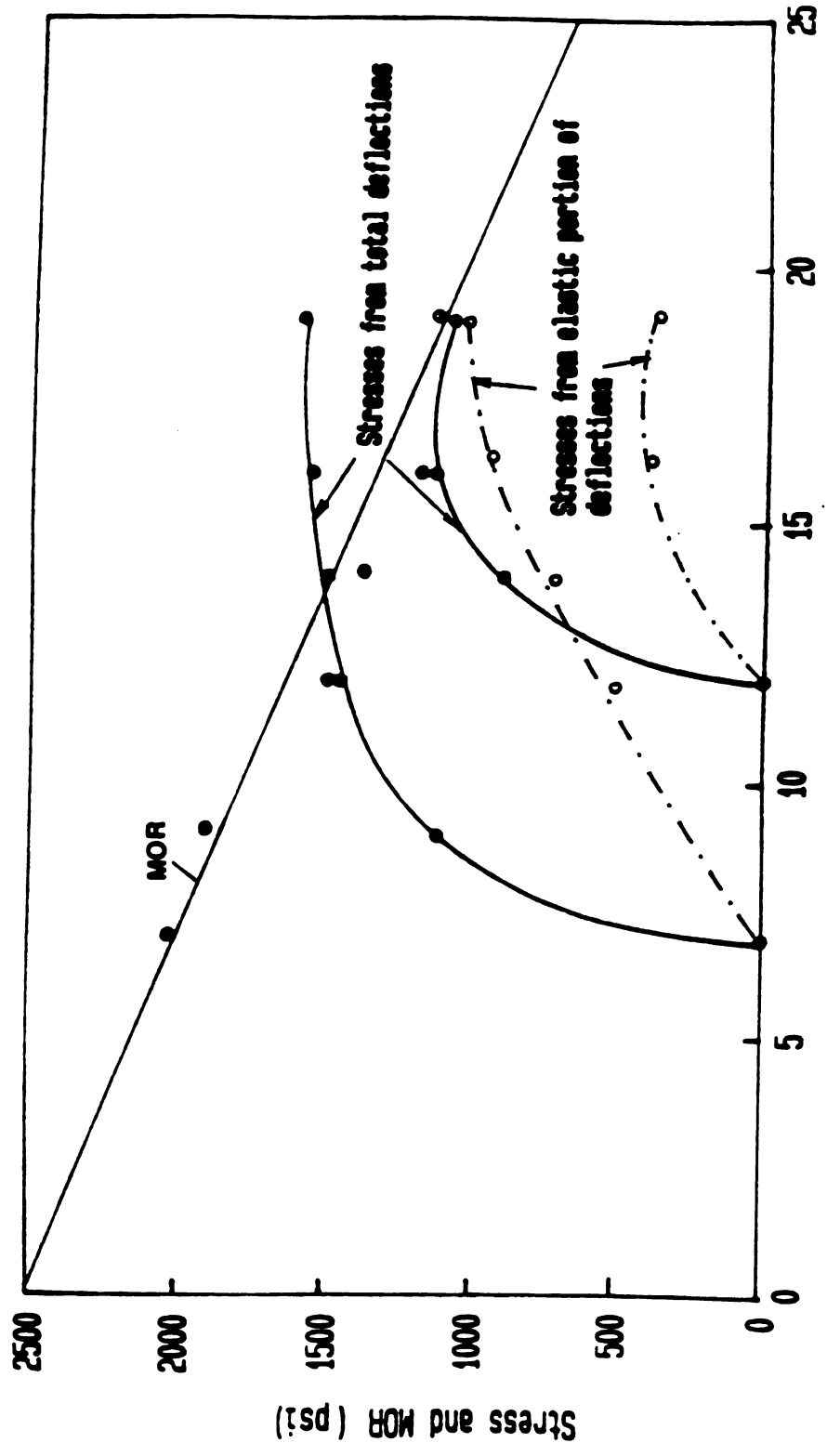

Figure 4.33. Theoretical bending stresses of restrained particleboard strips by using experimental buckling deflections.

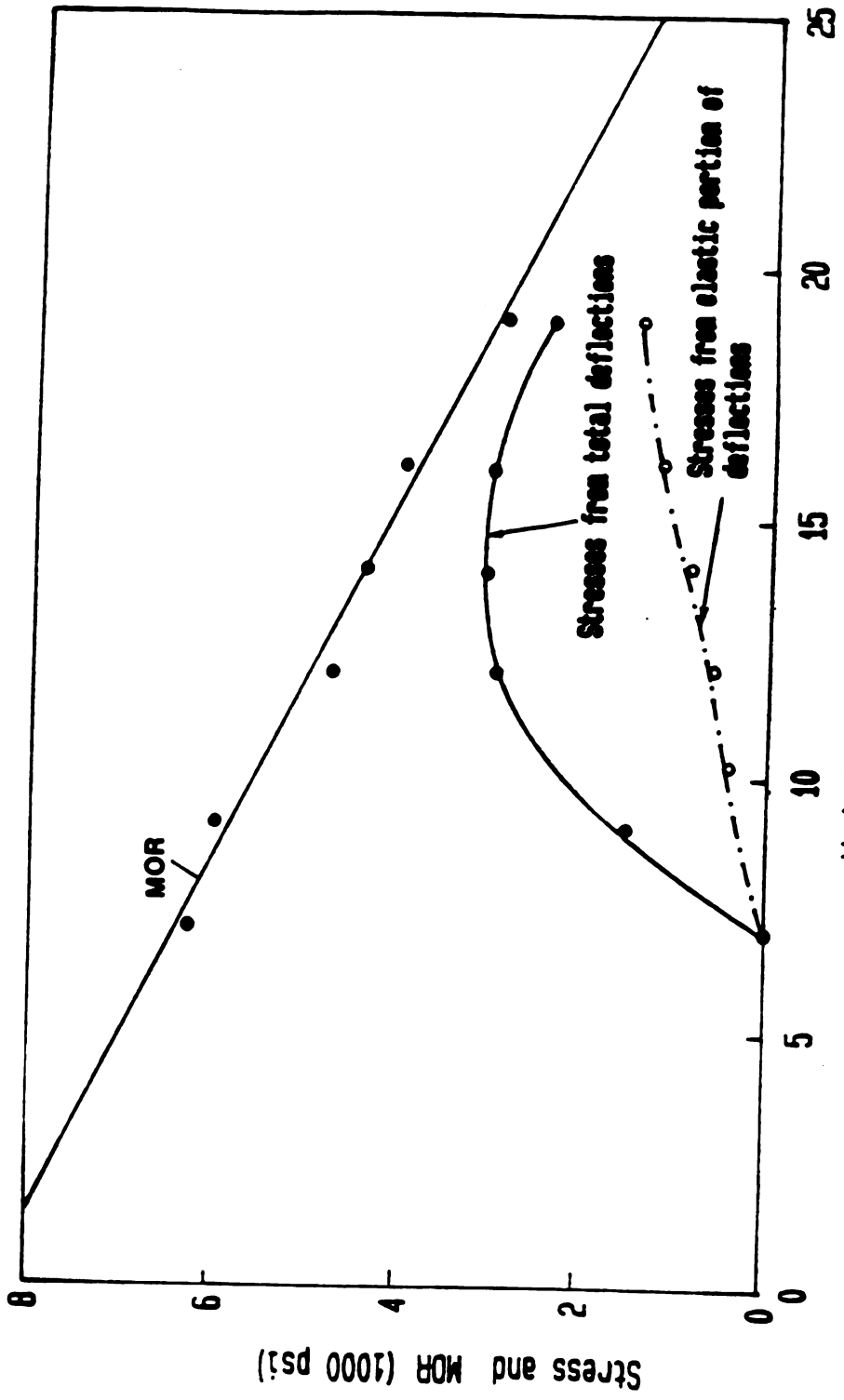

Figure 4.34. Theoretical bending stresses of restrained oriented strandboard strips by using experimental buckling deflections.

stresses, particularly when the elastic portion of the bending deflection is used as input. Still, even here, the bending stresses are substantial relative to the ultimate bending strength. However, this may be as close as this kind of analysis may get to the real bending stresses.

4.3.4. Theoretical Swelling and Shrinkage Stresses without Buckling

Theoretical swelling and shrinkage stresses of wood composites considered in this study were calculated based on the approximation which was explained in section 2.3.1.

As can be seen from Table 4.12 and Figure 4.35, 0 %, 7 % and 12 % initial moisture contents and average linear expansion values were used to compute compressive stresses for each type of wood composite.

Tension stresses of waferboard, particleboard and oriented strandboard for 19 %, 12 % and 7 % initial moisture contents were also calculated by using the same approximation in section 2.3.1. Figure 4.36 illustrates tension stresses of three types of wood composites.

Both theoretical shrinkage and swelling stresses without buckling for each type of structural product were found to be relatively higher than experimental test results.

WAFERBOARD		PARTICLEBOARD		ORIENTED STRANDBOARD	
Initial MC 0%		Initial MC 0%		Initial MC 0%	
MC (%)	Stress (psi)	MC (%)	Stress (psi)	MC (%)	Stress (psi)
7	599	7	955	7	1573
9	710	9	1266	9	1818
12	852	12	1674	12	1987
14	879	14	1698	14	2110
16	883	16	1616	16	2117
19	741	19	1396	19	1809
Initial MC 7%		Initial MC 7%		Initial MC 7%	
MC (%)	Stress (psi)	MC (%)	Stress (psi)	MC (%)	Stress (psi)
9	157	9	281	9	404
12	355	12	644	12	722
14	439	14	849	14	1055
16	496	16	909	16	1191
19	468	19	882	19	1142
Initial MC 12%		Initial MC 12%		Initial MC 12%	
MC (%)	Stress (psi)	MC (%)	Stress (psi)	MC (%)	Stress (psi)
14	125	14	121	14	452
16	220	16	303	16	661
19	273	19	441	19	761

Table 4.12. Theoretical swelling stresses.

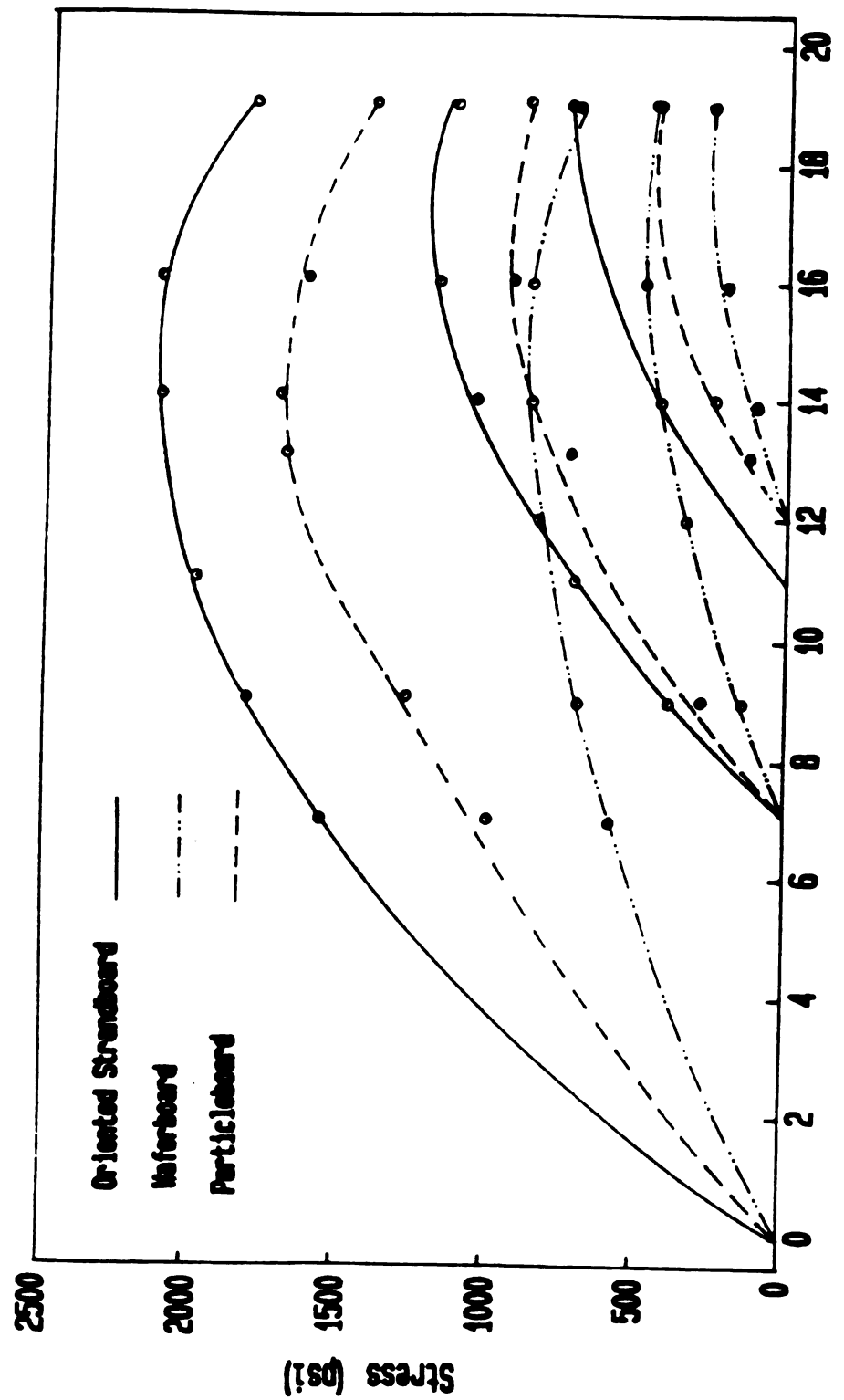

Figure 4.35. Theoretical swelling stresses without buckling.

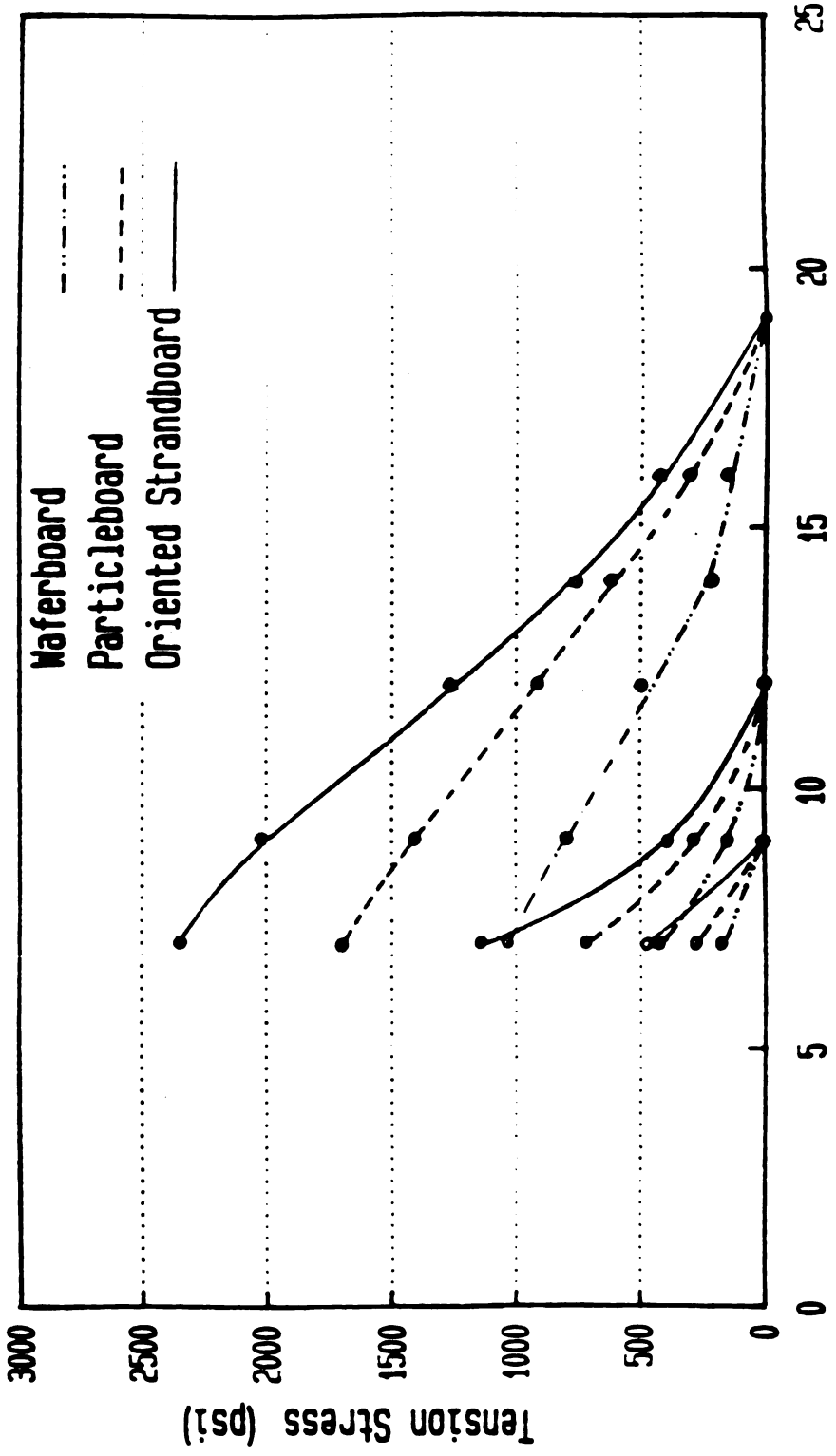

Figure 4.36. Theoretical shrinkage stresses without buckling.

WAFERBOARD		PARTICLEBOARD		ORIENTED STRANDBOARD	
Initial MC 19%		Initial MC 19%		Initial MC 19%	
MC (%)	Stress (psi)	MC (%)	Stress (psi)	MC (%)	Stress (psi)
16	165	16	303	16	419
14	188	14	606	14	747
12	497	12	901	12	1265
9	789	9	1407	9	2020
7	1030	7	1706	7	2343
Initial MC 12%		Initial MC 12%		Initial MC 12%	
MC (%)	Stress (psi)	MC (%)	Stress (psi)	MC (%)	Stress (psi)
9	157	9	281	9	404
7	429	7	711	7	1171
Initial MC 9%		Initial MC 9%		Initial MC 9%	
MC (%)	Stress (psi)	MC (%)	Stress (psi)	MC (%)	Stress (psi)
7	171	7	284	7	468

Table 4.13. Theoretical shrinkage stresses.

4.4. Visco-elasticity

It was one of the objectives of this study to predict development of stresses and buckling deformations of restrained wood composite columns due to changes in relative humidity by using the elasticity approach. However, it is clear that results from theoretical and experimental investigations of this study confirmed that all three types of structural wood composites presented rather inelastic behaviour. Therefore, in the following, theoretical aspects of visco-elasticity behaviour will be described in order to better understand the development of actual shrinkage, swelling stresses with combination of bending stresses as well as buckling deformations of wood composites.

Stress-strain relationship for many materials including most metals can be considered as independent of time. When a certain amount of load is applied to these types of materials, they do not exhibit any change in deformation unless the magnitudes of the loads which are applied to the members are changed. However, some other materials such as, high polymers, wood composites, silicon-organic rubber display both elastic and perfect liquid-like behavior depending on the time scale of measurement [11,15]. Materials which exhibit the above mentioned characterictics are known as visco-elastic material.

When a certain amount of load is applied to a wood composite, an initial elastic strain occurs immediately, and

then the strain varies as a function of time. This time dependent strain can be related to a number of characteristics of the composite as well as to environmental conditions.

Particle geometry, cross section pattern of composite, density and thickness of the board and press cycle are the most important factors which can be related to the time varying strain. Moreover, type of stress, duration of load, relative humidity and temperature can be considered as some of the enviromental factors.

Regrouping of segments of flexible chains without changing of the average distance between the chains is one of the major characteristics of visco-elastic deformation in polymers. The flexibility of the polymer molecules which could be considered as the main cause of the visco-elastic behavior is related to bonds which allow turning or rotating under applied load or the effect of change in hygrothermal conditions.

The model shown in Figure 4.37 illustrates the mechanics of visco-elastic deformation. U_a is the elastic deformation which is increased by viscous deformation U_b which occurs as a result of bond failure and the establishment of secondary bonds. Even after the load is removed the new bonds will remain causing the viscous deformation, U_b to be permanant[10].

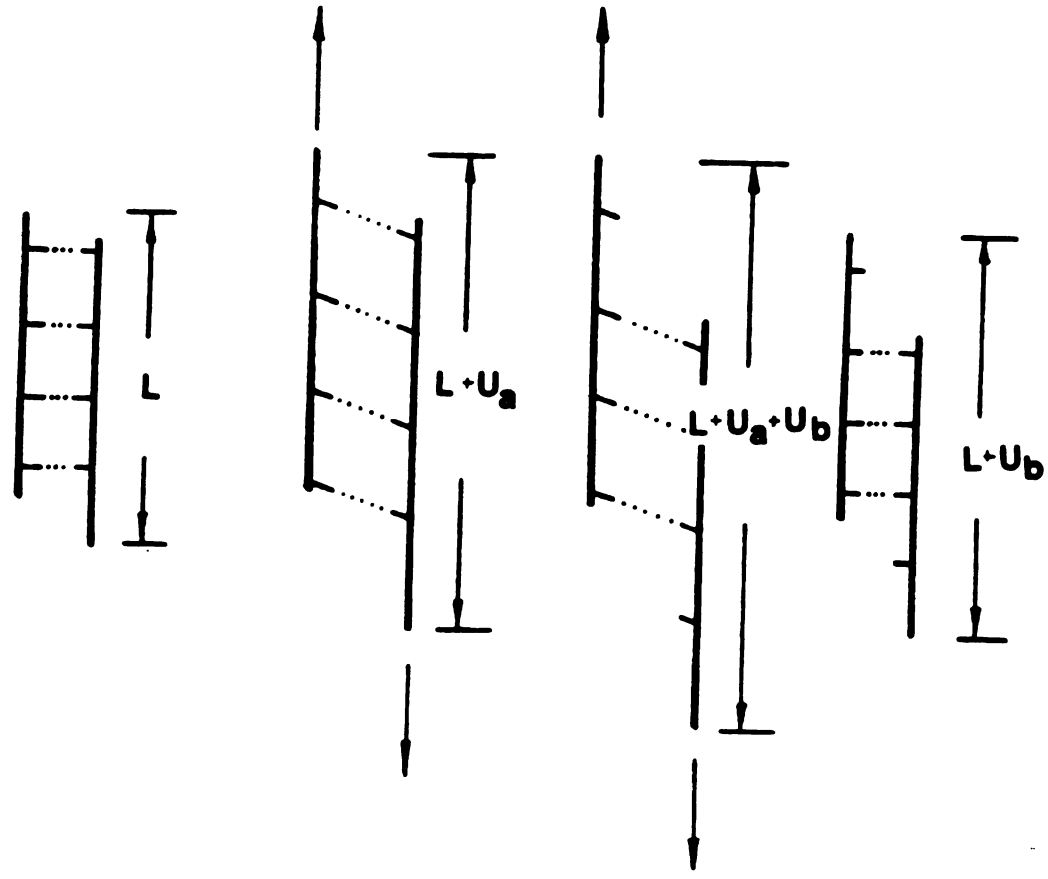

Figure 4.37. Schematic representation of viscous flow [10].

CHAPTER 5

CONCLUSIONS

Swelling and shrinkage stresses of restrained wood composites play a very important role on their utilizations, especially for structural purposes. Within the scope of this study the development of such stresses and deformations was investigated both experimentally and theoretically for particleboard, waferboard and oriented strandboard.

All types of wood composites considered throughout this study indicated a similar trend in stress development due to the cyclic relative humidity exposures in the laboratory conditions. Theoretical calculations within the perspective of elasticity and column mechanics showed that restrained swelling stresses and deformations in particleboard, oriented strandboard and waferboard may cause important problems. Although experimentally, no mechanical failures were detected in all three types of wood composites within the humidity ranges employed in the experiments, serious structural deformations were observed due to the excessive moisture content changes in these products. Moreover, it was found that structural deformations from the experiments do not only significantly deteriorate the physical properties, but they also manifest the reduction in the strength of the composite

panels. Consequently, when a wood composite panel is utilized in application where high humidity is inevitable, special care should be taken in order to minimize the adverse effects of the moisture content on the mechanical and physical properties of the wood composite products.

Following conclusive remarks can be drawn from the results of this investigation :

1- Wood composites under conditions of axial restraint develop swelling or shrinkage stresses when their moisture content changes due to changing environmental conditions.

2- These stresses are due to linear dimensional changes of the material which in the case of swelling can lead to buckling. The mechanism of the buckling of a column under an applied load can be applied to the case of restrained swelling.

3- Axial stresses due to restrained swelling and shrinkage as well as lateral deformation (buckling) can be determined experimentally. Bending stresses, associated with buckling, however, can only be determined theoretically, they cannot be measured.

4- Theoretical determinations of bending stresses of a buckling column is based (in the content of this study) on the assumption of elasticity of the material. This method is an unsatisfactory approach since it resulted in theoretical bending stresses exceeding the experimentally determined bending strength, in most cases. Even a modified approach (using experimental lateral deflections as input values, either

totally or further reduced to an "elastic" component) yielded bending stresses of considerable magnitude relative to the ultimate bending strength.

5- It is clear from the evidence that material such as those investigated cannot be analyzed accuratly under the assumption of elasticity. Rather, an accurate analysis must take their visco-elastic behaviour into consideration and must deal with certain inhomogeneities due to the structure of these materials and due to moisture content gradients developing during exposure.

6- Even with these qualification, the results should be taken seriously. They do indicate the strong possibility of the development of rather high bending stresses if the dimensional application parameters and the environmental conditions allow significant buckling to occur. These bending stresses may be of the same order of magnitude as other design stresses allowing for snow and rain loads, etc.

7- While it is generally desirable to develop a wood composite with a high modulus of elasticity, it is important to minimize its linear expansion in applications where restrained swelling could lead to buckling. This combination is being approached by the modern oriented strandboard composite. On the other hand, where linear expansion is high, the material can be applied only when plastic flow reduces developing stresses substantially. This seems to be the case with particleboard.

Plasticity of wood composites, in many application a serious disadvantages, is an asset in applications that favor the development of buckling because it substantially reduces potentially dangerous stresses.

APPENDIX A

TECHNICAL SPECIFICATIONS OF LOAD CELL

TECHNICAL SPECIFICATIONS OF LCC UNIVERSAL SHEAR BEAM LOAD CELL

Rated Capacity	: 1000 k.
Rated Output	: 3.0 0.003 mV/V
Nonlinearity	: 0.03 %
Hysteresis	: 0.02 %
Nonrepeatability	: 0.01 %
Creep in 20 Min.	: 0.03 %
Zero Balance	: 1.0 %
Compensated Temperature Range	: +15 to +115° F ; -10 to +45° C.
Temperature Effect	: Output : 0.08 % of load / 100° F ; Zero Balance : 0.15 % /100 ° F.
Terminal Resistance	: Input : 385 ohms minimum ; output 351 1 ohms.
Excitation Voltage	: 18 maximum V dc.
Insulation Resistance	: 5000 at 50 V dc megaohms/min.
Maximum Load Safe	: 150 %
Maximum Load Ultimate	: 250 %
Max.Side Load,Safe	: 100 %
Side Load Rejection	: 500:1
Deflection at Rated Load	: 0.005 in.
Weight	: 2.0 lb.

APPENDIX B

TECHNICAL SPECIFICATIONS OF DIGITAL STRAIN GAGE INDICATOR

TECHNICAL SPECIFICATIONS OF V/E-20A STRAIN GAGE INDICATOR

Input circuits	:	Strain gages and transducers, 50 to 1000 Ω Qarter, half and full bridge with 120, 350 Ω internal dummies provided. Five- way biding post on front panel.
Bridge Balance	:	Coarse 17-step switch selectible 8,000 $\mu\epsilon$ Fine 10 turn potentiometer 540 $\mu\epsilon$.
Bridge Excitation	:	Constant bridge current:0.5 to 20 mA per gage in 16 logarithmic steps. Voltage limits 13 Vdc.
Accuracy	:	Internal calibration 0.12 %, linearity 0.05 % 1 count.
Stability	:	2 counts (constant temperature after 15 minutes.) 0.25 Counts
Calibration	:	Quarter or half bridge, internal calibration by shunting internal half bridge which simulates 1000 (GF = 2). Full bridge : Shunts one leg of external bridge. External calibration provision on rear panel.
Range	:	Switch selectible: (X1) 1,999 with 1 count resolution, (X10) 19,999 with 10 counts resolution. Over-range indication by flashing digits. M option : 19,999 with 1 count resolution. 199,999 with 10 count resolution. Overrange indication by flashing digits.

Sensitivity	:	Quarter, half bridge, 120 Ω : 0.6 to 30 με /count. Full bridge 120Ω: 0.8 to 45 με /count. Quarter, half, bridge 350 Ω : 0.3 to 15 με / count.
Dynamic Output	:	Bandpass (-0.5 dB or 5 %) : dc to 2000 Hz. Linear Range : 5 Vdc. 0.5 mA. Output Impedance : 300 Ω .
Power	:	105 to 130 Vac 50-60 Hz, 10 W, or 210 to 260 Vac 50-60 Hz. (switchable)
Environment	:	Temperature : 0-40 C, Humidity : 0-90 %
Physical	:	Standard model: Weight 12.4 lb (5.6kg) Overall Size : 9.5 in W by 7.5 in H by 12.5 in D(241 W by 190 H by 318 D mm)

APPENDIX C

LOAD CELL CALIBRATION DATA

LOAD CELL CALIBRATION DATA

TENSION

MICROSTRAIN ($\mu\epsilon$)	LOAD (lb)
50	7.8
100	15.9
150	24.2
200	31.1
250	37.8
300	46.3
350	54.1
400	60.9
450	68.3
500	75.2
550	84.3
600	91.2
650	97.9
700	105.1
750	113.2
800	121.3
850	128.9
900	136.0
950	143.1
1000	150.1
1050	157.8
1100	164.8
1200	171.8
1250	185.5
1300	192.5
1350	200.5
1400	208.0
1450	215.0
1500	222.4
1550	229.6
1600	236.6
1650	244.0
1700	251.0
1750	257.6
1800	265.6
1850	273.4
1900	280.0
1950	287.1
2000	293.5
2050	300.0

MICROSTRAIN ($\mu\epsilon$)	LOAD (lb)
2100	306.8
2150	314.8
2200	322.6
2250	329.8
2300	337.2
2350	345.3
2400	352.8
2450	360.8
2500	368.7
50	50

Regression Output :

Constant : 3.13485
Std. Error of Y Est. : 1.11589
R Squared : 0.99999
No of Observations : 50
Degree of Freedom : 48

x Coefficient : 0.14571
Std. Error of Coefficient : 0.00021

Calibration was done at Instron Testing Machine Model 4206.

Cross-head speed : 0.008 inch/min.

COMPRESSION

MICROSTRAIN ($\mu\epsilon$)	LOAD (lb)
50	7.5
100	15.1
150	22.0
200	29.0
250	36.5
300	43.5
350	50.0
400	57.0
450	64.5
500	72.1
550	79.0
600	86.0
650	94.5
700	101.0
750	108.1
800	115.5
850	122.5
900	129.5
950	136.7
1000	144.8
1050	152.6
1100	159.6
1150	166.7
1200	174.0
1250	182.0
1300	189.0
1350	196.2
1400	203.4
1450	210.2
1500	218.0
1550	225.0
1600	232.0
1650	238.8
1700	245.6
1750	252.8
1800	260.6
1850	267.0
1900	275.0
1950	282.0
2000	290.2
2050	297.2
2100	304.4
2150	312.4
2200	319.0

MICROSTRAIN ($\mu\epsilon$)	LOAD (lb)
2250	326.0
2300	333.0
2350	340.2
2400	347.1
2450	354.1
2500	362.0
50	50

Regression Output :

Constant	:	-0.16204
Std. Error of Y Est.	:	0.54200
R Squared	:	0.99999
No of Observations	:	50
Degree of Freedom	:	48

X Coefficient	:	0.144920
Std. Error of coefficient	:	0.000106

Calibration was done at Instron Testing Machine Model 4206.

Cross-head speed : 0.008 inch/min.

APPENDIX D

TECHNICAL SPECIFICATIONS OF STRAIN GAGE EXTENSOMETER

SPECIFICATIONS OF STRAIN GAGE EXTENSOMETER

Catalog no	:	2630-0358
Gage Length	:	2 inch
Maximum Strain	:	10 %
Approximate Spring Load	:	0.20 inch range
Maximum Hysteresis	:	0.3 %
Non-linearity	:	0.25 %
Weight	:	45 grams

MAGNIFICATION AND DATA RANGE

Range Setting	:	0.2, 0.5, 1, 2, 5, 10, 20
Strain Factor	:	10,000-4,000-2,000-1,000-400-200
Magnification Ratio	:	5,000:1-2,000:1-2,000:1-500:1 200:1-100:1
Maximum Strain (20 in chart)	:	0.2%-0.5%-1%-2%-5%-10%
Range (inches)	:	0.004-0.010-0.020-0.040-0.100-0.200

LITERATURE CITED

LITERATURE CITED

[1] Albin, R. 1989. Durchbiegung und Lastannahmen im Korpusmobelbau. Holz als Roh-und Werkstoff. 47 (1) pp 4-10.

[2] American Society for Testing and Materials (ASTM), 1986 Method D1037-78. Evaluating the properties of wood based fiber and particle panel material.

[3] Anderson, G.R. 1988. A review of current structural panel markets and new opportunities. Structural wood composites, new technologies for expanding markets. FPRS Proc. 47359. Madison, Wisconsin.

[4] Bachmann, G. and Habler, W. 1978. Das Ver-halten von waagerechten tragenden Mobelbaugruppen bei Dauerstandbelastung. Holztechnologie. 19 (2) pp 44-48.

[5] Bartenev, G.M. and Zuyev, Y.S. 1968. Strength and failure of visco-elastic materials. Pergaman Press New York.

[6] Biblis, E.J. 1985. Properties of three-layer oriented strandboard from Southern hardwood. For. Prod. J. 35(2) pp 28-38.

[7] Brayn, E.L. and Schniewind, A.P. 1965. Strength and rheological properties of particleboard as effected by moisture content and sorption. For. Prod.J. 15(4) pp 143-148.

[8] Brayn, L.E. 1962. Dimensional stability of particleboard. For. Prod. J. 12(12) pp 572-576.

[9] Brumbaugh, J.I. 1960. Effect of flake dimension on properties of particleboard. For. Prod. J. 10(5) pp 243-246.

[10] Bodig, J.B. and Jayne, B.A. 1982. Mechanics of wood and wood composites. Van Nostrand Reinhold Co. New York.

[11] Chen, W.F. and Lui, E.M. 1987. Structural stability. Theory and implementation. Elsevier Science Pub.Co. New York.

[12] Chajes, A. 1974. Priciples of structural stability theory. Prentice Hall Inc.Englewood Cliffs, New Jersey.

[13] Dickerhoof, E.H. and Marcin, C.T. 1978. Factors influencing market potential for structural flakeboard. USDA. For. Serv. General Tech. Report WO-5. FPL. Madison, Wisconsin.

[14] DeTeresa, J.S., Porter, S.R. and Farris.J.R., 1985 A model for the compressive buckling of extended chain polymers. Journal of Material Sci. 20(9) pp 1645-1659.

[15] Flugge, W. 1967. Visco-elasticity, Blaisdell Pub. Company. Waltham, Massachusetts.

[16] Forest Industries, 1988 April. Panel Review.

[17] Garll, C. 1986. Wood, particleboard and flakeboard. Types, grades and uses. USDA For. Ser. General Tech. Report 53. FPL. Madison, Wisconsin

[18] Gatewood, B.E. 1957. Thermal stresses. Mc Graw-Hill Book Company Inc. New York.

[19] Gatchell, C.J., Heebink, B.G. and Hefty, F.J. 1966. Influence of component variables on properties of particleboard for exterior use. For. Prod.J. 25(3) pp 46-59.

[20] Geimer, R.L. 1982. Dimensional stability of flakeboard as affected by board specific gravity and flake alignment. For. Prod. J. 32(8) pp 47-51.

[21] Geimer, R. 1976. Flake alignment in particleboard as effected by machine variables and particle geometry. USDA. For. Serv. Research Paper FPL. Madison, Wisconsin.

[22] Geimer, R.L. and Price, E. W. 1978. Construction variables considered in fabrication of structural flakeboard. USDA. For. Serv. General Tech. Report WO-5. FPL. Madison, Wisconsin.

[23] Gertjejansen, R., Hyvarinen, H., Haygreen, J. and French, O. 1973. Physical properties of phenolic bonded wafer type particleboard from mixtures of aspen, paper birch and tamarac. For. Prod. J. 23(6) pp 24-28.

[24] Ivanov, Y.M. 1956. Measurement of swelling of wood. Composite Wood. 3 (5) pp 91-100.

[25] Halligan, A.F. 1970. A review of thickness swelling in particleboard. Wood Science and Tech. 4(4) pp 301-312.

[26] Halligan, A.F. and Schniewind, A.P. 1974. Prediction of mechanical properties of particleboard at various moisture content. Wood Science and Tech. 8(2) pp 68-78.

[27] Halligan, A.F. and Schniewind, A.P. 1972. Effect of moisture on physical and creep properties of particleboard. For. Prod.J. 22(4) pp 41-48.

[28] Harpole, B.G.1978. Overview of structural flakeboard production cost. USDA. For. Serv. General Tech. Report WO-5. FPL. Madison, Wisconsin.

[29] Haygreen, G.J. and Bowyer, J.L. 1982. Forest product and wood science. Iowa State University Press. Ames, Iowa.

[30] Hall, H., Haygreen, G.J. and Neisse, B. 1977. Creep of particleboard and plywood floor deck under concentrated loading. For. Prod.J. 27(5) pp 23-31.

[31] Hart, C.A. and Rice, J.T. 1963. Some observations on the development of a laboratory flakeboard process. For. Prod.J. 13(11) pp 483-488.

[32] Hann, R.A., Black, J.M. and Blomquist, R.F. 1963. How durable is particleboard? Part 2. The effect of temperature and humidity. For. Prod.J. 13(5) pp 169-174.

[33] Heebink, B.G., Hann, R.A. and Haskell, H.H. 1964. Particleboard quality as affected by planer shaving geometry. For. Prod.J. 14(10) pp 486-494.

[34] Heebink, B.G. and Hann, R.A. 1959. How wax and particle shape affect stability and strength of oak particleboard. For. Prod.J. 9(7) pp 197-203.

[35] Hoadley, B.R. 1969. Perpendicular to grain compression set induced by restrained swelling. Wood Science. 1(3) pp 157-166.

[36] Hse, C.Y. 1975. Properties of flakeboard from hardwood grown on southern pine sites. For. Prod.J. 25(3) pp 48-53.

[37] Jorgensen, R.N. and Odell, R.L. 1961. Dimensional stability of oak flakeboard. For. Prod.J. 11(3) pp 463-466.

[38] Kass, A.J. 1965. Shrinkage stresses in externally restrained wood. For.Prod.J. 15(6) pp 225-232.

[39] Keylwerth, R. 1962. Behinderte Quellung. Investigations on the free and restraint swelling. Part 2. Holz als Roh-und Werkstoff. 20(8) pp 292-303.

[40] Kollmann, F.P.and Kuenzi, E.W., and Stamm, A.J. 1975. Principles of wood science and technology. Wood based material. Vol.2. Springer-Verlag, New York.

[41] Kollmann, F.P. and Cote, W.A. 1968. Principles of wood science and technology. Solid wood. Vol.1. Springer-Verlag, New York.

[42] Langendorf, G. 1977. Beitrage zur Static von Mobelkonstrutionen. Holztechnologie. 18(2) pp 94-99.

[43] Langendorf, G. 1970. Zu aktuellen Problemen der Mobelstatic. Holztechnologie. 11(4) pp 237-248.

[44] Lee, W.C. and Biblis, E.J. 1976. Effect of high and low relative humidity cycle on properties of southern yellow pine particleboard. For. Prod. J. 26(6) pp 32-35.

[45] Lehmann, W.F. 1978. Cyclic moisture condition and their effect on strength and stability of structural flakeboard. For. Prod. J. 28(2) pp 23-31.

[46] Lehmann, W.F. 1974. Properties of structural particleboard. For. Prod. J. 24(1) pp 19-26.

[47] Lehmann, W.F. 1970. Resin efficiency in particleboard as influenced by density, atomization, and resin content. For. Prod.J. 20(11) pp 48-54.

[48] Lehmann, W.F. and Hefty, F.J. 1973. Resin efficiency and dimensional stability of flakeboards. U.S.D.A. For. Serv. Research Paper 207. FPL. Madison, Wisconsin.

[49] Liiri, O. 1960. Investigation on the effect of moisture and wax upon the properties of wood particleboard. The State Institute for Technical Research. Helsinki, Filland.Sarja. pp 1-15.

[50] Maloney, T.M. 1986. Modern particleboard and dry process fiberboard manufacturing. Miller Freeman Pub. San Francisco.

[51] Mc Natt, J.D. 1982. How cyclic humidity affects static bending and dimensional properties of some wood-base panel products. USDA. For. Serv. Southern Forest Exp. Station Technical Report. So.53. pp 67-76.

[52] Mc Natt, J.D. 1973. Buckling due to linear expansion of hardboard siding. For. Prod.J. 23(1) pp 37-43.

[53] Moslemi, A.A. 1964. Some aspects of visco elastic behaviour of hardboard. For. Prod. J. (13)8 pp 337-342.

[54] Narayanamurti, D. and Gupta, R.C. 1961. Swelling pressure of wood. Journal of Japan Soc. Test Material 10(12) pp 434-436.

[55] O'Halloran, R.M. 1981. Predicting buckling performance of plywood composite panels for roofs and floors. American Plywood Association. Research Report 144. Tacamo, Washington.

[56] Pentoney, R.E., Davidson, R.W., 1962. Rheology and study of wood. For. Prod. J. (12) 5 pp 243-248.

[57] Perkinty, T., Kinston, R.S., 1972. Review of the sufficient reseach on the swelling pressure of wood. Wood Science and Tech. (6)3 pp 215-229.

[58] Post, P.W. 1958. Effect of particle geometry and resin content on bending strength of oak particleboard. Forest Prod. J. 8 (10) pp 317-332.

[59] Post, P.W. 1961. Relationship of flake size and resin content to mechanical and dimensional properties of flakeboard. Forest Prod. J. 11(1) pp 34-37.

[60] Price, E.W. 1978. Properties of flakeboard made from southern specie. USDA. For. Ser. General Tech.Report WO-5. PFL. Madison, Wisconsin.

[61] Price,E.J. and Lehmann, W.F. 1978. Flaking alternatives USDA. For. Ser. General Tech. Report WO-5. FPL. Madison, Wisconsin.

[62] Popov, E.P. 1978. Strength of materials. Prentice-Hall Inc. Englewood Cliffs, New Jersey.

[63] Raczokowski, J. 1960. Anisotropy of swelling pressure of wood. Folis For. Poland. (2) pp 115-119.

[64] Remarker, T. and Lehmann, W. 1976. High performance structural flakeboards from Douglas fir logdepole pine forest residues.USDA. For. Serv. Research Paper. 286 FPL. Madison, Wisconsin.

[65] Sandor, I.B.1978. Strength of materials. Prentice-Hall Inc. Englewood Cliffs, New Jersey.

[66] Schniewind, A.P. 1968. Recent progress in the study of the rheology of wood. Wood Science and Tech. 2(3). pp 188-206.

[67] Schuler, C.E. and Kelly, A.R. 1976. Effect of flake geometry on mechanical properties of eastern spruce flake type particleboard. For. Prod. J. 26(6) pp 24-28.

[68] Siau, F.J. 1988. Sorption of the cell wall. Stabilization of the wood cell wall. Wood Science Seminar 1. Michigan State University. pp 29-40.

[69] Spalt, H.A. and Sutton, R.F., 1968. Buckling of thin surfacing materials due to restrained hydroexpansion. For. Prod. J. (18)4 pp 53-58

[70] Spetler, H. 1988. New panel technologies and their potential impact. Structural wood composites, new technologies for expanding markets. FPRS Proc. 47359 Madison, Wisconsin.

[71] Steck, F.E. 1988. An advanced press line system for structural composite boards. Structural wood composites, new technologies for expanding markets. FPRS. Proc. 47359. Madison, Wisconsin.

[72] Stewart, H.A. and Lehmann, W.F. 1973. High quality particleboard from cross grain knife planed hardwood flakes. For.Prod. J. 23(8) pp 53-60.

[73] Suchsland, O. 1976. Measurement of swelling forces with load cells. Wood Science. 8(3) pp 194-198.

[74] Suchsland, O. 1980. Determination of sorption isotherms in minidesiccators. Wood Science. 12(4) pp 214-217.

[75] Suchsland, O. 1972. Linear hygroscopic expansion of selected commercial particleboard. For. Prod. J. 22(11) pp 28-32.

[76] Suchsland, O. 1965. Swelling stresses and swelling deformations in hardboard. Michigan Agr. Exp. Stat. Quarterly Bull. 43(4) pp 591-605.

[77] Suchsland, O. 1974. Preventing the buckling of thin wood panels. Michigan State University, Extension Bull. E-778.

[78] Suchsland, O.and McNatt, J.D. 1985. On the warping of laminated wood panels. Michigan State University. East Lansing, Michigan.

[79] Suchsland, O., Lyon, D.E. and Short, P.E. 1987. Selected properties of commercial medium density fiberboard.For. Prod. J. 28(9) pp 45-48.

[80] Suchsland, O. 1989. Linear expansion and buckling of hardboard. (Unpublished paper) Michigan State University, Department of Forestry.

[81] Timoshenko, S.P. and Gere, J.M. 1961. Theory of elastic stability. Mc Graw-Hill Book Inc. New York.

[82] Turner, H.D. 1954. Effect of particle size and shape on strength and dimensional stability of resin bonded wood particle panels. For. Prod. J. 4(5) pp 210-220.

[83] Vital, B.R., Lehmann, W.F. and Boonie, R.J. 1974. How species and board densities affect the properties of exotic hardwood particleboard. For. Prod. J. 24(12) pp 37-44.

[84] Vital, B.R., Wilson, J. and Kanarek, P., 1980. Parameter affecting dimensional stability of flakeboard and particleboard. For. Prod. J. 30 (12) pp 23-28.

[85] Wood Handbook, 1987. USDA. Forest Service Agriculture Handbook 72.

[86] Youngquist, J.A. 1982. U.S. wood-based industry: Research and technologyical innovation. For. Prod. J. 32(8) pp 14-24.

[87] Zylkowski, S.C. 1986. Dimensional performance of wood-based siding. American Plywood Association. Research report 149. Tacoma, Washington.